



National Library  
of Canada

Bibliothèque nationale  
du Canada

Acquisitions and  
Bibliographic Services Branch

Direction des acquisitions et  
des services bibliographiques

395 Wellington Street  
Ottawa, Ontario  
K1A 0N4

395, rue Wellington  
Ottawa (Ontario)  
K1A 0N4

*Your file* *Votre référence*

*Our file* *Notre référence*

## NOTICE

## AVIS

The quality of this microform is heavily dependent upon the quality of the original thesis submitted for microfilming. Every effort has been made to ensure the highest quality of reproduction possible.

La qualité de cette microforme dépend grandement de la qualité de la thèse soumise au microfilmage. Nous avons tout fait pour assurer une qualité supérieure de reproduction.

If pages are missing, contact the university which granted the degree.

S'il manque des pages, veuillez communiquer avec l'université qui a conféré le grade.

Some pages may have indistinct print especially if the original pages were typed with a poor typewriter ribbon or if the university sent us an inferior photocopy.

La qualité d'impression de certaines pages peut laisser à désirer, surtout si les pages originales ont été dactylographiées à l'aide d'un ruban usé ou si l'université nous a fait parvenir une photocopie de qualité inférieure.

Reproduction in full or in part of this microform is governed by the Canadian Copyright Act, R.S.C. 1970, c. C-30, and subsequent amendments.

La reproduction, même partielle, de cette microforme est soumise à la Loi canadienne sur le droit d'auteur, SRC 1970, c. C-30, et ses amendements subséquents.

Canada

**A STUDY OF THE BEHAVIOUR OF VISCOELASTIC  
FLUIDS IN CONSTANT PRESSURE FILTRATION**

**Helen Tania Slegr**

**A thesis submitted to the School of Graduate Studies and Research  
in partial fulfillment of the requirements for the  
degree of  
MASTER OF APPLIED SCIENCE  
Department of Chemical Engineering  
University of Ottawa.**



**Helen Tania Slegr, Ottawa, Canada, 1992**



National Library  
of Canada

Acquisitions and  
Bibliographic Services Branch

395 Wellington Street  
Ottawa, Ontario  
K1A 0N4

Bibliothèque nationale  
du Canada

Direction des acquisitions et  
des services bibliographiques

395, rue Wellington  
Ottawa (Ontario)  
K1A 0N4

*Your file* *Voire référence*

*Our file* *Notre référence*

**The author has granted an irrevocable non-exclusive licence allowing the National Library of Canada to reproduce, loan, distribute or sell copies of his/her thesis by any means and in any form or format, making this thesis available to interested persons.**

**L'auteur a accordé une licence irrévocable et non exclusive permettant à la Bibliothèque nationale du Canada de reproduire, prêter, distribuer ou vendre des copies de sa thèse de quelque manière et sous quelque forme que ce soit pour mettre des exemplaires de cette thèse à la disposition des personnes intéressées.**

**The author retains ownership of the copyright in his/her thesis. Neither the thesis nor substantial extracts from it may be printed or otherwise reproduced without his/her permission.**

**L'auteur conserve la propriété du droit d'auteur qui protège sa thèse. Ni la thèse ni des extraits substantiels de celle-ci ne doivent être imprimés ou autrement reproduits sans son autorisation.**

ISBN 0-315-93610-X

**Canada**



**UNIVERSITÉ D'OTTAWA**  
**UNIVERSITY OF OTTAWA**

# Abstract

A filtration theory for constant pressure filtration in viscoelastic media is presented. The theory is based on the linearized capillary hybrid model for flow in a porous medium. The main filtration equation is quite similar to that for non-Newtonian filtration except for the parameter  $v_{me}$  representing a sum of two terms: one term characterizing the viscous (Newtonian) nature of the flow, and the second term portraying the elastic contribution to the flow.

Constant pressure filtration experiments are performed using slurries of calcium carbonate in aqueous solutions of high molecular weight polyacrylamide (viscoelastic slurries) and slurries of calcium carbonate and water (Newtonian slurries). Three pressure drops are employed: 345 *kPa*, 517 *kPa*, and 689 *kPa*. The filtration theory provides a means to compile the experimental data, wherein filter cake and filter medium resistances are computed and compared.

It is found that the filter cake resistances of the viscoelastic filtrations were considerably lower than those of the Newtonian filtrations. Furthermore, the filter medium resistances of the viscoelastic filtrations were, in general, higher than those of the Newtonian filtrations.

# Aknowledgments

Special gratitude is reserved for Dr. William Kozicki who supervised this thesis with infinite patience and understanding. I am extremely grateful for his invaluable advice, guidance, and technical expertise.

Other scholars I wish to thank include Adolf Cheung and Dionissios Kiriakidis for their helpful suggestions in the computer programming.

I would also like to thank Mr. Adreano Bonaldo for constructing the experimental apparatus as weil as Mr. Guiseppe Gasperetti. I also offer gracious thankfulness to Louis Tremblay for his kindness in answering my many technical questions.

I wish to add a special recommendation to Dr. David Boll who inexhaustibly proofread this document and whose sympathetic interest inspired me.

Finally, I extend much appreciation and love to my mother and father, Madeleine and John Sleg, for their financial and moral support.

# Nomenclature

$a, b$	geometric coefficients which characterize the shape of the conduit cross-section
$A$	function defined by Equation (2.59), $kPa \cdot s^N \cdot m^{-1-N}$
$c$	concentration of polymer in the solution used to determine an intrinsic viscosity, $g/dL$
$e$	$= \frac{\epsilon}{1-\epsilon}$ , void ratio
$g$	gravitational acceleration, $9.80606 \text{ m/s}^2$ for the Ottawa region
$h$	elevation, $m$
$\vec{i}, \vec{j}, \vec{k}$	unit vectors
$J_{RN}$	quantity defined by Equation (2.45), $m^{1-N}$
$k$	$= \frac{\epsilon R_h^2}{k_i}$ , permeability of the porous medium, $m^2$
$k'$	extensional coefficient, defined in $\dot{\epsilon} = k' \frac{(\xi n + 1)}{(n + 1)} \frac{(\langle v \rangle - \bar{u}_w)}{2 D_p}$
$k'$	Huggins coefficient, as employed in Appendix E
$k_i$	$= 2(a + b)$ , Kozeny constant
$k_o$	shape factor of pores, determined by the cake model
$K$	fluid consistency index as defined by the power-law fluid model, equal to $\mu$ for a Newtonian fluid, $Pa \cdot s^n$
$\bar{K}$	value of $K$ determined by the Mean Value Theorem, $Pa \cdot s^N$

$K_N$	quantity defined in Equation (2.89), $m^{1+\frac{1}{N}} \cdot s^{-1}$
$m$	moisture ratio, mass ratio of wet to dry cake
$\overline{M}_n$	number average molecular weight
$\overline{M}_v$	viscosity average molecular weight
$\overline{M}_w$	weight average molecular weight
$\overline{M}_z$	z-average molecular weight
$\overline{M}_{z+1}$	z+1-average molecular weight
$n$	flow behavior index defined by Ostwald-de-Waele fluid model
$N$	value of $n$ determined by the Mean Value Theorem
$p$	pressure applied at the surface of the filter cake, $kPa$
$p_x$	pressure exerted at distance $x$ from the filter medium, $kPa$
$p_1$	pressure at the filter cake-filter medium interface, $kPa$
$p_0$	pressure at the filter medium-atmosphere interface, $kPa$
$\mathcal{P}$	$= p + \rho gh$ , potential function, $kPa$
$q$	superficial velocity of the fluid, $m/s$
$q_1$	superficial velocity at the cake-septum interface, $m/s$
$q_s$	superficial velocity at the particle surface, $m/s$
$r$	superficial velocity of solid particles in a compressible filter cake, $m/s$
$R_h$	hydraulic radius, $m$
$R_m$	filter medium resistance for a Newtonian filtration, given in Equations (2.50) and (2.60), $m^{-1}$
$R_{ma}$	apparent filter medium resistance, defined in Equation (2.94), $m^{-N}$
$s$	mass fraction of the solids in the slurry

$t$	filter medium thickness, $m$
$T$	tortuosity of channels in porous medium, determined by cake model
$\langle u \rangle$	void velocity of fluid at cake section, $m/s$
$u_p$	particle velocity due to cake compaction at cake section, $m/s$
$\bar{u}_w$	effective velocity of fluid at particle surface, $m/s$
$v$	volume of filtrate collected, $mL$
$v_i$	volume of filtrate collected during initial period of filtration, $mL$
$v_m$	quantity defined in Equation (2.60), $mL$
$v_{me}$	quantity defined in Equations (2.80) and (2.90), $mL$
$w$	total weight of filter cake per unit area, $kg/m^2$
$w_x$	weight of filter cake per unit area at distance $x$ from filter, $kg/m^2$
$x$	distance measured from filter medium, opposite to direction of the flow, $m$

### Greek Letters:

$\alpha$	local specific cake resistance, $m/kg$
$\alpha_R$	Ruth average cake resistance, $m/kg$
$\beta_n$	quantity defined by Equation (2.30), $m^{1-n}$
$\gamma_{av}$	$= \alpha_R J_{RN}$ , overall average cake resistance, $m^{2-N}/kg$
$\epsilon$	porosity
$\dot{\epsilon}$	shear rate
$\eta_D$	Darcy viscosity defined by Equation (2.3), $Pa \cdot s$ ; $\eta_D$ is a "macro" quantity since it is defined in terms of <i>overall</i> quantities such as the average velocity, the Kozeny constant (which is considered constant for the entire packed bed), the average shear stress, and the hydraulic radius; $\mu$ and $\eta$ are "micro" quantities since they define the viscosity at one shear plane.

$\eta$	non-Newtonian viscosity in terms of Generalized Newtonian Fluid representation of fluid model, $Pa \cdot s$
$\theta$	time to collect volume of filtrate $v$ , $s$
$\theta_0$	effective time of commencement of filtration, $s$
$\mu$	Newtonian viscosity, $Pa \cdot s$
$\mu_s$	viscosity of the solvent, $Pa \cdot s$
$\xi$	aspect factor, $\frac{b}{a}$
$\bar{\pi}$	$= p + \bar{\tau}_{11}$ , contour average total normal stress, $kPa$
$\bar{\pi}_x$	contour average total normal stress at distance $x$ from the filter medium, $kPa$
$\bar{\pi}_1$	contour average total normal stress at filter cake-medium interface, $kPa$
$\bar{\pi}_0$	contour average total normal stress at the filter medium-atmosphere interface, $kPa$
$\bar{\Pi}$	$= p + \bar{\tau}_{11} + \rho gh$ , contour average normal stress potential at the cake surface, $kPa$
$\bar{\Pi}_x$	contour average normal stress potential at distance $x$ from the filter medium, $kPa$
$\bar{\Pi}_1$	contour average normal stress potential at the filter cake-medium interface, $kPa$
$\bar{\Pi}_0$	contour average normal stress potential at the filter medium-atmosphere interface, $kPa$
$\rho$	filtrate density, $kg/m^3$
$\bar{\tau}_{11}, \bar{\tau}_{22}, \bar{\tau}_{33}$	normal stresses, $kPa$
$\bar{\tau}_w$	contour integrated average shear stress at wall of conduit $= \frac{1}{s} \oint \tau_w ds$ where $s$ is the perimeter of the conduit and $\tau_w$ is the shear stress at the infinitesimal distance $ds$ along the contour, $kPa$
$\bar{\Phi}$	mapping tensor

## Abbreviations

$\nabla$	del operator
<i>BK</i>	Blake-Kozeny cake model
<i>CAS</i>	Chemical Abstract Service
<i>HDC</i>	Hydrodynamic Chromatography
<i>KC</i>	Kozeny-Carman cake model
<i>LALLS</i>	Low-Angle Laser Light Scattering
<i>rpm</i>	revolutions per minute

# Contents

<b>Abstract</b>	<b>i</b>
<b>Acknowledgment</b>	<b>ii</b>
<b>Nomenclature</b>	<b>iii</b>
<b>Table of Contents</b>	<b>viii</b>
<b>List of Tables</b>	<b>xi</b>
<b>List of Figures</b>	<b>xii</b>
<b>1 Introduction</b>	<b>1</b>
1.1 Scope of Research . . . . .	2
1.2 Literature Survey . . . . .	3
<b>2 Theoretical Aspects</b>	<b>4</b>
2.1 Porous Media Flow . . . . .	4
2.2 Anisotropic Porous Media . . . . .	7
2.3 Filtration . . . . .	9
2.4 Solution for $N \approx 1$ . . . . .	19
<b>3 Methodology</b>	<b>21</b>
<b>4 Properties of Materials</b>	<b>26</b>
4.1 Polyacrylamide . . . . .	26
4.1.1 Types of Polyacrylamide Used . . . . .	28
4.2 Calcium Carbonate . . . . .	30

4.3	Distilled Water . . . . .	31
4.4	Filter Cloth . . . . .	31
4.5	Materials Used in the Construction of the Apparatus . . . . .	32
<b>5</b>	<b>Experimental Aspects</b>	<b>33</b>
5.1	Apparatus . . . . .	33
5.2	Stock Polymer Solution Preparation . . . . .	38
5.3	Procedure for a Filtration Run . . . . .	38
<b>6</b>	<b>Results and Discussion</b>	<b>42</b>
6.1	Results . . . . .	42
6.2	Interpretation of the Results . . . . .	49
6.2.1	Flocculation . . . . .	49
6.2.2	Compressive Pressure Reduction . . . . .	53
6.2.3	Viscoelasticity . . . . .	55
6.2.4	Polymer Degradation . . . . .	57
6.3	Critical Evaluation of the Results . . . . .	58
6.4	Addendum . . . . .	59
<b>7</b>	<b>Conclusions</b>	<b>60</b>
<b>8</b>	<b>Recommendations</b>	<b>61</b>
	<b>References</b>	<b>63</b>
	<b>Appendix A</b>	<b>67</b>
	Computer Programs . . . . .	67
	<b>Appendix B</b>	<b>80</b>
	Types of Average Molecular Weight . . . . .	80
	<b>Appendix C</b>	<b>82</b>
	Determination of the Viscosity-Average Molecular Weight of the Non-ionic and the Anionic Polyacrylamides . . . . .	82
	<b>Appendix D</b>	<b>90</b>
	Definitions of Configuration, Conformation, Composition, and Constitution . . . . .	90

<b>Appendix E</b>	<b>93</b>
Calibration Data for the Diaphragm Pressure Gauge . . . . .	93
<b>Appendix F</b>	<b>96</b>
Sample Calculation . . . . .	96
<b>Appendix G</b>	<b>98</b>
Estimation of the Volume in the Piping and the Cone above the Filter Cloth . .	98
<b>Appendix H</b>	<b>100</b>
Filtration Data . . . . .	100
<b>Appendix I</b>	<b>146</b>
Verification of Assumptions . . . . .	146

# List of Tables

3.1	List of Experiments . . . . .	22
6.1	Constant Pressure Filtration Characteristics for Various Filtration Pressures and Polymer Solutions. Slurry Concentration = $10\% \frac{w}{w}$ $\text{CaCO}_3$ . . . . .	50
6.2	Comparison of thesis work in Constant Pressure Filtration of Rao (1970) and Fu (1977) to work in this thesis. Symbolic notation is employed for quick comparison of trends. . . . .	59

# List of Figures

2.1	Convention for Specifying Subscripts Relative to the Direction of the Flow.	6
2.2	Schematic Representation of the Filter Cake (Shirato, 1985).	11
2.3	Application of the Mean Value Theorem to Evaluate $\int_0^{\pi-\pi_1} \frac{d\beta_2}{\alpha}$ .	13
2.4	Application of the Mean Value Theorem to $\int_0^1 w\beta_n K q_1^n \left( \frac{q_x}{q_1} - \frac{e r_x}{q_1} - \frac{q_{2x}}{q_1} \right)^n d\left(\frac{w_x}{w}\right)$ .	14
3.1	An example of a set of data which cannot be fitted by a single curve. The slurry was comprised of 10% $\frac{w}{w}$ CaCO <sub>3</sub> in aqueous anionic polyacrylamide (50 ppm) and filtered at 345 kPa.	24
5.1	Schematic Diagram of the Filtration Equipment.	34
5.2	Detailed View of the Filter Unit.	36
5.3	Schematic Diagram Depicting the Addition of the Polymer Crystals to a Beaker of Distilled Water.	39
6.1	Volume of Filtrate Collected versus Time for Constant Pressure Filtration at 345 kPa (50 psi) of Slurries Comprising 10% $\frac{w}{w}$ CaCO <sub>3</sub> in Aqueous Anionic Polyacrylamide Solutions.	43
6.2	Volume of Filtrate Collected versus Time for Constant Pressure Filtration at 345 kPa (50 psi) of Slurries Comprising 10% $\frac{w}{w}$ CaCO <sub>3</sub> in Aqueous Non-ionic Polyacrylamide Solutions.	44
6.3	Volume of Filtrate Collected versus Time for Constant Pressure Filtration at 517 kPa (75 psi) of Slurries Comprising 10% $\frac{w}{w}$ CaCO <sub>3</sub> in Aqueous Anionic Polyacrylamide Solutions.	45
6.4	Volume of Filtrate Collected versus Time for Constant Pressure Filtration at 517 kPa (75 psi) of Slurries Comprising 10% $\frac{w}{w}$ CaCO <sub>3</sub> in Aqueous Non-ionic Polyacrylamide Solutions.	46

6.5	Volume of Filtrate Collected versus Time for Constant Pressure Filtration at 689 <i>kPa</i> (100 psi) of Slurries Comprising 10% <sub>w</sub> CaCO <sub>3</sub> in Aqueous Anionic Polyacrylamide Solutions. . . . .	47
6.6	Volume of Filtrate Collected versus Time for Constant Pressure Filtration at 689 <i>kPa</i> (100 psi) of Slurries Comprising 10% <sub>w</sub> CaCO <sub>3</sub> in Aqueous Non-ionic Polyacrylamide Solutions. . . . .	48

# Chapter 1

## Introduction

Cake filtration is the unit operation in which a heterogeneous mixture of liquid and solid particles is separated by flow through a septum to yield a liquid relatively free of particles and a cake of solids deposited on the septum. In non-Newtonian filtration, the filtrate is a non-Newtonian fluid.

Cake filtration is prevalent in virtually every chemical manufacturing process. Cake filtration of non-Newtonian fluids is usually encountered where the processing of polymeric substances occurs, such as in the processing of petroleum, pharmaceuticals, biological and fermentation products, soaps and detergents, plastics, and synthetic fibres.

An understanding of non-Newtonian filtration may provide economic improvement to the processing of a diversity of products. Also, as research in filtration includes consideration of porous media flow, the information gained in filtration studies may also serve to provide insight into the flow through porous media. Ultimately, there is a desire to predict the bulk flow phenomena of polymeric liquids from molecular properties, and to describe the stretching and orientation of the polymer molecules in arbitrary flow fields (Bird, et al., 1977b). Polymers could then be designed to have desired specific flow properties. The prediction or control of the microstructure of fabricated plastic products, the improvement of tertiary oil recovery, and enhancement of industrial filtration operations are examples of benefits from such advances in flow technology.

In cake filtration, the filtrate is often the desirable product; however, there are cases in which the cake is the valuable article.

Investigation of a special class of polymers, known as the viscoelastic polymers, has been greatly stimulated because of their unique mechanical behavior. Pye (1964) first described

a viscoelastic effect. He passed a 2% NaCl solution through a core from an oil reservoir and found the flowrate at the exit of the core to be approximately 10 mL/minute. He then passed through the same core a 500 ppm polyacrylamide solution in a 2% NaCl solution and observed a greatly reduced flowrate of about 1 mL/minute at the same pressure drop.

A viscoelastic material deforms when subjected to stress (e.g., by striking it, by causing it to flow, etc.). When the stress is removed, some of the deformation is recovered by recoil (Ferry, 1970). Viscoelastic effects occur in the presence of a polymer. Not all polymeric fluids are viscoelastic; those that do exhibit viscoelasticity include polymers of high molecular weight (i.e., greater than  $10^6$ ), either in solution or as polymer melts.

Viscoelastic effects are manifested in a variety of flow situations. In turbulent flow, the addition of a small amount of a high molecular weight polymer additive to a Newtonian fluid produces drag reduction, a phenomenon where a substantial reduction in pressure drop results at a given flowrate (Bird, et al., 1977a). In laminar flow the presence of small amount of the polymer causes a dramatic dilatant effect (Odell, et al., 1988) as the fluid flows through constricted geometries. Examples of constricted geometries are packed beds, porous media, capillary tubes, sudden contractions, orifices, and filters. Although viscoelastic fluids have been studied extensively, there appears to be no previous investigations of filtration in viscoelastic media. The aim of this thesis is to report the results of a preliminary study of constant pressure filtration of calcium carbonate suspensions in dilute aqueous polyacrylamide solutions.

## 1.1 Scope of Research

This research endeavours to experimentally test a new theoretical analysis for filtration in non-Newtonian media. The non-Newtonian media consisted of aqueous slurries containing calcium carbonate and small amounts of a viscoelastic polymer (high molecular weight polyacrylamide). During this present course of inquiry, experimental equipment was conceptualized and assembled. Filtration experiments were conducted maintaining a constant pressure drop across the filter cake. A FORTRAN computer program was utilized to estimate the unknown parameters. Careful scrutiny of the results was necessary in order to recognize how viscoelastic effects reveal themselves in cake filtration. An interpretation of the data collected for the systems investigated is presented.

## 1.2 Literature Survey

The complicating factor which impeded progress in filtration theory rests in the fact that filtration is a *moving boundary problem*. That is, the cake thickness is constantly changing throughout the experiment. Complicated integrals arise with even the simplest of models. Kozicki utilized the Mean Value Theorem and made logical assumptions to circumvent the mathematical obstacles (Kozicki, et al., 1972). Experimental data obtained by Shirato (Shirato, et al., 1977) validated the assumptions made by Kozicki and his associates. The existing filtration theory does not provide exact solutions to the complicating integrals which arise in filtration, although Shirato and co-workers have carried out evaluations for non-Newtonian filtration involving purely-viscous fluids based on compression-permeability cell measurements, and they found the theory to describe well the experimental findings. Filtration resistances provided a means for comparison for different filtration runs.

The filtration theory for time-independent fluids has been extended by Dr. W. Kozicki (Kozicki, 1990b) to include the viscoelastic effects of time-dependent fluids. The basis of this theory is the *linearized capillary hybrid model* of viscoelastic flow in packed beds or porous media. The final equation closely resembles that of the filtration of time-independent fluids. The principal difference is that one of the parameters,  $v_{me}$ , is the sum of two terms, one term characterizing the purely-viscous nature of the flow and the other term characterizing the elastic nature contribution to the flow. The development of this new theory is presented in the Theory section of this dissertation.

The literature consulted as an aid for the design of the equipment of this thesis project were the Ph.D. thesis of A.R.K. Rao (Rao, 1970) and the Master's thesis of C.T. Fu (Fu, 1977). The same filtration principle was employed with the distinguishing features of upward flow of the slurry as it approaches the septum, a transparent section to observe the cake build up, and a calming section to enhance the attainment of fully-developed flow of the slurry before being filtered. Marshall and Metzner (1967) and Shirato et al. (1977) used a cushion of compressed gas to force the fluid through their experimental apparatus. This idea is borrowed to drive the slurry to the filter unit. This method of propulsion reduces the possibility of mechanical and thermal perturbation of the slurry as might occur in the presence of a rotary gear pump.

## Chapter 2

# Theoretical Aspects

In this chapter, the derivation of the cake filtration equations is presented. The analysis considers the filtration to be of two stages: an initial stage and a main stage. The equations take into account the velocity of the particles in a compressible cake, surface effects (adsorption of the polymer on the particles, or the formation of a thin layer of pure solvent at the particle surface), and the fact that a filter cake is anisotropic. These equations may be interpreted in terms of any arbitrary fluid model and in terms of any porous bed model.

Since filtration is an operation involving the flow of a fluid through a porous structure (ie, through the filter cake and septum), filtration theory relies on porous media concepts.

### 2.1 Porous Media Flow

The fundamental equation describing viscoelastic flow in packed beds or porous media is the equation based on the *linearized capillary hybrid model* of flow in a porous medium. This equation, in its most general format,

$$\frac{\langle u \rangle - \bar{u}_w}{R_h} = \frac{(1 + \xi)T}{k_i} \left( \frac{\bar{\tau}_w}{T} \right)^{-\xi} \int_0^{\bar{\tau}_w^*} \tau^{\xi-1} f(\tau) d\tau \quad (2.1)$$

may be expounded by substituting in it the appropriate fluid and porous medium models.  $T$  and  $k_i$  are the tortuosity and Kozeny constants with values determined by the physical model assumed for the bed (Kozicki and Tiu, 1988);

Blake Model:	$T = 1$	$k_i = 5.0$
Blake-Kozeny Model:	$T = T_{BK} = 25/12$	$k_i = T_{BK} k_0 = 25/6$
Kozeny-Carman Model:	$T = T_{KC} = \sqrt{2}$	$k_i = T_{KC}^2 k_0 = 5.0$

Equation (2.1) may also be written

$$\frac{\langle u \rangle - \bar{u}_w}{R_h} = \frac{\bar{\tau}_w}{k_i \eta_D} \quad (2.2)$$

where

$$\eta_D = \frac{\left(\frac{\bar{\tau}_w}{T}\right)^{1+\xi}}{(1+\xi) \int_0^{\frac{\bar{\tau}_w}{T}} \tau^{\xi-1} f(\tau) d\tau} \quad (2.3)$$

which provides the definition of the Darcy viscosity for non-Newtonian flow in porous media. For purely viscous flow,

$$\bar{\tau}_w = R_h \left( \frac{-d\mathcal{P}}{dz} \right) \quad (2.4)$$

where

$$\mathcal{P} = p + \rho gh, \quad (2.5)$$

which is known as the potential function. For viscoelastic flow

$$\bar{\tau}_w = R_h \left( \frac{-d\bar{\Pi}_{11}}{dz} \right) \quad (2.6)$$

where  $\bar{\Pi}_{11}$  is the contour average normal stress potential at some section in the porous bed.  $\bar{\Pi}_{11}$  corresponds to the potential function when normal stresses are present,

$$\bar{\Pi}_{11} = p + \bar{\tau}_{11} + \rho gh \quad (2.7)$$

Setting  $\bar{\pi}_{11} = p + \bar{\tau}_{11}$ , then

$$\bar{\Pi}_{11} = \bar{\pi}_{11} + \rho gh \quad (2.8)$$

The subscript on  $\bar{\Pi}_{11}$  and on  $\bar{\pi}_{11}$  are defined with reference to the direction of flow (See Figure 2.1). These subscripts are omitted for the remainder of the theory presentation. Substituting Equation (2.8) into Equation (2.2) gives

$$\langle u \rangle - \bar{u}_w = \frac{R_h^2}{k_i \eta_D} \left( \frac{-d\bar{\Pi}}{dz} \right) \quad (2.9)$$

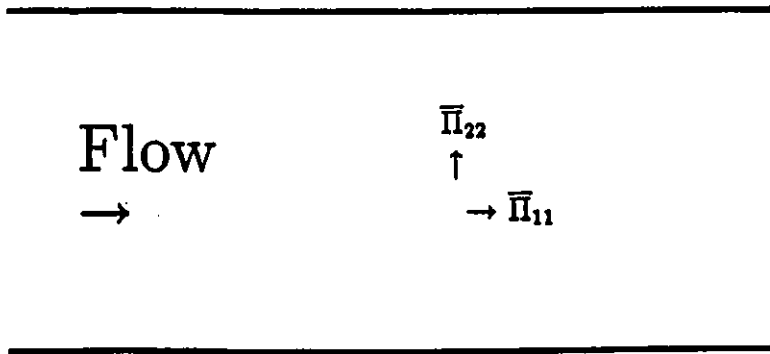


**Figure 2.1: Convention for Specifying Subscripts Relative to the Direction of the Flow.**

Equation (2.9) assumes that the particles comprising the porous bed are not moving. Since in a compressible cake the particles are moving, the velocity of the particles in the cake  $u_p$  may be accounted for as follows

$$\langle u \rangle - u_p - \bar{u}_w = \frac{R_h^2}{k_i \eta_D} \left( \frac{-d\bar{\Pi}}{dz} \right) \quad (2.10)$$

Introducing the Dupuit relations,  $\langle u \rangle = \frac{q}{\epsilon}$ ;  $u_p = \frac{r}{1-\epsilon}$ ;  $\bar{u}_w = \frac{q_s}{\epsilon}$ , and expressing Equation (2.10) in terms of superficial velocities yields

$$\frac{q}{\epsilon} - \frac{r}{1-\epsilon} - \frac{q_s}{\epsilon} = \frac{R_h^2}{k_i \eta_D} \left( \frac{-d\bar{\Pi}}{dz} \right) \quad (2.11)$$

Multiplying through by  $\epsilon$ ,

$$q - \frac{\epsilon}{1-\epsilon} r - q_s = \frac{\epsilon R_h^2}{k_i \eta_D} \left( \frac{-d\bar{\Pi}}{dz} \right) \quad (2.12)$$

Introducing the void ratio  $e = \frac{\epsilon}{1-\epsilon}$ , this equation becomes

$$q - er - q_s = \frac{\epsilon R_h^2}{k_i \eta_D} \left( \frac{-d\bar{\Pi}}{dz} \right) \quad (2.13)$$

For an isotropic porous medium,  $k_i$ ,  $\epsilon$ ,  $\eta_D$ , and  $R_h$  do not vary with a change in direction, and Equation (2.11) may be written as

$$\bar{q} - e\bar{r} - \bar{q}_s = -\frac{\epsilon R_h^2}{k_i \eta_D} \nabla \bar{\Pi} \quad (2.14)$$

In terms of the permeability  $k = \frac{\epsilon R_h^2}{k_i}$  of the porous medium, Equation (2.14) for viscoelastic flow in an isotropic porous medium becomes

$$\bar{q} - e\bar{r} - \bar{q}_s = \frac{-k}{\eta_D} \nabla \bar{\Pi} \quad (2.15)$$

## 2.2 Anisotropic Porous Media

In filtration the filter cakes are anisotropic; that is, the permeability  $k$  and Darcy viscosity  $\eta_D$  generally vary in the  $x$ ,  $y$ , and  $z$  directions. Therefore,  $k$  and  $\eta_D$  are tensors of rank 2 and may be represented as follows:

$$\begin{aligned} \bar{k} = & k_{xx}\bar{i}\bar{i} + k_{xy}\bar{i}\bar{j} + k_{xz}\bar{i}\bar{k} \\ & + k_{yz}\bar{j}\bar{i} + k_{yy}\bar{j}\bar{j} + k_{yz}\bar{j}\bar{k} \end{aligned}$$

$$+ k_{zx}\bar{k}\bar{i} + k_{zy}\bar{k}\bar{j} + k_{zz}\bar{k}\bar{k} \quad (2.16)$$

$$\begin{aligned} \bar{\eta}_D = & \eta_{Dxx}\bar{i}\bar{i} + \eta_{Dxy}\bar{i}\bar{j} + \eta_{Dxz}\bar{i}\bar{k} \\ & + \eta_{Dyx}\bar{j}\bar{i} + \eta_{Dyy}\bar{j}\bar{j} + \eta_{Dyz}\bar{j}\bar{k} \\ & + \eta_{Dzx}\bar{k}\bar{i} + \eta_{Dzy}\bar{k}\bar{j} + \eta_{Dzz}\bar{k}\bar{k} \end{aligned} \quad (2.17)$$

The concepts presented in the remainder of this section closely resemble those reported in Kozicki, et al. (1972).

The form of Equation (2.15) which applies to an anisotropic porous medium is

$$\bar{\eta}_D \cdot (\bar{q} - e\bar{r} - \bar{q}_s) = -\bar{k} \cdot \nabla \bar{\Pi} \quad (2.18)$$

The above formulation is based on the assumption that a tensor  $\bar{\Phi}$  can be determined which maps the vector on the left side into the vector on the right side as follows:

$$\nabla \bar{\Pi} = -\bar{\Phi} \cdot (\bar{q} - e\bar{r} - \bar{q}_s) \quad (2.19)$$

The apparent viscosity tensor of the fluid is thus derivable from a knowledge of the permeability tensor  $\bar{k}$  for the anisotropic medium and the mapping tensor  $\bar{\Phi}$  in accordance with the relationship

$$\bar{\eta}_D = \bar{k} \cdot \bar{\Phi} \quad (2.20)$$

By reference to the manner of formation of a filter cake, by deposition and compaction of the particles in conjunction with a compressive force, it can be conceived that the permeability tensor for a filter cake is a symmetric tensor; that is,  $k_{xy} = k_{yx} = 0$ ,  $k_{xz} = k_{zx} = 0$ ,  $k_{yz} = k_{zy} = 0$ .

If a rotation of the coordinate axes is considered, the manner in which the  $\bar{k}$  matrix transforms under such a rotation can be investigated. Such an investigation shows that if the  $\bar{k}$  matrix is symmetric, then rotation of the axes to a particular orientation produces a diagonal  $\bar{k}$  matrix.

In view of Equation (2.20), it is apparent that  $\bar{\eta}_D$  is also representable by a diagonal matrix with the same set of principal axes as the permeability matrix  $\bar{k}$ .

Hence, Equation (2.18) may be simplified to

$$\begin{pmatrix} \eta_{Dxx} & 0 & 0 \\ 0 & \eta_{Dyy} & 0 \\ 0 & 0 & \eta_{Dzz} \end{pmatrix} \begin{pmatrix} q_x - er_x - q_{sx} \\ q_y - er_y - q_{sy} \\ q_z - er_z - q_{sz} \end{pmatrix} = - \begin{pmatrix} k_{xx} & 0 & 0 \\ 0 & k_{yy} & 0 \\ 0 & 0 & k_{zz} \end{pmatrix} \begin{pmatrix} \frac{\partial \bar{\Pi}_x}{\partial x} \\ \frac{\partial \bar{\Pi}_y}{\partial y} \\ \frac{\partial \bar{\Pi}_z}{\partial z} \end{pmatrix} \quad (2.21)$$

The principal axes of the porous medium are thus defined in the direction of  $k_{xx}$ ,  $k_{yy}$ , and  $k_{zz}$ . Write  $k_x$  instead of  $k_{xx}$ ,  $k_y$  instead of  $k_{yy}$ , etc. for simplicity. Carrying out the indicated matrix multiplication,

$$q_x - e\tau_x - q_{sx} = \frac{k_x}{\eta_{Dx}} \left( -\frac{\partial \bar{\Pi}_x}{\partial x} \right) \quad (2.22)$$

$$q_y - e\tau_y - q_{sy} = \frac{k_y}{\eta_{Dy}} \left( -\frac{\partial \bar{\Pi}_y}{\partial y} \right) \quad (2.23)$$

$$q_z - e\tau_z - q_{sz} = \frac{k_z}{\eta_{Dz}} \left( -\frac{\partial \bar{\Pi}_z}{\partial z} \right) \quad (2.24)$$

Therefore, assuming diagonal tensors, one obtains three equations which are similar to the equation for the isotropic porous medium, Equation (2.15). The difference is that the above equations take into account that the permeability varies in the  $x$ ,  $y$ , and  $z$  directions. In filtration, the permeability in the plane perpendicular to the flow direction  $x$  through the cake will be constant for any orientation in the plane and  $k_y = k_z$ .

### 2.3 Filtration

For uni-dimensional filtration in the direction determined by the  $x$ -coordinate, the above equations reduce to the single equation:

$$q_x - e\tau_x - q_{sx} = \frac{k_x}{\eta_{Dx}} \left( -\frac{\partial \bar{\Pi}_x}{\partial x} \right) \quad (2.25)$$

In the following, the viscous response of the fluid will be represented by the power-law relation,

$$f(\tau) = \left( \frac{\tau}{K} \right)^{\frac{1}{n}} \quad (2.26)$$

in which  $n$  and  $K$  are assumed to vary throughout the cake. Evaluation of Equation (2.3) in terms of the power-law relation gives

$$\eta_D = \frac{(n\xi + 1)(KT)^{\frac{1}{n}}}{n(1 + \xi)} (\bar{\tau}_w)^{1 - \frac{1}{n}}. \quad (2.27)$$

in which  $n$  and  $K$  denote the fluid parameters corresponding to  $\bar{\tau}_w$ . Substituting  $\bar{\tau}_w = R_h \left( -\frac{\partial \bar{\Pi}_x}{\partial x} \right)$ , for flow in the  $x$ -direction,

$$\eta_{Dx} = \frac{(n\xi + 1)(KT)^{\frac{1}{n}}}{n(1 + \xi)} \left( R_h \left( -\frac{\partial \bar{\Pi}_x}{\partial x} \right) \right)^{1 - \frac{1}{n}} \quad (2.28)$$

which when substituted into Equation (2.25) produces

$$\begin{aligned}
q_x - er_x - q_{sx} &= \frac{kT}{(KT)^{\frac{1}{n}} (n\xi + 1)} (R_h)^{\frac{1}{n}-1} \left( \frac{-\partial \bar{\Pi}_x}{\partial x} \right)^{\frac{1}{n}} \\
(q_x - er_x - q_{sx})^n &= \frac{(kT)^n}{KT} \left( \frac{n(1 + \xi)}{(n\xi + 1)} \right)^n R_h^{1-n} \left( \frac{-\partial \bar{\Pi}_x}{\partial x} \right)^n \\
(q_x - er_x - q_{sx})^n &= \frac{k}{K} \left( \frac{Tk}{R_h} \right)^{n-1} \left( \frac{n(1 + \xi)}{(n\xi + 1)} \right)^n \left( \frac{-\partial \bar{\Pi}_x}{\partial x} \right)^n \\
(q_x - er_x - q_{sx})^n &= \frac{k}{K\beta_n} \left( \frac{-\partial \bar{\Pi}_x}{\partial x} \right)^n \tag{2.29}
\end{aligned}$$

where

$$\frac{1}{\beta_n} = \left( \frac{Tk}{R_h} \right)^{n-1} \left( \frac{n(1 + \xi)}{n\xi + 1} \right)^n \tag{2.30}$$

In filtration, the contribution of the gravity force is negligible in comparison to the pressure and normal forces, and the following simplification applies,

$$\bar{\Pi}_x = \bar{\pi}_x \tag{2.31}$$

The convention of measuring a distance  $x$  opposite to the direction of the flow (Shirato, 1985) is now considered, as in Figure 2.2. This convention dictates that the negative sign in Equation (2.29) must be changed to a positive sign.

Equation (2.29) may therefore be rewritten

$$(q_x - er_x - q_{sx})^n = \frac{k}{K\beta_n} \left( \frac{\partial \bar{\pi}_x}{\partial x} \right)^n \tag{2.32}$$

The partial derivative may be replaced by an ordinary derivative since  $\bar{\pi}_x$  is dependent only on  $x$  to give

$$(q_x - er_x - q_{sx})^n = \frac{k}{K\beta_n} \left( \frac{d\bar{\pi}_x}{dx} \right)^n \tag{2.33}$$

The solids compressive pressure is defined by

$$p_s = \bar{\pi} - \bar{\pi}_x \quad \text{and} \quad dp_s = -d\bar{\pi}_x \tag{2.34}$$

where  $\bar{\pi}$  is the total normal stress at the surface of the filter cake, and  $\bar{\pi}_x$  is the total normal stress at a distance  $x$  from the filter medium. The mass of solids in the thickness  $dx$  of filter cake is given by

$$dw_x = \rho_s(1 - \epsilon) dx \tag{2.35}$$

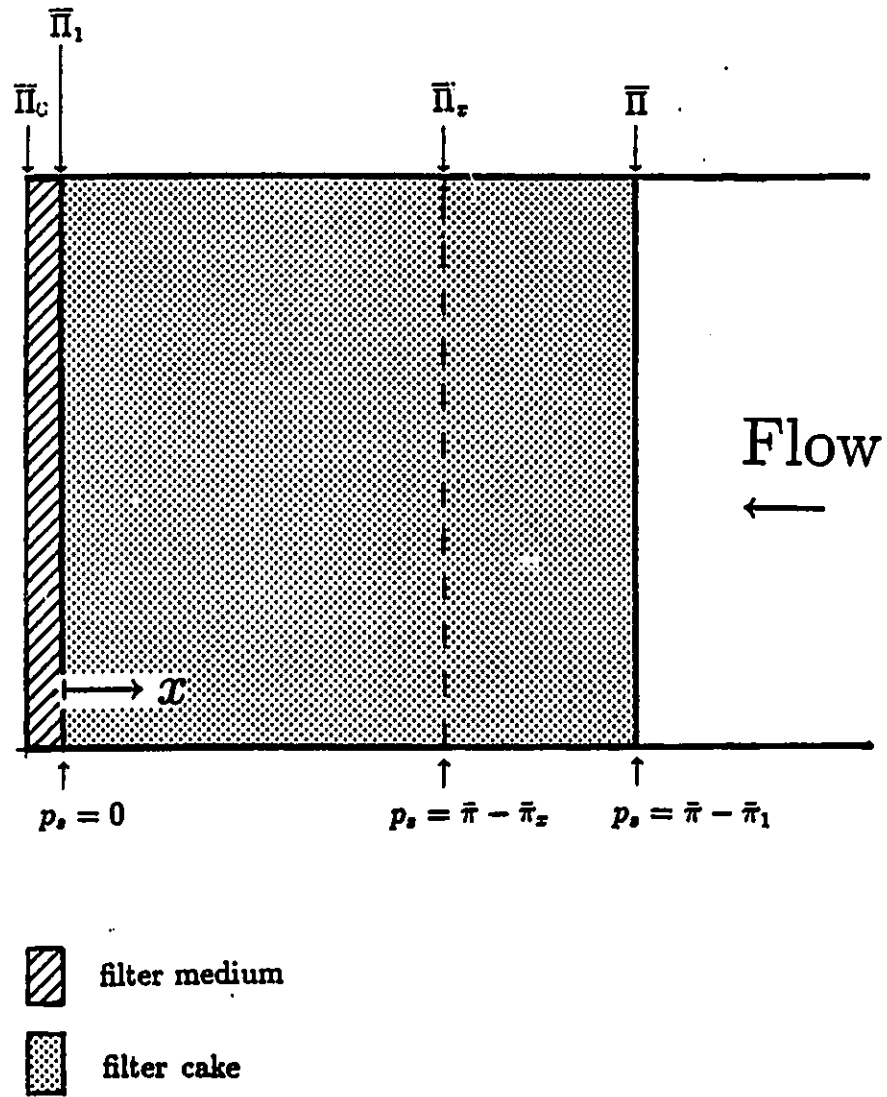


Figure 2.2: Schematic Representation of the Filter Cake

which gives

$$dx = \frac{dw_x}{\rho_s(1-\epsilon)} \quad (2.36)$$

Equation (2.33) therefore becomes

$$(q_x - er_x - q_{sx})^n = \frac{-\rho_s(1-\epsilon)k}{K\beta_n} \left( \frac{dp_s}{dw_x} \right) \quad (2.37)$$

Introduction of the local specific cake resistance  $\alpha = \frac{1}{\rho_s(1-\epsilon)k}$  yields

$$(q_x - er_x - q_{sx})^n = \frac{1}{K\alpha\beta_n} \left( -\frac{dp_s}{dw_x} \right) \quad (2.38)$$

Rearrangement results in

$$\begin{aligned} -\frac{dp_s}{dw_x} &= \alpha\beta_n K (q_x - er_x - q_{sx})^n \quad (2.39) \\ -\frac{dp_s}{\alpha} &= w\beta_n K (q_x - er_x - q_{sx})^n d\left(\frac{w_x}{w}\right) \end{aligned}$$

Integrating and applying the limits:

$$\text{At } \frac{w_x}{w} = 0, \quad p_s = \bar{\pi} - \bar{\pi}_1 \quad (2.40)$$

$$\text{At } \frac{w_x}{w} = 1, \quad p_s = 0 \quad (2.41)$$

where  $\bar{\pi}_1$  is the total normal stress present at the filter cake-septum interface, produces

$$\begin{aligned} \int_0^{\bar{\pi}-\bar{\pi}_1} \frac{dp_s}{\alpha} &= \int_0^1 w\beta_n K (q_x - er_x - q_{sx})^n d\left(\frac{w_x}{w}\right) \\ \int_0^{\bar{\pi}-\bar{\pi}_1} \frac{dp_s}{\alpha} &= \int_0^1 w\beta_n K q_1^n \left( \frac{q_x}{q_1} - \frac{er_x}{q_1} - \frac{q_{sx}}{q_1} \right)^n d\left(\frac{w_x}{w}\right) \end{aligned} \quad (2.42)$$

The left side of this equation  $\int_0^{\bar{\pi}-\bar{\pi}_1} \frac{dp_s}{\alpha}$  represents the area under the curve in Figure 2.3. According to the Mean Value Theorem, there exists a value of  $\frac{1}{\alpha}$ , say  $\frac{1}{\alpha_R}$ , where the area under the curve between  $p_s = 0$  and  $p_s = \bar{\pi} - \bar{\pi}_1$  is equal to a rectangular area. The area of the rectangle is  $\frac{\bar{\pi}-\bar{\pi}_1}{\alpha_R}$ . Therefore,  $\int_0^{\bar{\pi}-\bar{\pi}_1} \frac{dp_s}{\alpha} = \frac{\bar{\pi}-\bar{\pi}_1}{\alpha_R}$ .

This theorem may also be applied to the right side of Equation (2.42), as shown in Figure 2.4, to yield

$$\frac{\bar{\pi} - \bar{\pi}_1}{\alpha_R} = w\bar{K}q_1^N \int_0^1 \frac{\beta_n K q_1^n}{\bar{K}q_1^N} \left( \frac{q_x}{q_1} - \frac{er_x}{q_1} - \frac{q_{sx}}{q_1} \right)^n d\left(\frac{w_x}{w}\right) \quad (2.43)$$

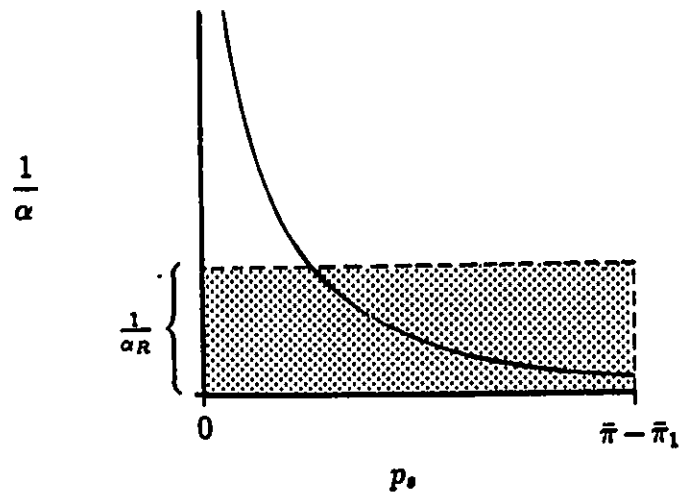


Figure 2.3: Application of the Mean Value Theorem to Evaluate  $\int_0^{\bar{\pi} - \bar{\pi}_1} \frac{dp_1}{\alpha}$ .

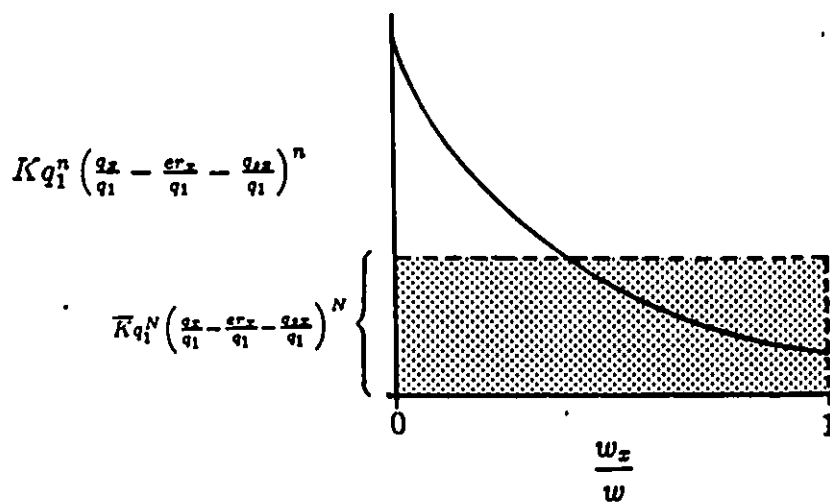


Figure 2.4: Application of the Mean Value Theorem to

Evaluate  $\int_0^1 w \beta_n K q_1^n \left( \frac{q_x}{q_1} - \frac{e r_x}{q_1} - \frac{q_{s_x}}{q_1} \right)^n d \left( \frac{w_x}{w} \right)$

where  $\bar{K}$  and  $N$  denote characteristic values of  $K$  and  $n$  yielded by application of the Mean Value Theorem.

Assuming the integrand

$$\frac{\beta_n K q_1^n}{\bar{K} q_1^N} \left( \frac{q_x}{q_1} - \frac{e r_x}{q_1} - \frac{q_{sx}}{q_1} \right)^n \quad (2.44)$$

satisfies the similarity criterion<sup>1</sup> for different cake thickness, the integral is constant in a filtration at constant normal stress difference and may be represented by  $J_{RN}$ .

$$J_{RN} = \int_0^1 \beta_n \frac{K q_1^n}{\bar{K} q_1^N} \left( \frac{q_x}{q_1} - \frac{e r_x}{q_1} - \frac{q_{sx}}{q_1} \right)^n d \left( \frac{w_x}{w} \right) \quad (2.45)$$

$J_{RN}$  is the correction term accounting for the particle movement due to cake compaction and the effects of surface phenomena, including polymer adsorption or slip, within the pores of the cake. Equation (2.42) may be rewritten

$$\frac{\bar{\pi} - \bar{\pi}_1}{\alpha_R} = W \bar{K} q_1^N J_{RN} \quad (2.46)$$

and rearranged as follows:

$$q_1^N = \frac{\bar{\pi} - \bar{\pi}_1}{\bar{K} W \alpha_R J_{RN}} = \frac{\bar{\pi} - \bar{\pi}_1}{\bar{K} W \gamma_{av}} \quad (2.47)$$

or

$$\bar{\pi} - \bar{\pi}_1 = \bar{K} W \gamma_{av} q_1^N \quad (2.48)$$

where  $\gamma_{av} = \alpha_R J_{RN}$  is the overall average cake resistance.

Apply Equation (2.39) across the filter medium. The particles comprising the filter medium are stationary; thus,  $r_x = 0$ .

$$-\frac{dp_s}{dt} = \beta_n R K (q_x - q_{sx})^n \quad (2.49)$$

where  $R$  = filter medium resistance, and  $t$  = filter medium thickness.

$$\int_0^1 \frac{dp_s}{\beta_n R} = - \int_t^0 K (q_x - q_{sx})^n dt = \int_0^t K (q_x - q_{sx})^n dt$$

---

<sup>1</sup>The *similarity criterion* says that whether the filter cake is thick or thin,  $J_{RN}$  is a unique function of  $\frac{w_x}{w}$  beyond the initial stage in constant total normal stress filtration. This uniqueness was established for filtration in Newtonian media by Tiller and Shirato (1964) and Shirato et al., (1967,1969) and corroborated for power-law fluids by Shirato and co-workers (1974, 1977).

$$\bar{\pi}_1 - \bar{\pi}_0 = \underbrace{\bar{K} \beta_n R t \left( \frac{q}{q_1} - \frac{q_s}{q_1} \right)^N}_{R_m} q_1^N \quad (2.50)$$

$$\bar{\pi}_1 - \bar{\pi}_0 = R_m \bar{K} q_1^N$$

$$\bar{\pi}_1 = \bar{\pi}_0 + R_m \bar{K} q_1^N \quad (2.51)$$

Substitution of Equation (2.51) in Equation (2.48),

$$\bar{\pi} - \bar{\pi}_0 - \bar{K} R_m q_1^N = \bar{K} W \gamma_{av} q_1^N \quad (2.52)$$

and rearrangement results in

$$q_1^N = \frac{\bar{\pi} - \bar{\pi}_0}{\bar{K}(W \gamma_{av} + R_m)} \quad (2.53)$$

Setting  $w = \frac{spv}{(1-ms)}$  and  $q_1 = \frac{dv}{d\theta}$  in Equation (2.53),

$$\left( \frac{dv}{d\theta} \right)^N = \frac{\bar{\pi} - \bar{\pi}_0}{\bar{K} \left( \frac{spv}{(1-ms)} \gamma_{av} + R_m \right)} \quad (2.54)$$

$$\left( \frac{d\theta}{dv} \right)^N = \frac{\bar{K}}{\bar{\pi} - \bar{\pi}_0} \left( \frac{spv}{(1-ms)} \gamma_{av} + R_m \right) \quad (2.55)$$

$$= \frac{\bar{K} \rho s \gamma_{av}}{(\bar{\pi} - \bar{\pi}_0)(1-ms)} \left( v + \frac{R_m(1-ms)}{\rho s \gamma_{av}} \right) \quad (2.56)$$

$$= \frac{A}{\Delta \bar{\pi}} (v + v_m) \quad (2.57)$$

$$\Delta \bar{\pi} = \frac{A}{\left( \frac{d\theta}{dv} \right)^N} (v + v_m) \quad (2.58)$$

$$\text{where } A = \frac{\bar{K} \gamma_{av} \rho s}{(1-ms)} \quad (2.59)$$

$$\text{and } v_m = \frac{R_m(1-ms)}{\gamma_{av} \rho s} \quad (2.60)$$

In the linearized capillary hybrid model of the flow in a filter cake, it is possible to write the following:

$$\begin{aligned} \bar{r}_{11} - \bar{r}_{22} &= -k' \bar{\eta} \frac{\xi n + 1}{n + 1} \frac{(\langle u \rangle - \bar{u}_w)}{2D_p} \\ &= -k' \bar{\eta} \frac{\xi n + 1}{n + 1} \frac{q}{2\epsilon D_p} \end{aligned} \quad (2.61)$$

Thus,

$$\begin{aligned}\Delta(\bar{\tau}_{11} - \bar{\tau}_{22}) &= \frac{-k'\Delta\bar{\eta}(\xi n + 1)q}{2\epsilon D_p(n+1)q_1} q_1 \\ &= -E q_1\end{aligned}\quad (2.62)$$

where

$$E = \frac{-k'\Delta\bar{\eta}(\xi n + 1)q}{2\epsilon D_p(n+1)q_1} \quad (2.63)$$

Recall that

$$\bar{\Pi} = \bar{p} + \bar{\tau}_{11} + \rho g h \quad (2.64)$$

$$= \bar{p} + \bar{\tau}_{22} + \rho g h + \bar{\tau}_{11} - \bar{\tau}_{22} \quad (2.65)$$

$$= \bar{\pi}_{22} + \rho g h + (\bar{\tau}_{11} - \bar{\tau}_{22}) \quad (2.66)$$

Similarly,

$$\bar{\Pi}_0 = \bar{\pi}_{22,0} + \rho g h_0 + (\bar{\tau}_{11} - \bar{\tau}_{22})_0 \quad (2.67)$$

Therefore,

$$\bar{\Pi} - \bar{\Pi}_0 = \bar{\pi}_{22} - \bar{\pi}_{22,0} + \rho g(h - h_0) + (\bar{\tau}_{11} - \bar{\tau}_{22}) - (\bar{\tau}_{11} - \bar{\tau}_{22})_0 \quad (2.68)$$

or,

$$\Delta\bar{\Pi} = \Delta\bar{\pi}_{22} + \rho g \Delta h + \Delta(\bar{\tau}_{11} - \bar{\tau}_{22}) \quad (2.69)$$

Neglecting gravitational effects,

$$\Delta\bar{\Pi} = \Delta\bar{\pi}_{22} + \Delta(\bar{\tau}_{11} - \bar{\tau}_{22}) = \Delta\bar{\pi} \quad (2.70)$$

The differential secondary total normal stress is the reading obtained in a differential pressure sensing device; hence  $\Delta\bar{\pi}_{22}$  is designated the filtration pressure. The preceding equation may be rewritten in terms of  $p$ .

$$\Delta\bar{\pi} = p + \Delta(\bar{\tau}_{11} - \bar{\tau}_{22}) \quad (2.71)$$

Substituting this equation and Equation (2.62) into Equation (2.58), one obtains

$$\frac{A}{\left(\frac{d\theta}{dv}\right)^N} (v + v_m) = p - E \left(\frac{dv}{d\theta}\right). \quad (2.72)$$

Rearranging,

$$A(v + v_m) = p \left(\frac{d\theta}{dv}\right)^N - E \left(\frac{dv}{d\theta}\right)^{N-1} \quad (2.73)$$

Assuming  $N \approx 1$ ,

$$p \left( \frac{d\theta}{dv} \right)^N - E = A(v + v_m) \quad (2.74)$$

$$p \left( \frac{d\theta}{dv} \right)^N = A(v + v_m) + E \quad (2.75)$$

$$p \left( \frac{d\theta}{dv} \right)^N = A \left( v + v_m + \frac{E}{A} \right) \quad (2.76)$$

Or,

$$\left( \frac{d\theta}{dv} \right)^N = \frac{A}{p} (v + v_{me}) \quad (2.77)$$

where

$$v_{me} = v_m + \frac{E}{A} \quad (2.78)$$

$$= \frac{R_m(1 - ms)}{\gamma_{av}\rho s} + \frac{k'\Delta\bar{\eta}}{2\epsilon D_p} \left( \frac{\xi n + 1}{n + 1} \right) \left( \frac{q}{q_1} \right) \frac{(1 - ms)}{\bar{K}\gamma_{av}\rho s} \quad (2.79)$$

$$= \frac{1 - ms}{\gamma_{av}\rho s} \left[ R_m + \frac{k'\Delta\bar{\eta}}{2\epsilon D_p \bar{K}} \left( \frac{\xi n + 1}{n + 1} \right) \left( \frac{q}{q_1} \right) \right] \quad (2.80)$$

It is noted that for filtration in purely viscous media  $v_{me} = v_m$ . The analysis therefore predicts an effective medium resistance in viscoelastic filtration which is greater than the actual medium resistance.

Expanding  $\frac{A}{p}$ , one obtains

$$\frac{A}{p} = \frac{\bar{K}\gamma_{av}\rho s}{p(1 - ms)} = \left[ \frac{1 + N}{N K_N} \right]^N \quad (2.81)$$

where

$$K_N = \frac{1 + N}{N} \left[ \frac{p(1 - ms)}{\bar{K}\gamma_{av}\rho s} \right]^{\frac{1}{N}} \quad (2.82)$$

which is expressed in terms of  $p$ . Therefore,

$$\left( \frac{d\theta}{dv} \right)^N = \left( \frac{1 + N}{N K_N} \right)^N (v + v_{me}) \quad (2.83)$$

$$\frac{d\theta}{dv} = \frac{1 + N}{N K_N} (v + v_{me})^{\frac{1}{N}} \quad (2.84)$$

Filtration at constant pressure drop is comprised of two stages:

1. The *Initial Filtration Stage* occurs during the time when the filtration apparatus is being brought from the pressure of 0 psi to the desired operating pressure. It is of relatively short duration.  $p_1$  is appreciable in relation to  $p$  (in fact, at the beginning of the filtration,  $p = p_1$ ). The quantities  $m$ ,  $\alpha_R$ ,  $N$ ,  $J_{RN}$  and therefore  $\gamma_{av}$  are varying continuously.

2. The *Main Filtration Stage* is of primary interest.  $p_1$  is negligible compared to  $p$ . The quantities  $m$ ,  $\alpha_R$ ,  $N$ ,  $J_{RN}$ , and  $\gamma_{av}$  are constant.

Integrating the latter equation, using the boundary conditions

$$v = 0 \quad \text{at} \quad \theta = 0 \quad (2.85)$$

$$v = v > v_i \quad \text{at} \quad \theta = \theta \quad (2.86)$$

where  $v_i$  is the filtrate volume at the onset of the main filtration stage, gives

$$\theta = \frac{1}{K_N} [(v + v_{me})^{1+\frac{1}{N}} - v_{me}^{1+\frac{1}{N}}] + \theta_0 \quad (2.87)$$

where  $\theta_0$  is the effective time of commencement of the filtration. Equation (2.87) represents the effective coupling of the primary variables in the main filtration stage with the effects of the initial stage. This equation applies only for  $v > v_i$ .

## 2.4 Solution for $N \approx 1$

For  $N \approx 1$ , this becomes

$$\theta = \frac{1}{K_N} (v^2 + 2v_{me}v) + \theta_0 \quad (2.88)$$

where

$$K_N = 2 \left( \frac{p(1-ms)}{\mu\rho s\gamma_{av}} \right) \quad (2.89)$$

and

$$v_{me} = \frac{R_{ma}(1-ms)}{\rho s\gamma_{av}} \quad (2.90)$$

which is amenable to evaluation of  $K_N$ ,  $v_{me}$ , and  $\theta_0$  by linear least-squares fitting. By rearranging Equations (2.89) and (2.90), the overall average cake resistance  $\gamma_{av}$  and the effective filter medium resistance  $R_{ma}$  may be evaluated.

$$\gamma_{av} = \frac{2p(1-ms)}{K_N\mu\rho s} \quad (2.91)$$

$$R_{ma} = \frac{v_{me}\gamma_{av}\rho s}{(1-ms)} \quad (2.92)$$

Recall that

$$v_{me} = \frac{1-ms}{\gamma_{av}\rho s} \left[ R_m + \frac{k'\Delta\bar{\eta}}{2\epsilon D_p K} \left( \frac{\xi n + 1}{n + 1} \right) \left( \frac{q}{q_1} \right) \right] \quad (2.93)$$

which may be rearranged as

$$R_{ma} = \frac{v_{mc} \gamma_{av} \rho s}{(1 - ms)} = R_m + \frac{k' \Delta \bar{\eta}}{2 \epsilon D_p \bar{K}} \left( \frac{\xi n + 1}{n + 1} \right) \left( \frac{q}{q_1} \right) \quad (2.94)$$

$$= R_m + \text{an elastic contribution}$$

The units of  $\gamma_{av}$ ,  $R_m$ , and  $R_{ma}$  are:

$$\gamma_{av} \quad [=] \quad \frac{kg \frac{m}{s^2} \cdot \frac{1}{m^2}}{\frac{m^2}{s} \cdot \frac{kg}{m \cdot s} \cdot \frac{kg}{m^3}} \quad (2.95)$$

$$[=] \quad \frac{m}{kg} \quad (2.96)$$

$$R_m \text{ and } R_{ma} \quad [=] \quad m \cdot \frac{m}{kg} \cdot \frac{kg}{m^3} \quad (2.97)$$

$$[=] \quad m^{-1} \quad (2.98)$$

## Chapter 3

# Methodology

The experiments consisted of filtering slurries at constant pressure drop across the filter cake. The slurry was comprised of calcium carbonate, polyacrylamide, and distilled water. Two types of polyacrylamide, four polymer concentrations, and three pressure drops were employed. A list of the experiments is presented in Table 3.1.

The conditions held constant throughout the experimentation were the temperature at 25°C, the weight fraction of calcium carbonate at 0.10, and the pH of approximately 7 for distilled water before making the slurry. To be consistent in technique the same balances, stop watch, thermocouple in the autoclave, brand of calcium carbonate, graduated cylinders, density meter, viscometer and viscometer bath were used.

The data recorded during each experiment were the volume of filtrate collected  $v$  as a function of the elapsed time  $\theta$ . Each experiment was allowed to proceed until either of the following conditions was reached:

1. The total volume of filtrate collected was 3500 mL, a limitation imposed by the design of the equipment. The autoclave held only 4000 mL of solution and the piping, approximately 500 mL. Filtering more than 3500 mL of liquid resulted in large bubbles of nitrogen gas shooting through the filter unit.
2. 75 minutes had elapsed. A filter cake of appreciable thickness was obtained in this time interval when the flowrate of filtrate was slow.

Other data collected were the weights of the wet filter cakes, weights of the oven-dried filter cakes, the viscosities and the densities of the filtrates.

Table 3.1: List of Experiments

<b>anionic polyacrylamide</b>	
pressure drop	polymer conc.
kPa	ppm by weight
345	0
	25
	50
	100
517	0
	25
	50
	100
689	0
	25
	50
	100

<b>non-ionic polyacrylamide</b>	
pressure drop	polymer conc.
kPa	ppm by weight
345	0
	25
	50
	100
517	0
	25
	50
	100
689	0
	25
	50
	100

These data were entered into a data file on the mainframe computer. A FORTRAN computer programme compiled the data and evaluated the three unknown parameters  $a_0$ ,  $a_1$ , and  $a_2$  by linear least-squares fitting of the equation

$$\theta = a_2 v^2 + a_1 v + a_0 \quad (3.1)$$

which when compared to the main filtration equation

$$\theta = \frac{1}{K_N}(v^2 + 2 v_{me} v) + \theta_0 \quad (3.2)$$

allowed for the evaluation of  $K_N$ ,  $v_{me}$ , and  $\theta_0$  through

$$\theta_0 = a_0 \quad (3.3)$$

$$v_{me} = \frac{a_1 K_N}{2} \quad (3.4)$$

and

$$K_N = \frac{1}{a_2} \quad (3.5)$$

Knowing the values of  $K_N$ ,  $v_{me}$ ,  $\theta_0$ , and  $N$ , the filter cake resistance  $\gamma_{av}$  and the filter medium resistance  $R_m$  was evaluated from

$$\gamma_{av} = \frac{2p(1 - ms)}{\mu \rho s K_N} \quad (3.6)$$

$$R_m = \frac{v_{me} \gamma_{av} \rho s}{(1 - ms)} \quad (3.7)$$

A comparison of  $\gamma_{av}$  and  $R_m$  for the various experiments was possible.

The IMSL subroutine IFLSQ was used to execute the linear least-squares approximation. A listing of this programme, called COUNT FORTRAN is found in Appendix A. This programme fitted the parameters of the first five data points of an experiment and stored the fitted parameters in the output file. It then fitted the first six data points, then the first seven, and proceeded in this manner until finally all data points were included in the fit. The calculation was continued, but in the opposite direction, to fit the last five data points, then the last six, the last seven, etc., storing the results of each fit in the output file. A typical data file and a representative output file is presented in Appendix A. This information was useful when attempting to fit a data set that included a large settling effect. Figure 3.1 displays a data set which could not be fitted by a single curve. Two curves best describe the experiment. The subroutine entitled SOLVE may be modified to solve for four

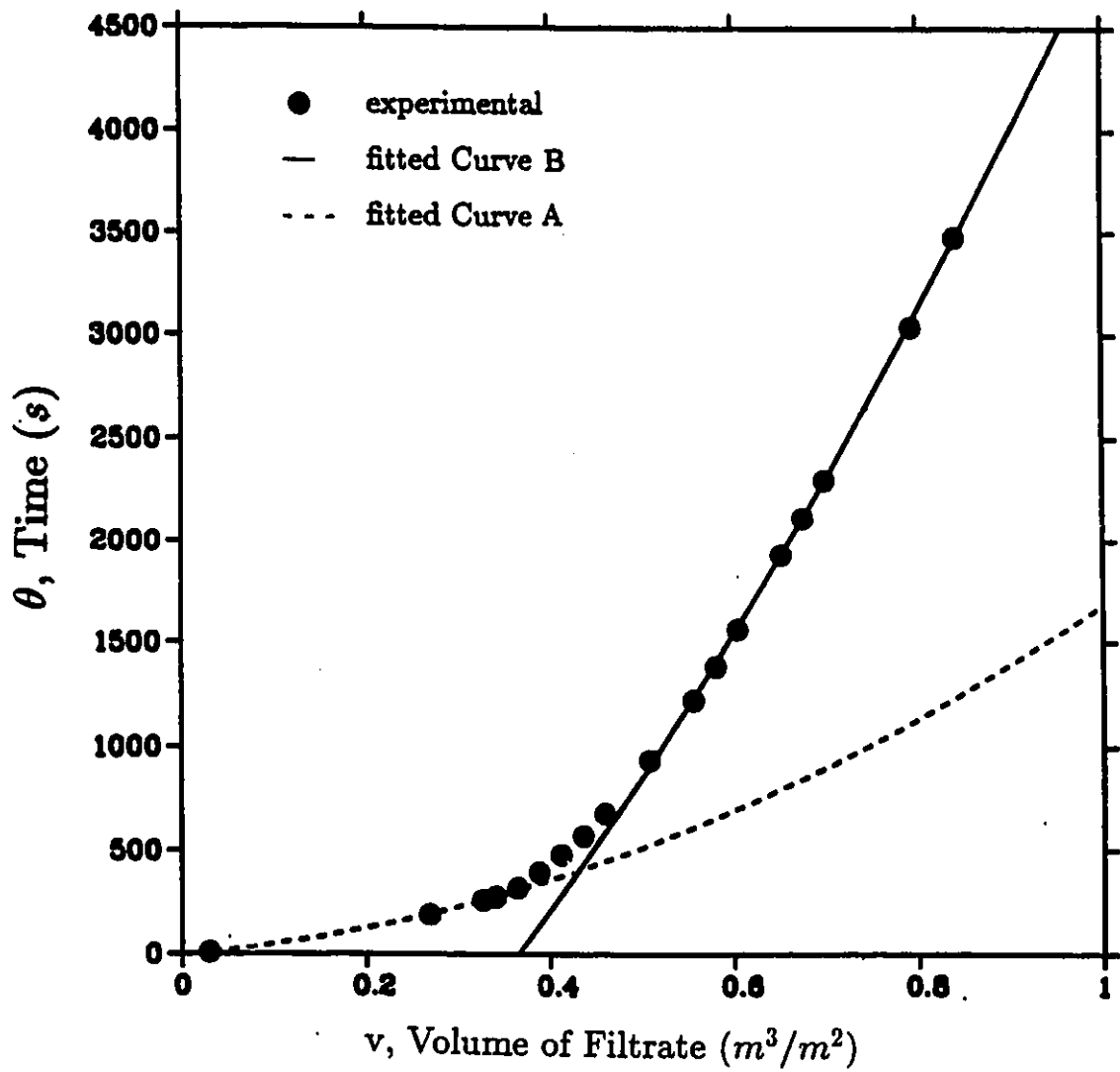


Figure 3.1: An example of a set of data which cannot be fitted by a single curve. The slurry was comprised of 10%<sub>w</sub> CaCO<sub>3</sub> in aqueous anionic polyacrylamide (50 ppm) and filtered at 345 kPa.

parameters by removing the commented statements and commenting out others. Solving for four parameters  $N$ ,  $K_N$ ,  $v_{me}$ , and  $\theta_0$  in the equation

$$\theta = \frac{1}{K_N}[(v + (v + v_{me})^{1+\frac{1}{N}} - v_{me}^{1+\frac{1}{N}})] + \theta_0 \quad (3.8)$$

requires a non-linear least-squares approximation. The IMSL subroutine ZXSSQ lends itself to a solution of this nature. A copy of this version of the programme is entitled MERGE FORTRAN, which may also be found in Appendix A.

To run COUNT FORTRAN or MERGE FORTRAN, the driving programme F EXEC was found useful (see Appendix A.).

## Chapter 4

# Properties of Materials

### 4.1 Polyacrylamide

High molecular weight polyacrylamide became the polymer of choice for this study project because of its well-known ability to produce viscoelastic effects when dilute aqueous solutions of this polymer flow through constricted geometries (Marshall and Metzner, 1967; Durst, et al., 1982; Haas and Durst, 1982; Kulicke and Haas, 1984(a,b); Odell, et al., 1988). Polyacrylamide is highly soluble in water, and the advantage of working with water as opposed to working with other solvents is obvious. Polyacrylamide is non-irritating to the skin under normal use conditions and has a low single-dose toxicity (Teot, 1978). The polymer is an off-white, granular, free-flowing substance which is rather easy to measure.

At room temperature, an aqueous solution of polyacrylamide will not separate into two phases, nor will the polymer normally precipitate from the solution when electrolytes are present.

Other chemical names, abbreviations, and trade names of this synthetic polymer are poly(acrylamide); polyacrylic amide; poly(1-carbamoylethylene) [IUPAC]; PAm; PAAM; PAM; *Cyanamer* (American Cyanamid); *Purifloc* (Dow); *Separan* (Dow); and *Pusher* (Dow).

Only commercial grades of the polymer were used and, therefore, the results should be applicable to the actual use of the material. The main source of information of the polyacrylamide is the technical literature of the manufacturer, and for commercial reasons, the literature is vague. The manner by which the polymer was produced is uncertain with the corresponding ambiguity regarding such features as the average molecular weight and the molecular weight distribution (Molyneux, 1984). The two polyacrylamide sam-

ples were characterized in the solvent in which the main studies were performed, allowing their viscosity-average molecular weights<sup>1</sup> to be estimated. The viscosity-average molecular weight determination is presented in Appendix C.

### **Solution Aging**

One complicating feature of a study of the behavior of high molecular weight polyacrylamide is the 'aging' effect of the solution that occurs. There is a progressive fall in the viscosity of the solution with time. This effect seems to be largely physical - relating to the disentangling or the disaggregation of the polymer molecules (Molyneux, 1984). The literature supplied by Dow Chemical Company states that an aqueous stock solution of 0.5%<sub>w</sub> polyacrylamide may be prepared according to particular instructions, which have been included in the experimental section of this thesis, and that the solution will keep for three to four weeks in dark glass bottles.

To minimize the effects of aging of the solution due to exposure to light, air, and vibration, the stock polymer solution was stored in tightly-capped, brown glass bottles in a cupboard in a laboratory.

### **Hygroscopicity**

Polyacrylamide is slightly hygroscopic (absorbing water from the air). No attempt was made to dehydrate the polymer. The minute amount of water that was present in the polymer was considered to have no effect on the results of the experiments, especially since the polymer was dissolved in water for the filtration runs.

### **Concentrations:**

A concentration of the stock polyacrylamide solution of 0.5%<sub>w</sub> polyacrylamide proved to be suitable since the solution was not too viscous for measuring a specific quantity during an experiment.

Concentrations of 0 ppm, 25 ppm, 50 ppm, and 100 ppm of polyacrylamide were chosen for the experimentation.

---

<sup>1</sup> See Appendix B for a description of the various types of average molecular weights.

## Viscoelastic Character

Polyacrylamide has been reported (Pye, 1964; Marshall and Metzner, 1967; Dauben and Menzie, 1967; Kulicke and Haas, 1984(a,b); Odell, et al., 1988) to possess viscoelastic character. The three principal features of viscoelastic polymers are (a) very high molecular weight (greater than  $10^6$ ), (b) a chain containing single-bonded carbon atoms which allow a change in conformation, and (c) able to sequester large amounts of solvent in their coils.

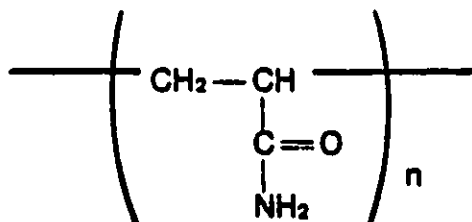
### 4.1.1 Types of Polyacrylamide Used

Two types of polyacrylamide were employed for this research, non-ionic polyacrylamide and anionic polyacrylamide. Utilizing these two types of the polymer permitted a comparison of the effect of the surface charge on the macromolecule<sup>2</sup>.

The polyacrylamides used were linear, polydisperse polymers.

#### Non-Ionic Polyacrylamide

Non-ionic polyacrylamide (or unhydrolyzed polyacrylamide) is a homopolymer of 2-propenamide,  $C_3H_5NO$ , and has the representation as shown below.



The 500 gram sample was supplied by Polysciences, Inc. of Warrington, Pennsylvania. The only chemical reaction of this polymer in aqueous solution is the hydrolysis of the amide groups. In neutral solvents, Silberberg et al. (1957) found that this reaction only occurred above temperatures of  $67^\circ\text{C}$ . At the operating temperature of this thesis experimentation,  $25^\circ\text{C}$ , it is unlikely that the amide groups underwent any chemical reaction or that the polymer gained a surface charge during the experiments of this study.

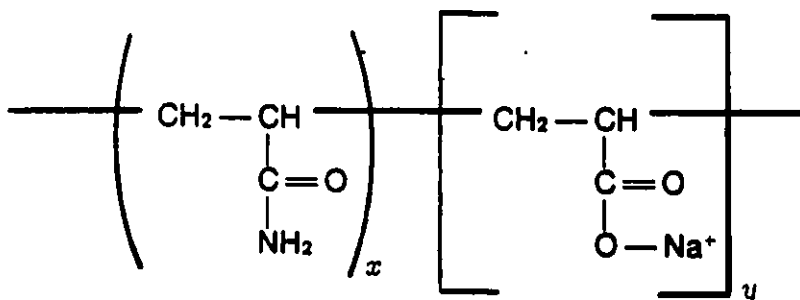
Non-ionic polymers are generally considered to have random coiling (Merrill, 1962). A randomly coiled molecule has the ability to hold a large volume of solvent within its coils.

<sup>2</sup>The word macromolecule and polymer are used interchangeably in this thesis.

The random coils are easily deformed, and under an applied stress, change conformation<sup>3</sup> and change from spherical coils to elongated ellipsoids. The coils are also extensively entangled with one another, and when a coil moves, it must drag along the other coils with much solvent (Dauben and Menzie, 1967).

#### Anionic Polyacrylamide:

Anionic polyacrylamide (or partially-hydrolyzed polyacrylamide) is a modified form of the non-ionic polymer, and is represented schematically below. It is a copolymer of 2-propenamide and the sodium salt of 2-propenoic acid.



The brand name of the anionic polyacrylamide is *Pusher 500* (CAS Registry Number [54182-67-1]) which was manufactured for the purpose of mobility control<sup>4</sup> in enhanced oil recovery. It has been cited (Baijal and Dey, 1982) to be 37% hydrolyzed; i.e., that in the previous diagram  $x=63\%$  and  $y=37\%$ . This chemical was supplied by Dow Chemical Company of Midland, Michigan. Langhorst, et al., (1986) determined two average molecular weights of *Pusher 500* to be

$$\overline{M}_w = 5.56 \times 10^6$$

$$\overline{M}_n = 2.80 \times 10^6$$

using hydrodynamic chromatography (HDC) and a low-angle laser light scattering (LALLS) detector.

<sup>3</sup>Appendix D offers the definitions of the terms conformation, configuration, and similar words.

<sup>4</sup>i.e., increasing oil displacement efficiency by reducing the mobility ratio, (permeability of the reservoir)/(viscosity of the driving phase). This mobility reduction may be achieved by a permeability reduction, a viscosity increase of the driving phase, or a combination of the two. A reduced driving phase mobility results in improvements in areal sweep efficiency and in the vertical coverage in stratified reservoirs (Dauben and Menzie, 1967).

The macromolecule is said to be anionic because of the net negative charge existing on the polymer. Because of the repulsion between neighbouring indentically charged groups on the main chain, the macromolecule expands more and more, from the random coil into a semi-stiff rod (Merrill, 1967). Under applied stress, the anionic polymer does not deform as much as the nonionic polyacrylamide. Scissioning of the macromolecules is possible.

## 4.2 Calcium Carbonate

Precipitated calcium carbonate was the source of particulates to be filtered in this study. The term 'precipitated calcium carbonate' applies to the commercial type of calcium carbonate produced chemically in a precipitation process. The precipitated products are distinguished by a finer, more uniform particle size, a narrower size range, and a higher degree of chemical purity (Lepley, 1978).

There are minimal health and safety concerns associated with precipitated calcium carbonate. It is listed as a nutrient and dietary-supplement food additive; however, the dust is classified as a nuisance particulate and inhalation should be avoided.

Calcium carbonate occurs naturally in two crystal structures, calcite and aragonite. The type used in this study consisted of calcite, thermodynamically stable at all investigated pressures and temperatures (Lepley, 1978).

Product information is as listed:

- Supplier: Anachemia, Mississauga, Ontario
- Manufacturer: Pfizer, Inc., Minerals, Pigments and Metals Division, New York, New York
- Description: light powder, lab-grade, in bags of 50  $lb_m$
- Chemical Formula:  $CaCO_3$
- Molecular Weight: 100.09
- Density:  $2710 \text{ kg}/m^3$  (Lepley, 1978)
- Solubility in Water:  $0.0014 \text{ g}/100 \text{ cm}^3$  of water (Lepley, 1978)
- Average Particle Diameter:  $0.8 \mu m$  (Kozicki, 1990a).

A weight fraction of 0.10 of calcium carbonate in the slurry was found satisfactory for the purpose of this study because filter cakes of appreciable thickness were obtained.

### 4.3 Distilled Water

The distilled water used in the slurry was double-distilled tap water from the distillation unit located on the fifth floor of the Colonel By Building. The distilled water was kept microbe-free by infra-red lamps within the distillation unit. The quality of the distilled water varied, depending on demand.

A comparison of this distilled water with a sample of the distilled water from the Chemistry department<sup>5</sup> was carried out. The pH (Beckman Zeromatic SS-3 pH Meter, Beckman Instruments, Inc., Fullerton, California) of the two liquids was identical at 7.1. A conductimetry test was also performed using a CDM 80 Conductivity Meter (Radiometer, Copenhagen)<sup>6</sup>. The conductivity of the distilled water from the Colonel By Building was  $1.16 \mu S/cm$ , while that of the distilled water from the Chemistry department was  $1.55 \mu S/cm$ . This suggests that the water from the Colonel By Building contained fewer ions than that obtained from the Chemistry Department. For comparison, tap water had a conductivity of  $125.6 \mu S/cm$ . The water used was considered to be pure enough for the purpose of this study; however, this observation, by itself, is no basis for concluding that the water quality was consistently good.

### 4.4 Filter Cloth

The filter cloth was purchased in 1978 from the T. Shriver Co., Harrison, New Jersey. The filter cloth (Style 3627) is classified as a twill (fabric woven with diagonal ribbing) having a weight of 15.5 ounces per square foot. The cloth is woven of cotton with a small quantity of some other unknown fibre. The cloth was cut into circles 0.064 metres (2.5 inches) in diameter. A new filter cloth was used for every filtration run because a reused filter cloth offered more resistance than an unused filter cloth. A used filter cloth has particles deeply imbedded within its fibres.

It should be noted that there is considerable difficulty in securing a clear filtrate with a dry filter cloth. In the case where a wetted filter cloth is employed, the filtrate is clear from almost the beginning of the filtration. The efficacy of the filter cloth is enhanced when wetted because the water serves to swell the cloth fibres and reduce the size of the pores

<sup>5</sup> which was triple-distilled and passed through a four-cartridge purifier (a particulate remover, an activated carbon cartridge, an anion exchange resin, and a cation exchange resin).

<sup>6</sup>The conductivity is given in  $\mu S/cm$ , or *micro Siemens per centimetre*. Please note that 1 *Siemens* = 1 *mho*.

in the fabric. The water may also permit a double electrical layer to form on the fibres, possibly ionizing the hydroxyl groups in the cotton, and initiating the adherence of the slurry particles to the filter cloth.

#### **4.5 Materials Used in the Construction of the Apparatus**

The materials utilized in the construction of the filtration apparatus were stainless steel and plexiglass. The choice was based on the fact that these materials did not react chemically with high molecular weight polyacrylamide, nor with the calcium carbonate. The perforated support plate for the filter cloth was of brass.

For the preparation of the stock polyacrylamide solutions, Teflon-coated stirring bar and pyrex beakers were employed.

## Chapter 5

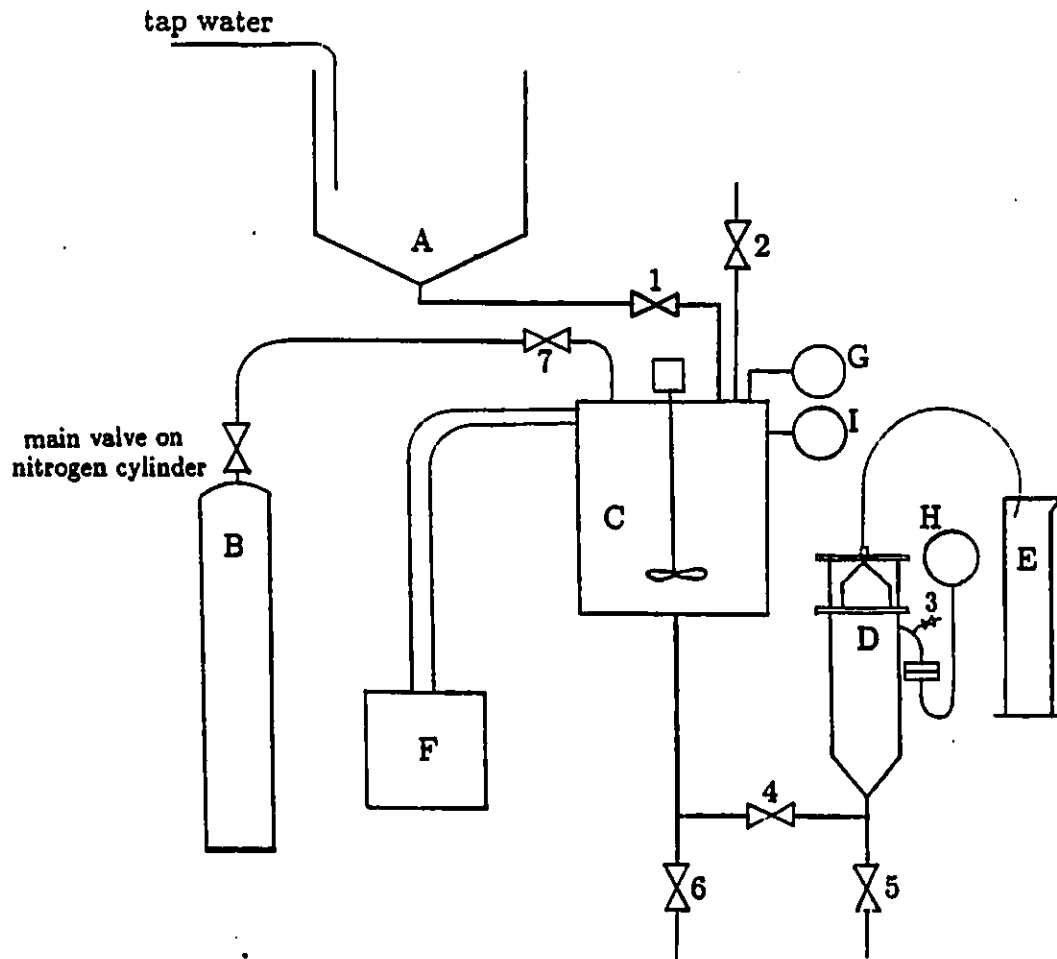
# Experimental Aspects

### 5.1 Apparatus

A schematic diagram of the filtration apparatus used in the filtration experiments is shown in Figure 5.1. The equipment included a mixing tank, autoclave, a cylinder of compressed nitrogen gas, filter, a graduated cylinder, thermocouple, and two pressure gauges. There were two unusual features of the design that made it different from conventional filters. The first difference was that the flow moved upwards. This was beneficial for the type of experimentation undertaken in the study; in the event that an air bubble becomes entrained in the slurry, the upward flow allows the bubble to escape. In downward flow, it is likely that the air bubble would have become entrapped within the filter cake and would have affected the evaluations of the porosity and moisture ratio of the cake. Since the filter cake formed on the underside of the septum, artificial compaction of the cake due to gravity was eliminated. The second major difference of this filtration equipment was that compressed nitrogen gas was used to force the slurry through the system. This was a desirable alternative to the use of a pump since it was important that the slurry not be subjected to any mechanical or thermal trauma. Vibrations associated with a mechanical pump might have caused oscillations in the two pressure gauges, and, possibly, resulted in inaccurate readings.

#### Mixing Tank

The tank was necessary in order to combine all of the constituents of the slurry. No stirring was done in the tank since the slurry was stirred in the autoclave.



- A ... Mixing tank
- B ... Cylinder of nitrogen gas
- C ... Autoclave with stirrer and water jacket
- D ... Filter unit
- E ... Graduated cylinder
- F ... Constant temperature bath
- G ... Standard pressure gauge
- H ... Diaphragm pressure gauge
- I ... Thermocouple
- ⊗ ... Valve, numbered 1 to 7

Figure 5.1: Schematic Diagram of the Filtration Equipment.

The mixing tank was positioned above the autoclave to allow transfer of the slurry from the tank to the autoclave by gravity flow.

### **Filter**

The filter unit, shown in Figure 5.2, consists of two flanged plates, three plexiglass cylinders having an inside diameter of 0.073 metres, a perforated brass plate, a filter cloth, Teflon gaskets, and eight threaded steel rods with nuts. The plexiglass allowed for observation of the cake build-up. One of the plexiglass cylinders had an opening housing a removable plug, which facilitated the withdrawal of filtrate remaining above the filter cake after an experiment. The perforated brass plate served to support the filter cloth. It was a brass disk drilled with evenly spaced holes (20 holes/cm<sup>2</sup>, each hole 0.0016 m inside diameter).

The components of the filter had to be dismantled after each run in order to permit a thorough cleaning in preparation for the next experiment.

### **Driving System**

Nitrogen gas entered through an opening at the top of the autoclave, forming a gas pocket above the slurry. The pressure exerted by this gas caused the slurry to flow out of the autoclave. The amount of nitrogen gas had to be closely monitored to ensure that filtration occurred at the desired constant pressure drop.

The autoclave was equipped with a stirrer, which was set at the lowest possible speed (approximately 150 rpm).

The autoclave was positioned at a level higher than the filter so that the slurry would flow from the autoclave into the filtering unit by gravity. This was useful when filling the equipment with the slurry and later, when cleaning the apparatus between runs.

### **Pressure Gauges**

There were two pressure gauges utilized, a standard pressure gauge (USG, U.S.A., dial type with a range of 0 psi to 600 psi, subdivisions of 2 psi) and a diaphragm pressure gauge (ACCO Helicoid Gage, U.S.A., dial type with a range of 0 psi to 200 psi, subdivisions of 2 psi.). For the location of the gauges, please refer to Figure 5.1). Both gauges provided readings of *gauge pressure*, not *absolute pressure*.

Before any experiments were performed, the diaphragm pressure gauge was calibrated against the standard gauge. The calibration involved filling the entire system with water,

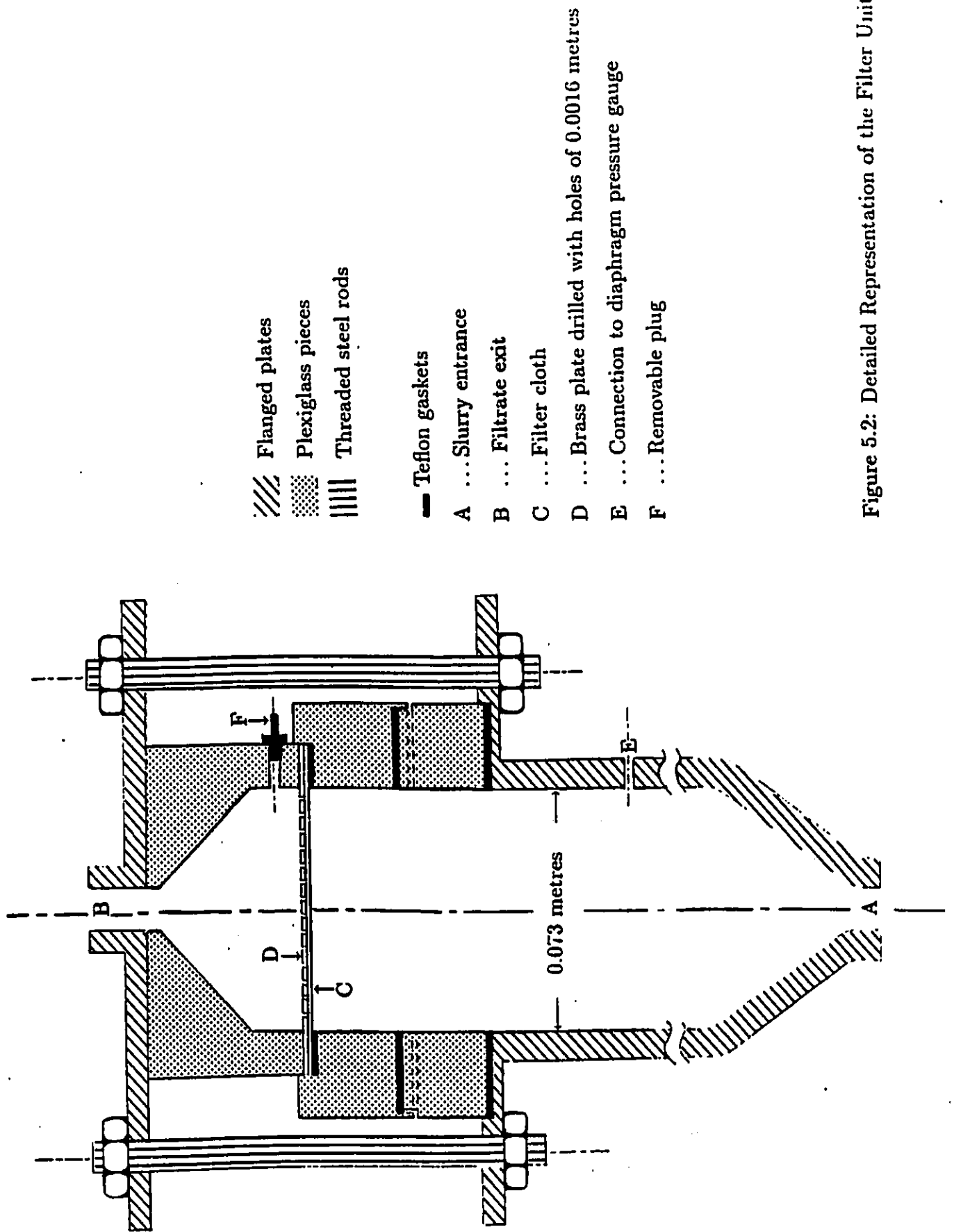


Figure 5.2: Detailed Representation of the Filter Unit.

tightly capping the outlet of the filtering unit with a swage lock closure, and closing all other valves. Using the nitrogen gas, the autoclave was then pressurized to various levels, and the readings were recorded. A calibration curve for the diaphragm pressure gauge is presented in Appendix E. This procedure was also convenient for the detection of any leaks in the system.

### **Temperature Control**

The autoclave was equipped with an external water jacket. This was connected to an automatically-controlled constant temperature water bath set at 25°C. The autoclave had a thermowell which extended toward the bottom of the autoclave, and a thermocouple rests in the thermowell. A digital readout of the temperature in degrees Celsius was provided (Thermo Electric Canada Ltd., Brampton, Ontario). An incidental advantage was in having the pilot plant housing the equipment registering a temperature range between 22°C to 25°C for the duration of the experiments. This was found to be convenient because the filtering unit (containing the filter cake) was without insulation since this section of the equipment needed to be dismantled for cleaning after each experiment.

### **Viscosity Measurements**

Viscosity was measured with a Cannon-Fenske routine viscometer for transparent liquids, size 50, immersed in a constant temperature bath at 25°C (GCA Precision Scientific Temp-Trol Viscosity Bath). The procedure for measuring viscosity conformed to ASTM standards<sup>1</sup>. After each viscosity measurement, the viscometer was washed thoroughly with distilled water, ethanol, and acetone, and was then air-dried.

### **Density Measurements**

Density was measured at 25°C using a DMA 48 Digital Density Meter (Anton Paar Co., Graz, Austria). Each day, the density meter was calibrated. The procedure for measuring the density of a sample followed the manufacturer's directions. The density meter was cleaned after each sample using distilled water, ethanol, and acetone, and was then air-dried. The accuracy of the density reading (listed in the operating manual) was  $\pm 1 \times 10^{-4}$  g/cm<sup>3</sup>.

---

<sup>1</sup>Standard Specification for Kinematic Glass Viscometers ASTM Designation: D 2515-66; and Standard Method for Test for Viscosity of Transparent and Opaque Liquids ASTM Designation: D445-65.

## 5.2 Stock Polymer Solution Preparation

The aqueous polyacrylamide solutions were prepared as a concentrate, 0.5%<sub>w</sub> polyacrylamide in distilled water, and diluted to the desired concentrations, as needed before a filtration experiment. A 1.0 L batch of polymer solution would suffice for three to four weeks of experimentation. The procedure for the preparation of the aqueous polyacrylamide solutions is according to instructions supplied by Dow for *Pusher* polyacrylamide.

The appropriate amount of distilled water was put into a beaker. A magnetic stirrer was added and the speed adjusted so that the bottom of the water vortex was thirty to fifty percent the diameter of the beaker. The polymer crystals were poured just below the curve of the vortex (See Figure 5.3). The polymer was added to the water over a period of fifty to sixty seconds. When all of the polymer had been added, the magnetic stirrer was adjusted to the lowest possible speed. The solution was stirred for three hours, and then filtered through a 75 $\mu$ m sieve. The solution was stored at room temperature in a tightly-capped, brown glass bottle in a closed, dark cupboard. A new batch of this stock solution was prepared every three to four weeks.

## 5.3 Procedure for a Filtration Run

In preparation for a filtration run, a filter cloth was soaked in distilled water in a closed container overnight to ensure saturation. The following day, the filter cloth, porous brass plate, gaskets, and the plexiglass sections of the filter were assembled and secured with eight bolts and nuts. The eight bolts and nuts were first hand-tightened, and tightened again using a crescent wrench and a socket wrench in a criss-cross pattern, tightening each bolt only one revolution at a time (as one would tighten the wheel bolts when changing an automobile tire). Valves 1,4,5 and 6 were closed. The desired amounts (Appendix F) of polymer solution, calcium carbonate, and distilled water were weighed. The distilled water was poured into the mixing tank, and then the polymer solution was added. The calcium carbonate powder was slowly and carefully added to the mixing tank. The stirrer in the autoclave was started and Valves 1 and 2 were opened. The slurry was allowed to drain into the autoclave by gravity. When liquid had begun to flow through Valve 2, this valve was closed. Valves 3 and 4 were opened to allow the slurry to fill the pipes, and the filtering unit. When the slurry reached Valve 3, this indicated that the air had been expelled from the pipe connected to the Maniragm pressure gauge. Valve 3 was then closed. By this

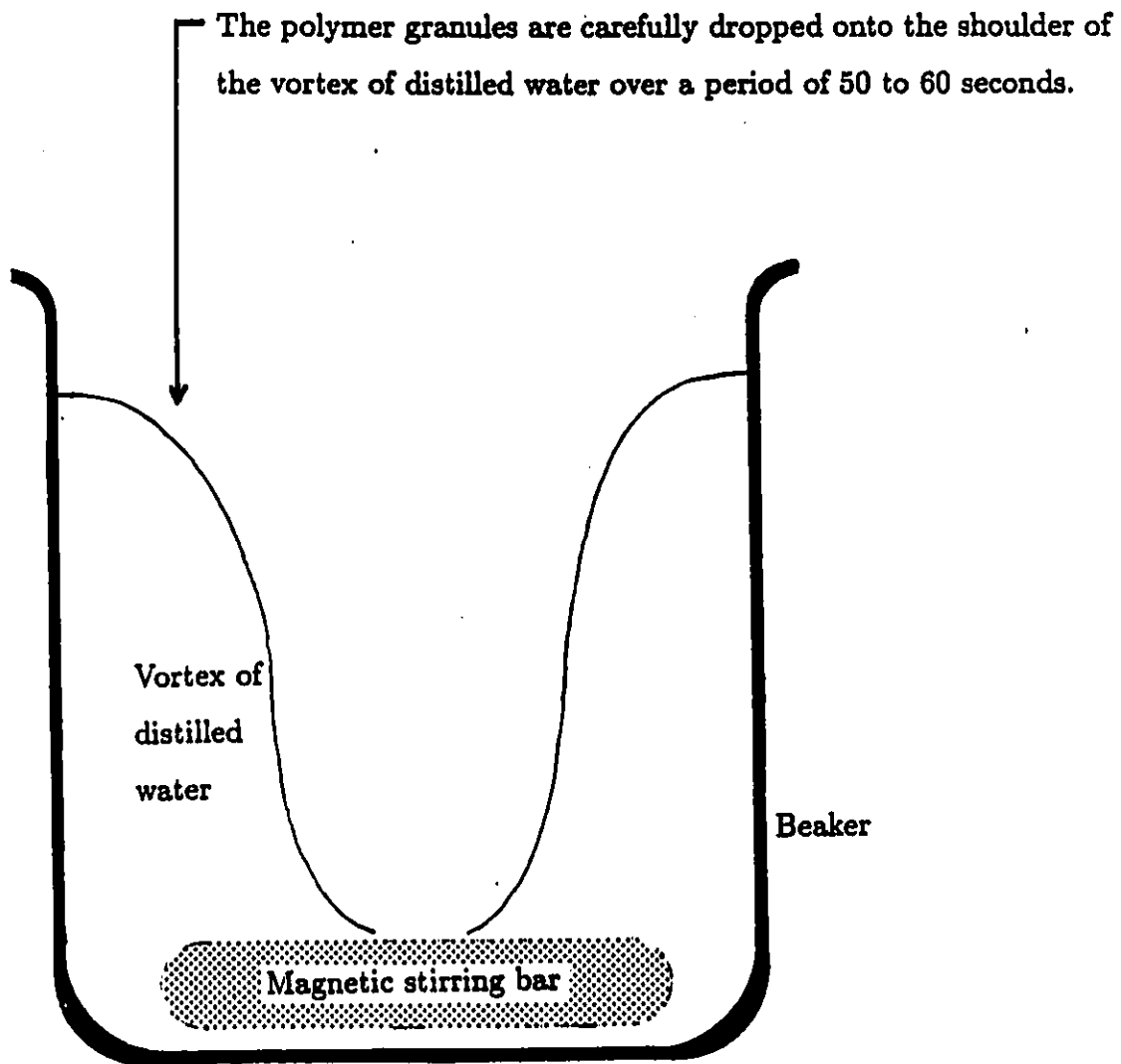


Figure 5.3: Schematic Diagram Depicting the Addition of the Polymer Crystals to a Beaker of Distilled Water.

time, the mixing tank had been depleted of slurry. Valve 1 was closed.

The main valve on the nitrogen cylinder was opened, and Valve 7 was then gently opened to allow the flow of nitrogen into the autoclave. The nitrogen slowly forced some of the slurry out of the autoclave causing the level of the slurry in the filtering unit to rise, and eventually, the slurry reached the filter cloth. When the first drop of filtrate had permeated the filter cloth and porous brass plate, a calibrated (NRC Time Signal) stop watch was started. When the first drop of filtrate fell into the graduated cylinder, the time was observed and recorded and became the initial reading of the experiment. At this time, 122 mL of filtrate had been produced<sup>2</sup>. The pressure in the system was allowed to rise gradually until the desired operating pressure had been attained. Then Valve 7 was partially closed as required to allow a small flow of nitrogen into the autoclave to maintain a constant pressure in the system. Valve 7 had to be adjusted frequently during the experiment. The temperature indicated by the digital thermocouple was constantly monitored to ensure that the temperature remained at  $25 \pm 1^\circ\text{C}$ . The temperature of the filtrate was also checked periodically.

For every 100 mL of filtrate collected, the time was recorded. The experiment was terminated in one of two ways: either when 3400 mL had been collected; or, when 75 minutes had elapsed.

A sample of filtrate was collected in a vial to determine viscosity and density, and at this time, the thickness of the filter cake was measured.

The system was shut down by first closing Valves 4 and 7 which caused the pressure to decrease rapidly. A flexible tube attached to a large syringe was inserted into the filtering unit. This syringe produced the required suction necessary to prevent the filter cake from falling down into the pipe below the filter. Valve 5 was opened followed by the opening of Valve 3, and when the slurry had drained from this section, the plug in the plexiglass cylinder was removed. The syringe was inserted into the plexiglass cylinder. The syringe was used to withdraw the liquid remaining above the filter cake. The eight bolts were removed as quickly as possible, and the filter cake was removed from the assembly. The cake was placed in a clean glass dish and weighed. The cake and dish were then placed in an oven at approximately  $115^\circ\text{C}$  for 24 hours, and the cake was weighed again. Following this, the cake was returned to the oven and another weight recorded after 48 hours had elapsed. When the two weights of the dried cake corresponded to within  $\pm 0.002$  grams, the

<sup>2</sup>122 mL was the amount of water that the section of the filtering assembly above the filter cloth held. This measurement was taken before any experiments were performed. This data is purveyed in Appendix G.

cake was discarded. The moisture ratio of the cake was calculated taking into account the weight of the clean, dry dish.

The equipment was then flushed of all slurry. The cleaning of the filtration equipment was achieved by slowly opening Valve 4, allowing the pressure to be released from the autoclave. Valve 3 was also opened to allow the nitrogen to escape. Care had to be taken in opening Valves 3 and 4 since the slurry tended to splatter as it escaped from the pressurized autoclave. When the system was depressurized, all valves, except Valve 7, were opened. Copious amounts of water were flushed through the system, and a final rinse with distilled water was mandatory. The valves were always left in the open position to allow the water to drain out and evaporate.

## Chapter 6

# Results and Discussion

### 6.1 Results

The record data for the filtration experiments conducted at constant pressure drop are presented in tabular and graphical form in Appendix H.

The volume-time data collected during the filtration experiments were compiled, and  $K_N$ ,  $v_{me}$ ,  $\theta_0$ , and  $N$  were evaluated. For the different experiments the  $N$ 's varied erratically between 0.8 and 1.1. The corresponding values for  $K_N$ ,  $v_{me}$ , and  $\theta_0$  were also scattered. The reason for this is that for the non-linear model, i.e.,

$$\theta = \frac{1}{K_N}[(v + v_{me})^{1+\frac{1}{N}} - v_{me}^{1+\frac{1}{N}}] + \theta_0 \quad (6.1)$$

the data are not conducive to the level of discrimination required to yield all four parameters by minimization of the sum of squares of residuals, using a search procedure, as has been pointed by a previous worker (Rao, 1970). The problem becomes tractable when the equation is linearized by fixing  $N$ , requiring the estimation of only three parameters. The flow behavior index  $N$  was assigned the value of unity, since the concentrations of polymer used were quite low.

In several of the experimental runs involving the polyacrylamides, the graphs of the time-volume data reveal a distinct change in direction developing at 25 ppm, and more visible at 50 ppm. Figures 6.1 through 6.6 are typical examples (The data points have been connected with straight lines to make the change in direction visible.). The discontinuity occurring at 50 ppm of polymer may be explained as a collapse in the filter cake occurring after a certain time in the experiment. The agglomerates deform or break down with a

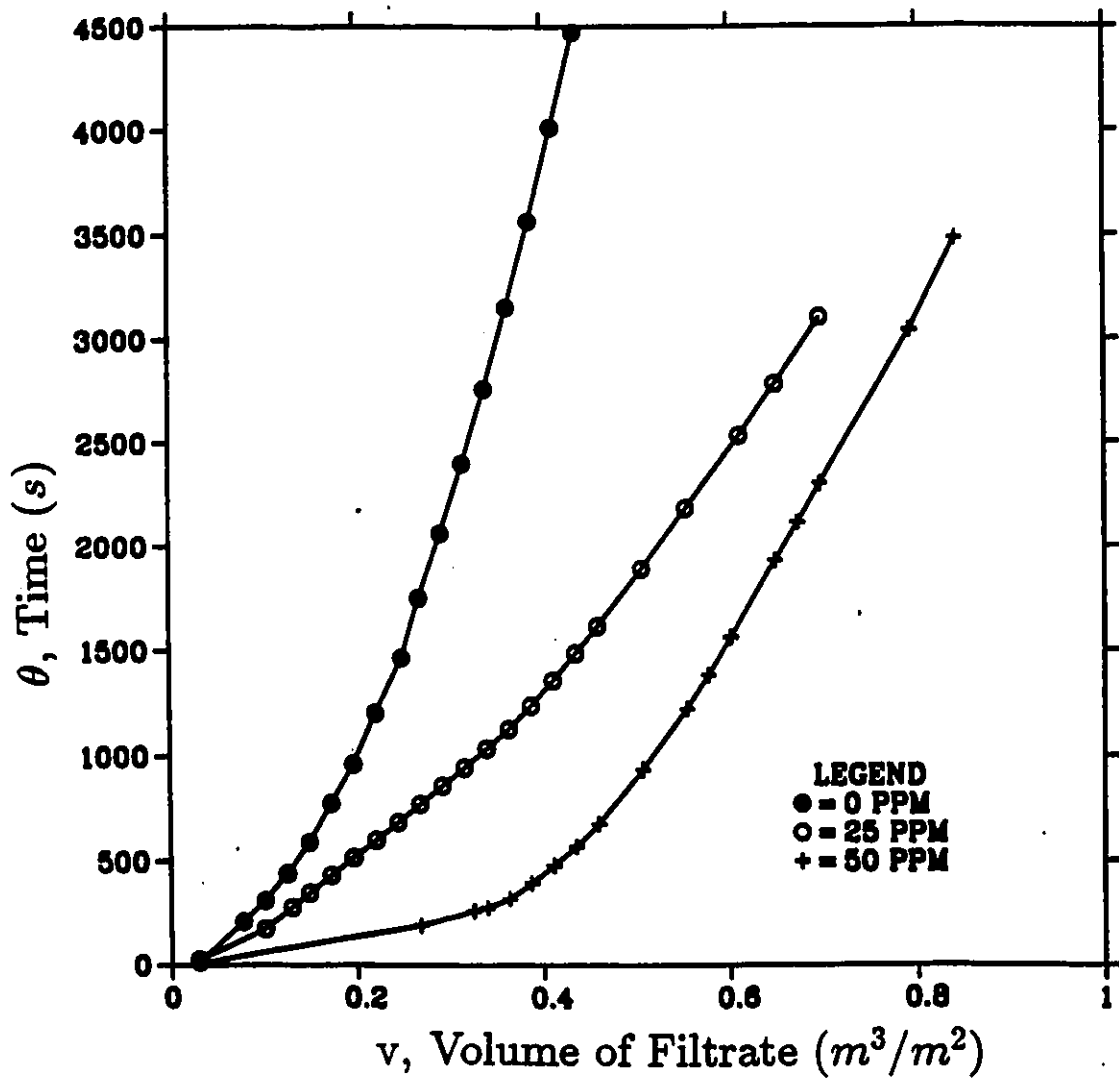


Figure 6.1: Volume of Filtrate Collected versus Time for Constant Pressure Filtration at 345 kPa (50 psi) of Slurries Comprising 10%<sub>w</sub> CaCO<sub>3</sub> in Aqueous Anionic Polyacrylamide Solutions.

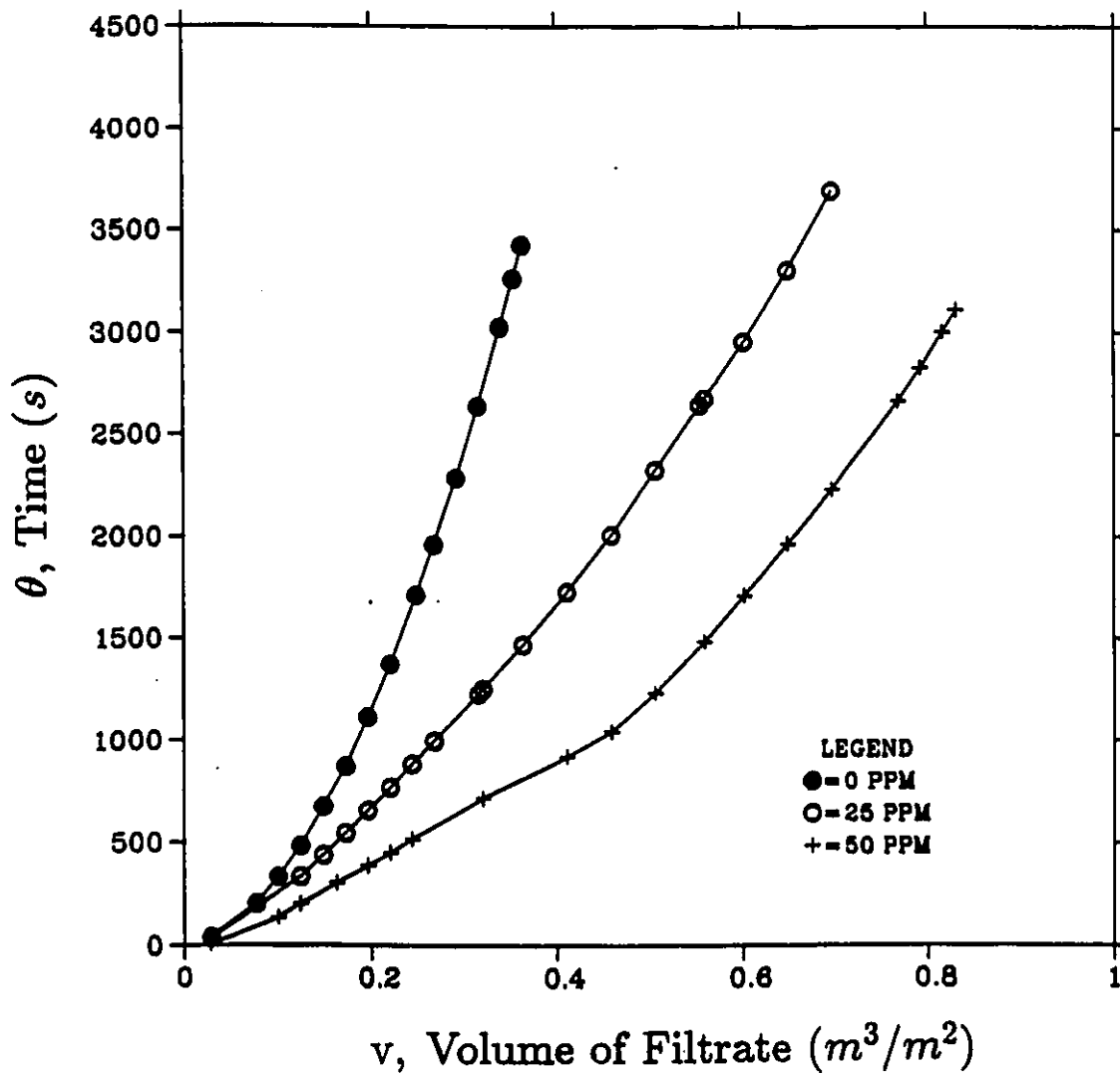


Figure 6.2: Volume of Filtrate Collected versus Time for Constant Pressure Filtration at 345 kPa (50 psi) of Slurries Comprising 10%<sub>w</sub> CaCO<sub>3</sub> in Aqueous Non-ionic Polyacrylamide Solutions.

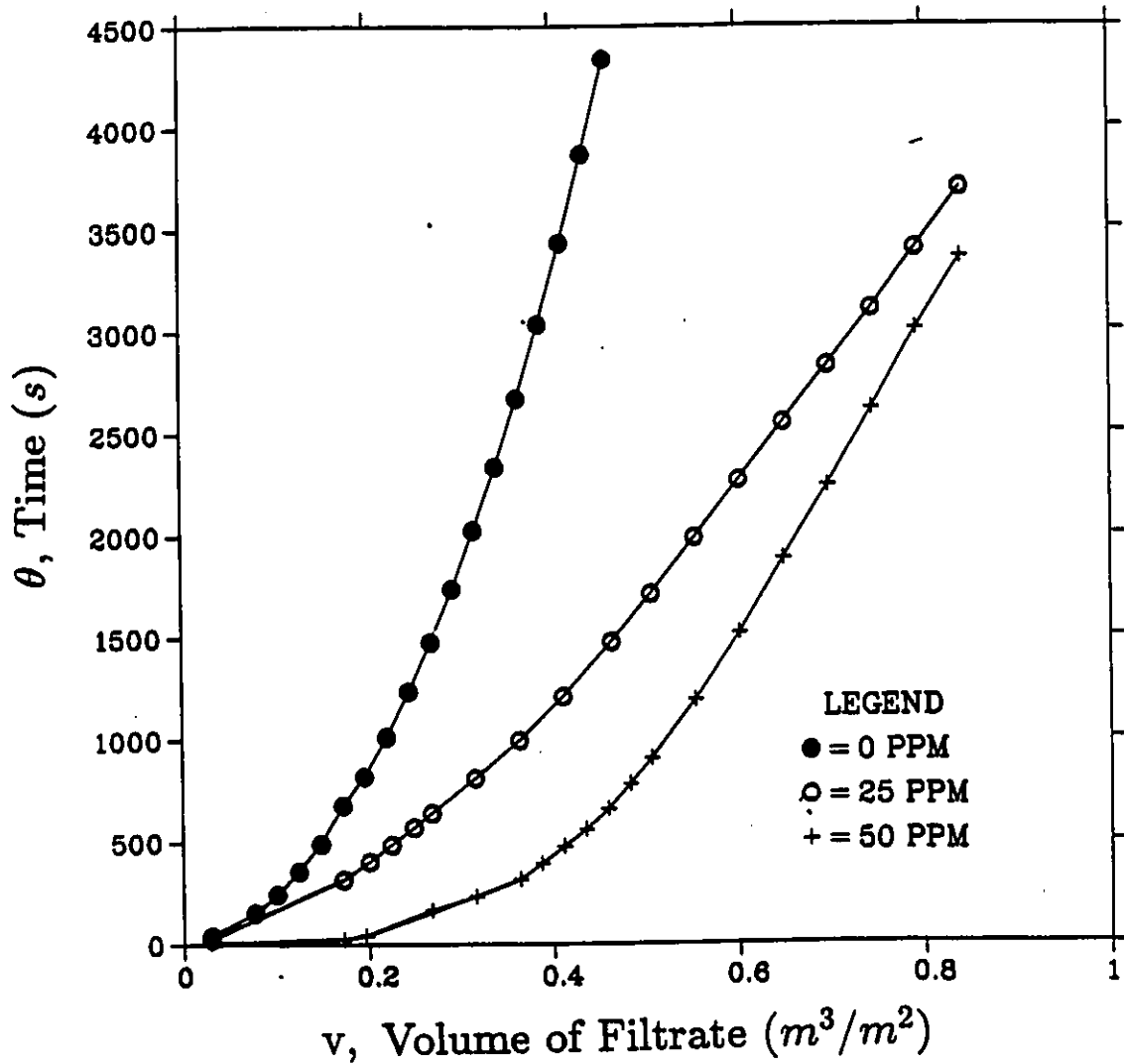


Figure 6.3: Volume of Filtrate Collected versus Time for Constant Pressure Filtration at 517 kPa (75 psi) of Slurries Comprising 10%<sub>w</sub> CaCO<sub>3</sub> in Aqueous Anionic Polyacrylamide Solutions.

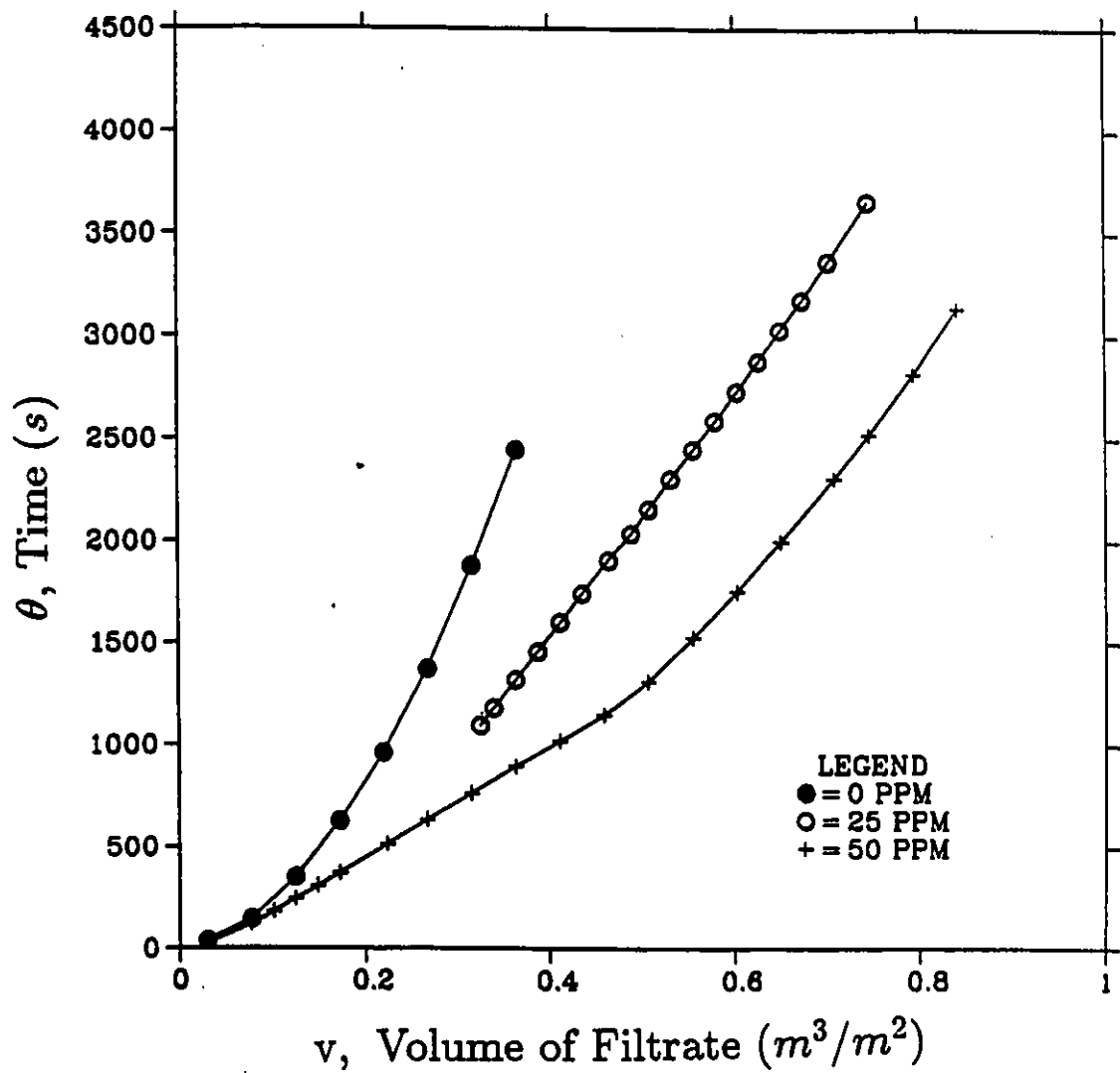


Figure 6.4: Volume of Filtrate Collected versus Time for Constant Pressure Filtration at 517 kPa (75 psi) of Slurries Comprising 10%<sub>w</sub> CaCO<sub>3</sub> in Aqueous Non-ionic Polyacrylamide Solutions.

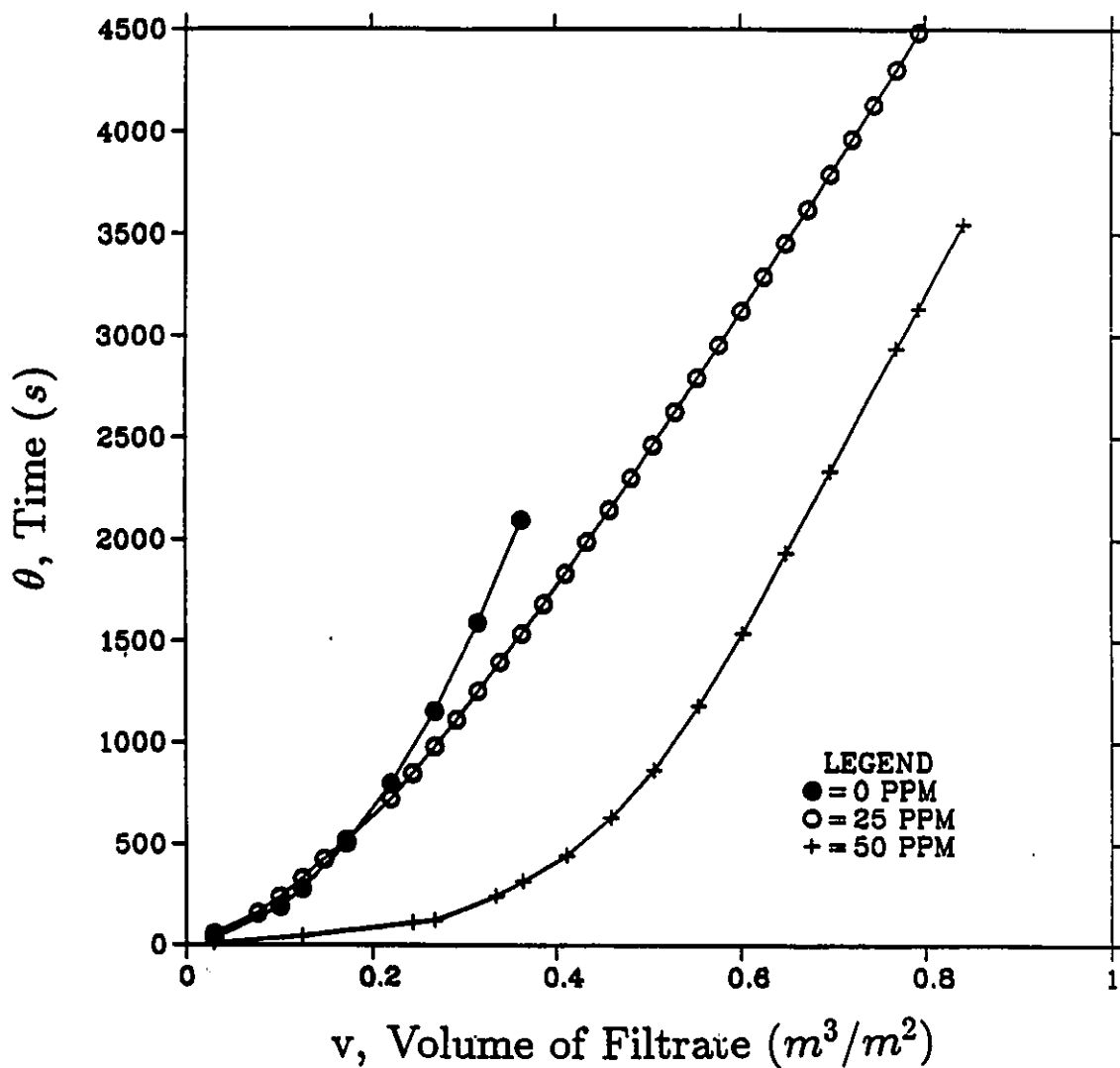


Figure 6.5: Volume of Filtrate Collected versus Time for Constant Pressure Filtration at 689 kPa (100 psi) of Slurries Comprising 10% $\frac{w}{w}$  CaCO<sub>3</sub> in Aqueous Anionic Polyacrylamide Solutions.

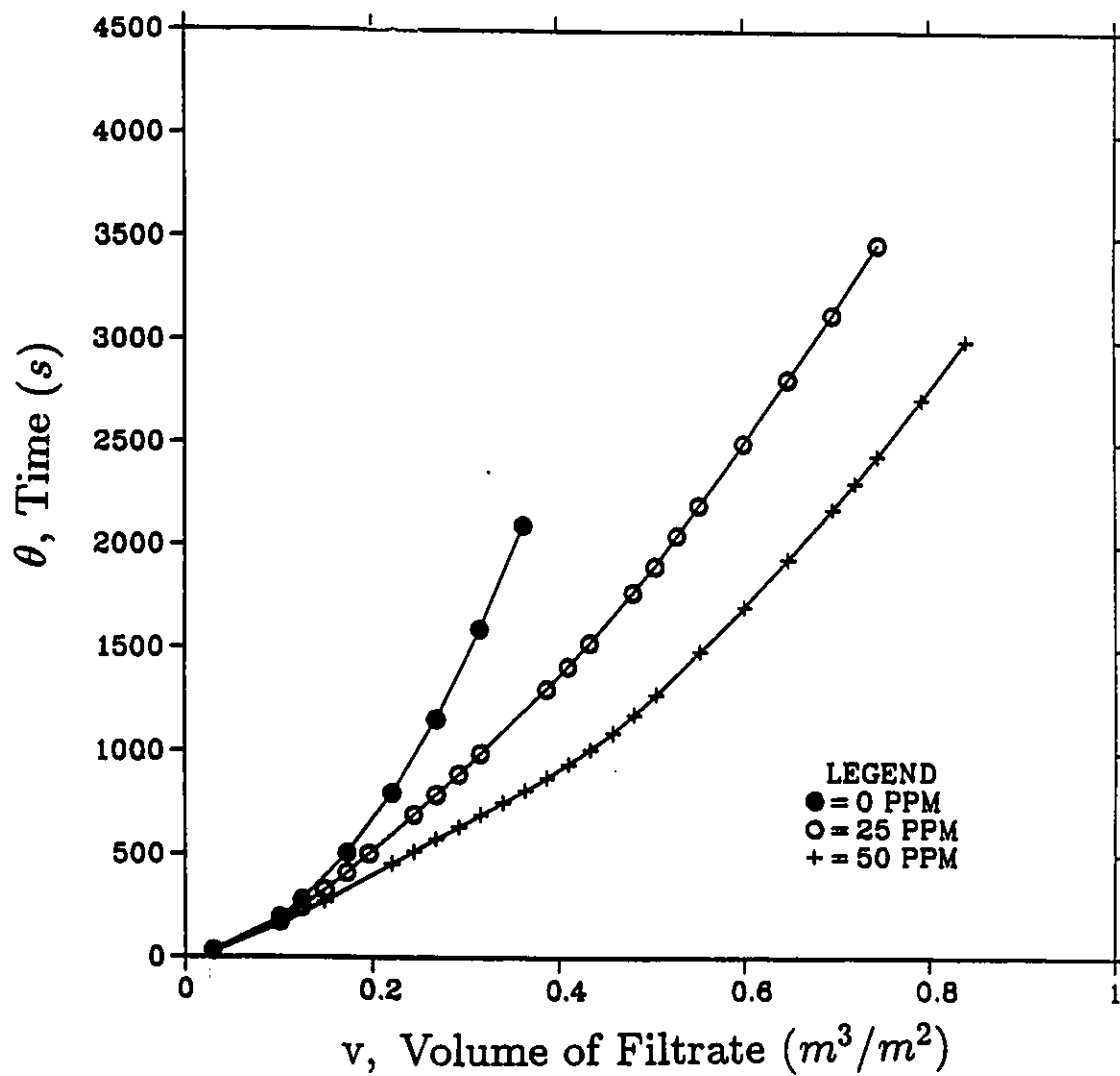


Figure 6.6: Volume of Filtrate Collected versus Time for Constant Pressure Filtration at 689 kPa (100 psi) of Slurries Comprising 10%  $w/w$   $CaCO_3$  in Aqueous Non-ionic Polyacrylamide Solutions.

reduction in the large voids, tending to cause a more uniform packing and voidage distribution (Grace, 1953). It may also be noted that when the polymer content in the slurry is augmented, the discontinuity occurs earlier and is more pronounced suggesting a collapse of greater extent in the cake. It appears that since the flocs and void spaces were larger when the polymer concentration of the solution was increased, the agglomerate structure was more labile and the filter cake began to collapse earlier in the experiment.

When the data sets with an anomaly were fitted with only a single curve, rather poor fits were obtained. The data were then fitted with two curves – Curve A fitting the data for the first part of the experiment, and Curve B fitting the data for the latter part of the experiment. This resulted in variances that were a good deal lower implying that an improvement was achieved. Table 6.1 displays the results of this compilation.

Runs were also carried out using 100 ppm polymer solutions for which data are not included in Table 6.1. Only three experiments out of the six tests using 100 ppm were accomplished. These results have been included in Appendix H for reference. It was impossible to obtain any readings for the three other tests because the flocs immediately fell to the bottom of the filter unit when filtration was commenced. The upward flow was not strong enough to counteract the gravitational acceleration of the large flocs.

In the ensuing discussion, the terms ‘water slurry’ and ‘Newtonian slurry’ will refer to a slurry composed of calcium carbonate and distilled water. The term ‘polymer slurry’ will describe a slurry of calcium carbonate in aqueous polyacrylamide solutions.

## **6.2 Interpretation of the Results**

Three phenomena were considered to occur during the constant pressure filtrations: flocculation, viscoelasticity, and polymer degradation.

### **6.2.1 Flocculation**

There was visual verification of flocculation occurring during the preparation of the slurries. Addition of calcium carbonate to a solution of distilled water and polyacrylamide

Table 6.1: Constant Pressure Filtration Characteristics for Various Filtration Pressures and Polymer Solutions. Slurry Concentration = 10% $\frac{w}{w}$  CaCO<sub>3</sub>.

<b>345 kPa, Anionic Polyacrylamide</b>						
Conc. ppm	Stage	$R_{ma} \times 10^{-11}$ $m^{-1}$	$\gamma_{av} \times 10^{-11}$ $m \cdot kg^{-1}$	$K_N$ $m \cdot s^{-2}$	$\theta_0$ $s$	$v_{mc}$ $m$
0		2.7	1.4	0.00015	0.8	0.016
25	A:	8.5	0.1	0.0014	-70.8	0.53
	B:	11.8	0.1	0.0014	-474.5	0.73
50	A:	1.2	0.08	0.0023	-4.4	0.12
	B:	13.4	0.2	0.0012	-1815.1	0.70

<b>345 kPa, Non-Ionic Polyacrylamide</b>						
Conc. ppm	Stage	$R_{ma} \times 10^{-11}$ $m^{-1}$	$\gamma_{av} \times 10^{-11}$ $m \cdot kg^{-1}$	$K_N$ $m \cdot s^{-2}$	$\theta_0$ $s$	$v_{mc}$ $m$
0		2.7	1.4	0.00015	0.8	0.016
25	A:	10.6	0.2	0.0011	-71.8	0.016
	B:	10.5	0.2	0.0010	-85.9	0.46
50	A:	6.6	0.07	0.0027	-54.8	0.79
	B:	1.0	0.22	0.00082	51.5	0.037

Table 6.1, continued

**517 kPa, Anionic Polyacrylamide**

Conc. ppm	Stage	$R_{ma} \times 10^{-11}$ $m^{-1}$	$\gamma_{av} \times 10^{-11}$ $m \cdot kg^{-1}$	$K_N$ $m \cdot s^{-2}$	$\theta_0$ $s$	$v_{mc}$ $m$
0		0.5	1.9	0.00018	0.4	0.023
25	A:	11.0	0.2	0.0012	-134.0	0.40
	B:	12.4	0.2	0.0012	-203.8	0.46
50	A:	0.3	0.02	0.0013	16.0	0.12
	B:	18.8	0.2	0.0012	-1689.0	0.64

**517 kPa, Non-Ionic Polyacrylamide**

Conc. ppm	Stage	$R_{ma} \times 10^{-11}$ $m^{-1}$	$\gamma_{av} \times 10^{-11}$ $m \cdot kg^{-1}$	$K_N$ $m \cdot s^{-2}$	$\theta_0$ $s$	$v_{mc}$ $m$
0		0.5	1.9	0.00018	0.4	0.023
25	A:	10.3	0.2	0.0014	-33.2	0.43
	B:	15.2	0.3	0.0011	-165.1	0.49
50	A:	8.8	0.2	0.0017	-0.1	0.43
	B:	2.5	0.3	0.00088	131.3	0.067

Table 6.1, continued

**689 kPa, Anionic Polyacrylamide**

Conc. ppm	Stage	$R_{ma} \times 10^{-11}$ $m^{-1}$	$\gamma_{av} \times 10^{-11}$ $m \cdot kg^{-1}$	$K_N$ $m \cdot s^{-2}$	$\theta_0$ $s$	$v_{me}$ $m$
0		1.4	2.2	0.00021	15.7	0.0055
25	A:	1.4	0.3	0.0014	-4.5	0.046
	B:	1.7	0.3	0.0014	-8.8	0.052
50	A:	1.0	0.07	0.0055	-0.5	0.13
	B:	31.2	0.3	0.0012	-2138.2	0.88

**689 kPa, Non-Ionic Polyacrylamide**

Conc. ppm	Stage	$R_{ma} \times 10^{-11}$ $m^{-1}$	$\gamma_{av} \times 10^{-11}$ $m \cdot kg^{-1}$	$K_N$ $m \cdot s^{-2}$	$\theta_0$ $s$	$v_{me}$ $m$
0		1.4	2.2	0.00021	15.7	0.0055
25	A:	16.7	0.3	0.0011	-83.6	0.43
	B:	17.3	0.4	0.0010	-199.8	0.40
50	A:	13.9	0.4	0.0014	-23.6	0.34
	B:	15.0	0.4	0.0012	-313.0	0.34

produced a slurry of tiny white curds and clear supernatant liquid. This was somewhat divergent from the appearance of the slurry consisting of distilled water and calcium carbonate, which displayed a milky consistency. The extent of flocculation was greater with the anionic polyacrylamide than for the non-ionic polyacrylamide, since the flocs of the anionic polyacrylamide tended to be larger, and the supernatant liquid, clearer.

The filter cakes produced with the polymer slurries also appeared quite different from those obtained with water slurries. The water slurry created a smooth cake in contrast to the cake from the polymer slurry, which had a coarse appearance of curds and voids at the bottom, and these curds and voids gradually diminished in size towards the top of the cake, approaching the septum. This polymer cake appeared less compacted than the Newtonian filter cake.

The primary effect of the flocculation was the creation of larger voids in the cake. The filter cake resistance  $\gamma_{av}$  reveals this effect. Table 6.1 clearly indicates that for all of the pressure drops investigated, the  $\gamma_{av}$  for the slurries containing either polymer (anionic or non-ionic), is lower than the  $\gamma_{av}$  for the water slurries. Grace (1953) reported a similar result with the use of the flocculent Dow polystyrene latex and calcium carbonate; and Rao (1970), who employed hydroxyethyl cellulose<sup>1</sup> and calcium carbonate, found that the porosities of the cakes were much greater than obtained with the water slurries.

## 6.2.2 Compressive Pressure Reduction

Flocculation is not solely responsible for the large decrease in  $\gamma_{av}$ . A decline in the compressive pressure is the second reason why  $\gamma_{av}$  was lower for the slurries containing polymer.

Figure 6.7 indicates that the lower the compressive pressure, the higher the specific cake resistance. Since the  $\gamma_{av}$ 's were lower for the slurries containing the polymer, then the compressive pressures must, of necessity, have been lower where the polymer was involved. The viscoelastic nature of the polyacrylamide diminished the compressive pressure in two ways: (1) in the uncoiling, or stretching<sup>2</sup> of the elastic molecules; and possibly, (2) in degradation due to the fracture of the polymer molecules. In mathematical terms, the

---

<sup>1</sup>The hydroxyethyl cellulose, Natrosol 250 HR, is a high molecular weight polymer with viscoelastic character.

<sup>2</sup>The terms "uncoiling" and "stretching" are utilized in the literature to refer to the changes in conformation of the polymer which causes the macromolecule to extend over a greater length. These terms do not imply that the carbon-carbon bond length is made longer.

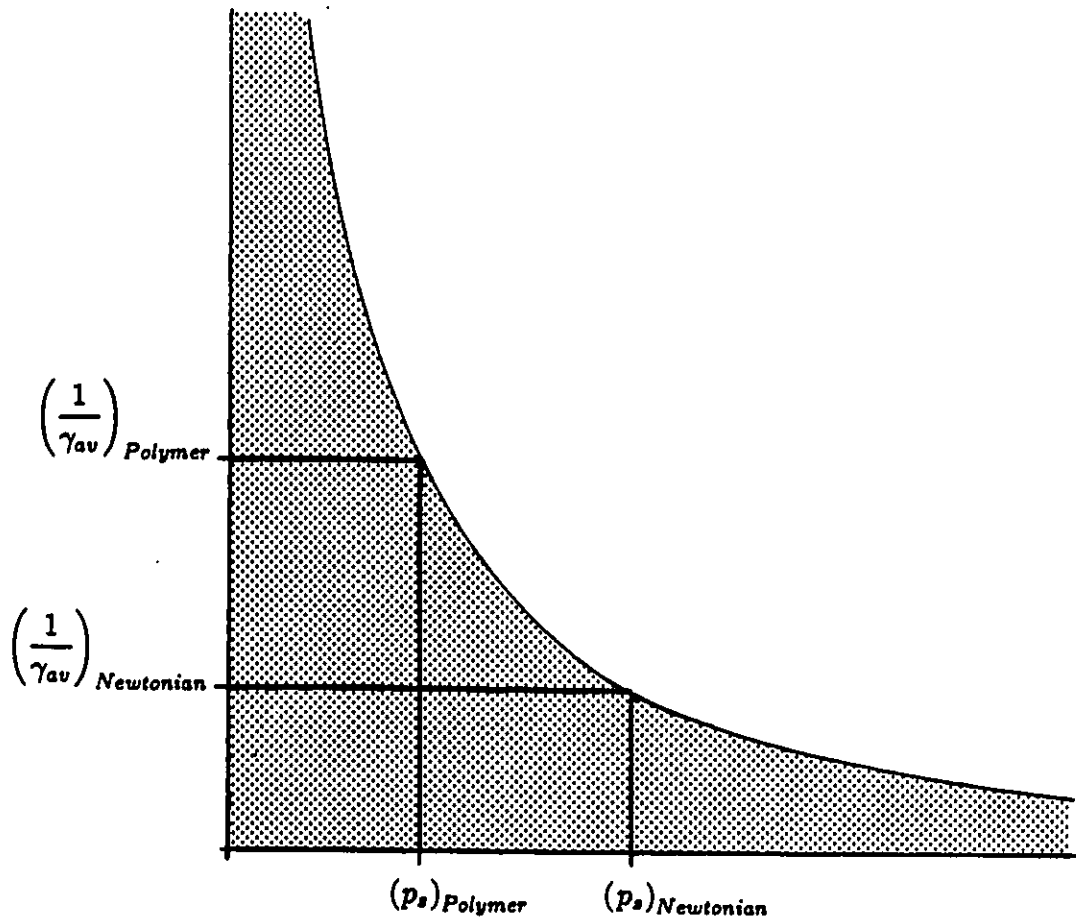


Figure 6.7: Plot of  $\frac{1}{\gamma_{av}}$  versus compressive pressure  $p_s$  to illustrate the effect of the compressive pressure on the specific cake resistance.

compressive pressure  $p_s$  in viscoelastic filtration is

$$p_s = p + \underbrace{\Delta\bar{\tau}_{11}}_{\text{a negative quantity}} \quad (6.2)$$

whereas for the Newtonian filtration, the compressive pressure is simply

$$p_s = p \quad (6.3)$$

The principal difference between the viscoelastic filtration and the Newtonian filtration is that additional normal stresses were present in the filtration involving the viscoelastic polymer. Although the viscoelastic and the Newtonian filtrations were carried out at constant pressure drop, the viscoelastic filtration may not have been rendered at *constant potential*. That is to say that for a Newtonian filtration, the potential is given by

$$\Delta\mathcal{P} = p + \rho g \Delta h \quad (6.4)$$

which is higher than the potential in a viscoelastic filtration,

$$\Delta\bar{\Pi}_{11} = p + \rho g \Delta h + \underbrace{\Delta\bar{\tau}_{11}}_{\text{a negative quantity}} \quad (6.5)$$

for the same filtration pressure.

In industry, viscoelastic filtration would have to be carried out at higher operating pressure drops to achieve the same endpoint as in the Newtonian filtration.

### 6.2.3 Viscoelasticity

An explanation is required for the increase in the  $\gamma_{av}$  from Part A to Part B in the filtration experiments. The ensuing elaboration on viscoelasticity affords insight.

#### Role of Viscoelasticity

Dauben and Menzie (1967) described well the role of viscoelasticity in flow through a porous medium:

“For polymers of extremely high molecular weight to propagate through a low-permeability porous media system, the polymer molecules must be capable of deforming sufficiently to flow through the tight and tortuous flow channels. This would indicate that polymers most suitable for propagation in porous media

would exhibit viscoelastic effects... Extremely high molecular weight polymer solutions showing little or no elastic effects will likely plug a low-permeability porous matrix."

### Normal Stresses

In flowing through a filter cake, the macromolecules undergo a series of accelerations and decelerations as they flow through the tortuous, compressing filter cake. These accelerations and decelerations, expressed mathematically as  $\frac{\partial v_x}{\partial x}$ , generate normal stresses which act on the polymer molecules. The capillaries become more narrow approaching the filter cloth, thereby accelerating the molecules further with a corresponding increase in the normal stress level. Under this applied stress, the polymer coils become distorted and less able to interpenetrate neighbouring coils (Merrill, 1963). This disentangling of the network of loops a macromolecule forms with other macromolecules is known as a *reversible decay of fluid elasticity*. If the rate at which the molecules are strained is high, the molecules may stretch to the extent that they fracture.

### Increased Flow Resistance

Viscoelastic fluids develop a measurable elastic potential energy during flow (Dauben and Menzie, 1967). In other words, a viscoelastic polymer molecule is much like an ordinary spring. When the spring is stretched, kinetic energy is consumed and stored as potential energy.

When the polymer molecule is made to flow through a conduit, the macromolecule and the surrounding solvent have kinetic energy. Part of this kinetic energy is stored as potential energy in the macromolecule when the polymer extends. The macromolecule and surrounding solvent now have a lower kinetic energy and are moving more slowly than before. The fluid behind this slower-moving polymer is therefore hindered to move forward at the speed it previously had, and the flow resistance is greater.

From this information, it was expected that the values of  $\gamma_{av}$  would be higher in Stage B than in Stage A. From Table 6.1, this result is not apparent at 25 ppm, but is observable at 50 ppm. At 25 ppm, the polymer concentration is low, and after flocculation, the corresponding polymer concentration in the fluid flowing through the filter cake is quite small. It is suspected that because the specific cake resistance is unchanged from Stage A to Stage B, that little energy is consumed by the flowing fluid for the trials at 25 ppm.

At 50 ppm, the polymer concentration was high enough to reveal an increase in the  $\gamma_{av}$ 's. The collapsing of the filter cake further contributed to narrowing of the cake pores in Stage B, thereby increasing the flow resistance. It is also possible that there was adsorption of polymer molecules to the walls of the capillaries in the cake. This adsorbed polymer built up over time. The capillaries were narrowed and offered greater flow resistance. Hence, it is conceivable that the cake resistance was larger in Stage B than in Stage A.

#### 6.2.4 Polymer Degradation

##### Apparent Filter Medium Resistance:

If the rate at which the molecules are strained is high, the molecules may stretch to the extent that they are fractured. The filter cloth provides an environment dramatically different from that of the filter cake, and it is likely that this sudden change in porous structure altered the strain level. As a consequence, scissioning of the polymers may have occurred in addition to the disaggregating and uncoiling of the polymer molecules.

The filter medium resistance for a Newtonian filtration is calculated from the expression

$$R_m = \frac{\gamma_{av} v_m \rho s}{(1 - ms)} \quad (6.6)$$

while for a filtration involving polymer, an apparent filter medium resistance  $R_{ma}$  is appropriate,

$$R_{ma} = \frac{\gamma_{av} v_{me} \rho s}{(1 - ms)} \quad (6.7)$$

Since  $R_{ma}$  is directly proportional to the filter cake resistance  $\gamma_{av}$ , it was expected that the  $R_{ma}$  would follow the trend of  $\gamma_{av}$ . However, this is not the case. For instance, considering the simplest case – the water slurries – with an increase in pressure, the  $\gamma_{av}$  increased, but the filter medium resistance decreased. The theoretical analysis affords insight into the tendency of the filter medium resistance.

In the theoretical development, it was shown that

$$v_{me} = \frac{(1 - ms)}{\gamma_{av} \rho s} \left[ R_m + \frac{k' \Delta \bar{\eta}}{2\epsilon D_p} \left( \frac{\xi n + 1}{n + 1} \right) \left( \frac{q}{q_1} \right) \left( \frac{1}{K} \right) \right] \quad (6.8)$$

which may be rearranged to define the apparent filter medium resistance

$$R_{ma} = \frac{v_{me} \gamma_{av} \rho s}{(1 - ms)} = R_m + \underbrace{\frac{k' \Delta \bar{\eta}}{2\epsilon D_p} \left( \frac{\xi n + 1}{n + 1} \right) \left( \frac{q}{q_1} \right) \left( \frac{1}{K} \right)}_{\text{elastic contribution}} \quad (6.9)$$

elastic contribution

(a positive quantity)

Hence, the filter medium resistance of a viscoelastic filtration is the filter medium resistance of the Newtonian filtration (at the same operating conditions) plus an "elastic contribution". The elastic contribution is the additional resistance offered by the presence of the viscoelastic polymer in the filtration. Mathematically, it was expected that the  $R_{ma}$ 's would be larger than the  $R_m$ 's.

The majority of the experimental results indicate the  $R_{ma}$ 's of Stage B to be larger than the  $R_m$  values for the water slurries. When the polymer molecules are not present, as in the filtration of the water slurries, the resistance to flow stems only from viscous drag. However, when the viscoelastic macromolecules are present in the slurry, the flow resistance is the result of both viscous drag and the elastic contribution.

The  $R_{ma}$  values of Stage B were remarkably larger than the  $R_{ma}$  values of Stage A, and it is deduced that the elastic contribution in Stage B is much larger than in Stage A. The discrepancy between the  $R_{ma}$ 's of Stages A and B is remarkably larger than the discrepancy between the  $\gamma_{av}$ 's of Stages A and B. To present such a large increase in the filter medium resistance, the elastic contribution of the polymer is likely to include fracturing of the polymer molecules as they proceeded from the filter cake to the dramatically different environment of the filter cloth.

### 6.3 Critical Evaluation of the Results

The experimental error was estimated to be approximately 3% in the values of  $R_{ma}$  and  $\gamma_{av}$ .

A comparison to the works of Rao (1970) and Fu (1977) show similar trends in the  $\gamma_{av}$ 's and  $R_{ma}$ 's of this thesis. For instance, it is apparent that with an increase in pressure drop, both the filter cake and filter medium resistances increase. Furthermore, with an increase in polymer concentration, Rao (1970) and Fu (1977) found the  $\gamma_{av}$ 's to decrease, which concurs with the findings of this thesis. Table 6.2 gives a summary of this comparison. The data provided in this thesis are, perhaps, more revealing of viscoelastic effects than that of Rao (1970) and Fu (1977) because the equipment design in this work was more conducive to viscoelastic flow (i.e., utilizing a  $N_2$  gas-driven filtration apparatus, instead of employing a gear pump to propagate the slurry through the filter unit).

Table 6.2: Comparison of thesis work in Constant Pressure Filtration of Rao (1970) and Fu (1977) to work in this thesis. Symbolic notation is employed for quick comparison of trends.

author	with an increase in pressure drop	with an increase in polymer concentration
Rao	$\gamma_{av}$ ↓ $R_{ma}$ (irregular)	$\gamma_{av}$ ↑ $R_{ma}$ ↑
Fu	$\gamma_{av}$ ↓ $R_{ma}$ ↑	$\gamma_{av}$ ↑ $R_{ma}$ ↑
Slegr	$\gamma_{av}$ ↓ $R_{ma}$ ↑	$\gamma_{av}$ ↑ $R_{ma}$ ↑

### Possible Significance

The possible significance of the experimental work of this thesis was to provide a preliminary perspective on filtration in viscoelastic media. Experimentation still plays an essential role in the prediction of filtration characteristics, particularly when compressible cakes are involved (Shirato, et al., 1977). Furthermore, an understanding of filtration in viscoelastic media may provide economic improvement and operating efficiency to the processing of a diversity of polymeric products.

## 6.4 Addendum

A summary of the answers to the question 'How are viscoelastic effects revealed in constant pressure cake filtration?' will be presented.

It was determined that the viscoelasticity of the polyacrylamides was partially responsible for reducing the compressive pressure in the cakes, thereby decreasing the values of  $\gamma_{av}$  compared to the  $\gamma_{av}$  of the water slurries.

In comparing the filter medium resistance of the water slurry filtrations with the apparent values  $R_{ma}$  for the polymer slurry filtrations, it was apparent that the  $R_{ma}$  of Stage B of most of the experiments was larger by one order of magnitude than the  $R_{ma}$  values for the water slurries.

## Chapter 7

# Conclusions

1. The filter cake resistance  $\gamma_{av}$  for the filtrations involving the polyacrylamides are lower than for those not involving the polymer.
2. The filter medium resistance  $R_{me}$  for filtration of the polymer slurries were much higher than the  $R_{me}$  for the water slurries.
3. For the non-linear filtration equation, Equation (2.87), the  $v, \theta$  data were not conducive to the level of discrimination required to yield all four parameters  $K_N, v_{me}, \theta_0$  and  $N$  by minimization of the sum squares of residuals, using a search procedure.
4. The extent of flocculation was greater with the anionic polyacrylamide than with the non-ionic polyacrylamide.
5. Although the viscoelastic filtrations were carried out at constant pressure drop, they may not have been rendered at constant potential.

## Chapter 8

# Recommendations

1. The moisture ratio of the cakes included with each data set are not the *true* moisture ratios because the cake weights also included the weight of the polyacrylamide. To obtain the *true* moisture ratio, an additional weight is required. Following the heating of the cake at 115°C and weighing, the cake should be returned to a hot oven, at a temperature which would completely burn away the polyacrylamide, and reweighed. In this way, the exact polymer content may be established. This quantity may then be subtracted from the weight of the wet cake, and from the weight of the cake after it was taken out of the oven at 115°C.
2. A pressure gauge should be added on the downstream side of the filter unit to ensure that the pressure at this location is atmospheric pressure (i.e., that the gauge pressure is zero).
3. After the polymer slurry has been prepared, and before the slurry is about to be filtered, the viscosity of a sample of the supernatant liquid should be measured. The sample taken must be as small as possible so as not to change the concentration of the slurry. This viscosity measurement should be compared to that of the filtrate to give an idea about the extent of the polymer degradation occurring during the filtration. Also, the filtrate should be stored for a day to allow the polymer networks to reform. An additional viscosity measurement at this time could give an indication of the extent of the polymer fracture that took place in the filtering process.
4. Brass is not a suitable material for the porous plate supporting the filter cloth. This porous support plate should be of another material, for example, stainless steel, be-

cause polyacrylamide degrades in the presence of brass (Cohen, 1981). A plexiglass porous plate was employed for a filtration run, and it proved to be incapable of withstanding the large pressures. A stainless steel plate would be more suitable.

5. To better evaluate  $[\eta]$  and  $\overline{M}_v$ , viscosity measurements of more concentrated aqueous solutions of polyacrylamide should be made (e.g., in the concentration range of 1000 ppm and larger.).
6. A survey of the quality of the distilled water available from the fourth floor of the Colonel By Building should be instigated, to establish how the quality varies from day to day, week to week, etc., and to exercise some control over the range of variation of pH and the composition of the water.

## References

- Bajjal, S.K. and N.C. Dey. "Role of Molecular Parameters during Flow of Polymer Solutions in Consolidated Porous Media". *J.Appl.Polym.Sci.*, 27:121-131, (1982).
- Billmeyer, F.W. "*Textbook of Polymer Science*". John Wiley & Sons, New York, N.Y., 3<sup>rd</sup> edition, (1984).
- Bird, R.B., R.C. Armstrong and O. Hassanger. "*Dynamic Behavior of Polymeric Liquids: Fluid Mechanics*". Volume 1, John Wiley & Sons, New York, N.Y., (1977a).
- Bird, R.B., R.C. Armstrong and O. Hassanger. "*Dynamic Behavior of Polymeric Liquids: Kinetic Theory*". Volume 2, John Wiley & Sons, New York, N.Y., (1977b).
- Brandrup, J. and E.H. Immergut. "*Polymer Handbook*". John Wiley & Sons, New York, N.Y., (1989).
- Cohen, Y. "*Behavior of Polymer Solutions in Non-Uniform Flows*". PhD thesis, University of Delaware, (1981).
- Dauben, D.L. and D.E. Menzie. "Flow of Polymer Solutions Through Porous Media". *J.Petrolm.Technol.*, 240:1065-1071, (1967).
- Daza, A. "*Agglomeration and Flocculation of Calcium Carbonate Particles in Polymer Solutions*". B.A.Sc. Thesis (Chemical Engineering), University of Ottawa, Ottawa, Canada, (1991).
- Durst, F., R. Haas and W. Interthal. "Laminar and Turbulent Flows of Dilute Polymer Solutions: A Physical Model". *Rheol.Acta*, 21:572-577, (1982).
- Ferry, John D. "*Viscoelastic Properties of Polymers*". John Wiley & Sons, New York, N.Y., 2<sup>nd</sup> edition, (1970).

- Fu, C.T. "Filtration of Drag Reducing Fluids". Master's thesis, University of Ottawa, Ottawa, Canada, (1977).
- Grace, H.P. "Resistance and Compressibility of Filter Cakes". *Chem.Eng.Progress*, 49:303-318, (1953).
- Haas, R. and F. Durst. "Viscoelastic Flow of Dilute Polymer Solutions in Regularly Packed Beds". *Rheol.Acta*, 21:566-571, (1982).
- James, D.F. and D.R. McLaren. "Laminar Flow of Dilute Polymer Solutions through Porous Media". *J.Fluid.Mech.*, 70(4):733-752, (1975).
- Keller, A. and J.A. Odell. "Flow-Induced Chain Fracture of Isolated Linear Macromolecules in Solution". *Colloid.Polym.Sci.*, 263:181, (1985).
- Klein, J. and K.-D. Conrad. "Molecular Weight Determination of Poly(acrylamide) and Poly(acrylamide-co-sodium acrylate)". *Makromol.Chem.*, 179:1635, (1978).
- Kozicki, W. "Factors Affecting Cake Resistance in Non-Newtonian Filtration". *Can.J.Chem.Eng.*, 68:75, (1990a).
- Kozicki, W. "Theoretical Aspects for Constant Pressure Filtration in Viscoelastic Media". (1990b). unpublished manuscript.
- Kozicki, W. and C. Tiu. "A Unified Model for Non-Newtonian Flow in Packed Beds and Porous Media". *Rheol.Acta.*, 27:31-38, (1988).
- Kozicki, W., A.R.K. Rao and C. Tiu. "Filtration of Polymer Solutions". *Chem.Eng.Sci.*, 27:615-625, (1972).
- Kulicke, W.-M., and R. Haas. "Flow Behavior of Dilute Polyacrylamide Solutions Through Porous Media. 1. Influence of Chain Length, Concentration, and Thermodynamic Quality of the Solvent". *Ind.Eng.Chem.Fundam.*, 23:308-315, (1984a).
- Kulicke, W.-M., and R. Haas. "Flow Behavior of Dilute Polyacrylamide Solutions Through Porous Media. 2. Indirect Determination of Extremely High Molecular Weights and Some Aspects of Viscosity Decrease over Long Time Intervals". *Ind.Eng.Chem.Fundam.*, 23:316-319, (1984b).

Langhorst, M.A., F.W. Stanley Jr., S.S. Cutié, J.H. Sugarman, L.R. Wilson, D.A. Hoagland and R.H. Prud'homme. "Determination of Non-ionic and Partially Hydrolyzed Polyacrylamide Molecular Weight Distributions Using Hydrodynamic Chromatography". *Anal. Chem.*, 58(11):2242-2247, (1986).

Lepley, R.H. "*Kirk-Othmer Encyclopedia of Chemical Technology*", chapter entitled "Resins, Water Soluble", pages 427-432. Volume 4, John Wiley & Sons, New York, N.Y., 3<sup>rd</sup> edition, (1978).

Marshall, R.J. and A.B. Metzner. "Flow of Viscoelastic Fluids Through Porous Media". *Ind.Eng.Chem.Fund.*, 6:393-400, (1967).

Merrill, E.W., H.S. Mickley, A. Ram and W.H. Stockmayer. "Upper Newtonian Regime in Polymer Solutions. II: General Observations". *Trans.Soc.Rheology*, VI:119-129, (1962).

Molyneux, P. "*Water Soluble Synthetic Polymers*". Volume 1, CRC Press, Inc., Boca Raton, Florida, (1984).

Odell, J.A., A.J. Müller and A. Keller. "Non-Newtonian Behavior of Hydrolyzed Polyacrylamide in Strong Elongational Flows: A Transient Approach". *Polymer*, 28:1179-1190, (1988).

Perry, John H. "*Chemical Engineers' Handbook*". McGraw-Hill Book Company, Inc., New York, N.Y., 3<sup>rd</sup> edition, (1950).

Pye, D.J. "Improved Secondary Recovery by Control of Water Mobility". *J.Pet.Tech.*, 16:911-916, (1964).

Rao, A.R.K. "*Filtration of Non-Newtonian Fluids*". PhD thesis, University of Ottawa, Ottawa, Canada, (1970).

Shirato, M., M. Sambuichi, H. Kato and T. Aragaki. "Flow Through Compressible Cake Under Constant Pressure Filtration". *J.Chem.Eng.Japan*, 31:359-364, (1967).

Shirato, M., M. Sambuichi, H. Kato and T. Aragaki. "Internal Flow Mechanisms in Filter Cakes". *AIChE J.*, 15:405-409, (1969).

- Shirato, M., M. Sambuichi, T. Murase, T. Aragaki, K. Kobayashi and E. Iritani. "Theoretical and Experimental Studies in Cake Filtration". *Nagoya Daigaku, Faculty of Engineering Memoirs*, 37:1-91, (1985).
- Shirato, M., T. Aragaki and S. Fujiyoshi. "Generalized Filtration Theory for Newtonian and Non-Newtonian Fluids". *First World Filtration Congress*, A8:1-5, May 14-17 (1974).
- Shirato, M., T. Aragaki, E. Iritani, M. Wakimoto, S. Fujiyoshi and S. Nanda. "Constant Pressure Filtration of Power Law Non-Newtonian Fluids". *J.Chem.Eng.Japan*, 10:54-60, (1977).
- Silberberg, A., J. Eliassaf and A. Katchalsky. "Temperature-Dependence of Light Scattering and Intrinsic Viscosity of Hydrogen Bonding Polymers". *J.Polym.Sci.*, 23:259-260, (1957).
- Smith, D.A. "*Addition Polymers: Formation and Characterization*". Plenum Press, New York, N.Y., (1968).
- Teot, A.S. "*Kirk-Othmer Encyclopedia of Chemical Technology*", chapter entitled "Calcium Carbonate", pages 212-216. Volume 20, John Wiley & Sons, New York, N.Y., 3<sup>rd</sup> edition, (1978).
- Ternay, A.L. "*Contemporary Organic Chemistry*". W.B. Saunders Company, Philadelphia, (1976).
- Tiller, F.M. and M. Shirato. "New Definition of Filtration Resistance". *AIChE J.*, 10:61-67, (1964).
- Tobolsky, A.V. and H.F. Mark. "*Polymer Science and Materials*", chapter 2, pages 12-13. Volume 1, John Wiley & Sons, New York, N.Y., (1971).
- Williams, D.J. "*Polymer Science and Engineering*". Prentice-Hall, Inc., Englewood Cliffs, N.J., (1971).

# Appendix A

## 9.1 Computer Programs

- COUNT FORTRAN
- data file which may be used with either COUNT FORTRAN or MERGE FORTRAN
- output file of COUNT FORTRAN
- MERGE FORTRAN
- F EXEC

The following is a copy of the programme COUNT FORTRAN.

```

C.....
C THIS PROGRAMME IS FOR SOLVING FOR THE THREE UNKNOWN PARAMETERS
C KAPPA, VO, AND THETA FOR CONSTANT PRESSURE FILTRATION.
C IT USES IMSL SUBROUTINE IFLSQ(...) WITH THE FLOW BEHAVIOR
C INDEX EQUAL TO 1.0 TO EVALUATE X(1,2,3).
C
C USE F EXEC TO RUN THE PROGRAM.
C
C M = NO. OF DATA POINTS
C L = NO. OF PARAMETERS
C X(1,2,3) = UNKNOWN PARAMETERS
C F(I) = EXPT. VALUE MINUS YOUR MODEL
C BKAPPA=X(1), BTHETA=X(2), BVO=X(3)
C UNITS: THETA IN SECONDS
C KAPPA IN SQUARE FEET PER SECOND
C VO IN FEET
C N IS DIMENSIONLESS
C ALPHA IN FEET PER POUND
C RM IN RECIPROCAL FEET.
C.....
PROGRAM COUNT
IMPLICIT DOUBLE PRECISION (A-H,O-Z)
EXTERNAL FCN
DIMENSION V(50),THETA(50),Q(50),QTHETA(50),BKAPPA(50),
+BTHTAO(50),BVO(50),BN(50),F(50),X(10),BF(50)
COMMON/AA/IN,IO,M,L,N,ITER
COMMON/CC/AKAPPA,ATHTAO,AN
COMMON/DD/BKAPPA,BTHTAO,BVO,BN
COMMON/EE/V,THETA,J
COMMON/GG/BF
COMMON/HH/IDRCTN
COMMON/KK/ES,P,AMOIST
COMMON/LL/RHO,AMU
COMMON/MM/Q,QTHETA
COMMON/NN/K
COMMON/OO/JJ

C
C IN=15
C IO=16
C N=3

C
C CALL READ
C DO 100 IDRCTN=1,2
100 CALL SOLVE
C
C STOP
C END

C
C
C SUBROUTINE READ
C IMPLICIT DOUBLE PRECISION (A-H,O-Z)
C DIMENSION VV(50),V(50),VMETRC(50),FLOW(50),THETA(50),X(10),F(50)
C CHARACTER*72 TITLE,TITLE1,TITLE2
C COMMON/AA/IN,IO,M,L,N,ITER
C COMMON/BB/F,X,IXJAC,NSIG,EPS,DELTA,MAXFN,IOPT
C COMMON/EE/V,THETA,J
C COMMON/KK/ES,P,AMOIST
C COMMON/LL/RHO,AMU
C COMMON/NN/K
C COMMON/PP/FLOW

C
C READ(IN,50)TITLE
C WRITE(IO,50)TITLE
C READ(IN,80)M
C WRITE(IO,80)M
C ITER=M-4

C

```

..., continued

```

READ(IN,50)TITLE
WRITE(10,50)TITLE
C
READ(IN,50) TITLE1
WRITE(10,60) TITLE2
C
DO 10 I=1,M
READ(IN,65) VV(I),THETA(I)
V(I) = VV(I)*0.00003531467/0.0450819
VMETRC(I) = V(I)/3.28084
WRITE(10,70) VV(I),V(I),VMETRC(I),THETA(I)
10 CONTINUE
C
READ(IN,50)TITLE
WRITE(10,85)TITLE
C
READ(IN,400)ES,P,AMOIST,RHO,AMU
WRITE(10,400)ES,P,AMOIST,RHO,AMU
C
P = P*144.0
RHO = RHO/0.016018
AMU = AMU*6.7197*(-4.0)
WRITE(10,500)TITLE
WRITE(10,450)ES,P,AMOIST,RHO,AMU
C
CONVERT TO METRIC
PMETRC = P/144.0*100.0/14.5038
RMETRC = RHO*0.016018*1000.0
WRITE(10,505)TITLE
WRITE(10,455)PMETRC,RMETRC
C
FORMAT STATEMENTS
50 FORMAT(A72)
60 FORMAT(4X,'VV(ML)',2X,'V(CUFT/SQFT)',4X,'V(METRES)',
+2X,'THETA(SECONDS)')
65 FORMAT(2F10.1)
70 FORMAT(1F10.1,4X,1F10.4,3X,1F10.3,6X,1F10.1)
80 FORMAT(I10)
85 FORMAT(/,A72)
400 FORMAT(1F10.3,1F10.1,1F10.4,2F15.4,/)
450 FORMAT(1F10.3,1F10.1,6X,1F10.4,4X,1F10.4,5X,1F10.6)
455 FORMAT(1F10.0,6X,1F10.1)
500 FORMAT(2X,'S(FRACT)',5X,'P(LBF/SQ.FT.)',3X,'MOIST',3X,'RHO(LBM/CU.
+FT.)',2X,'MU(LBM/FT.S.)')
505 FORMAT(/,4X,'P(KPA)',3X,'RHO(KG/CU.M.)')
C
RETURN
END
C
C
SUBROUTINE ARRAY
IMPLICIT DOUBLE PRECISION (A-H,O-Z)
DIMENSION Y(50),THETA(50),Q(50),QTHETA(50)
COMMON/AA/IN,IO,M,L,N,ITER
COMMON/EE/V,THETA,J
COMMON/HH/IDRCTN
COMMON/MM/Q,QTHETA
COMMON/NN/K
C
IF (IDRCTN.EQ.1) THEN
DO 10 I=K,M
Q(I-K+1)=V(I)
QTHETA(I-K+1)=THETA(I)
10 WRITE(10,990)K,I,Q(I-K+1),QTHETA(I-K+1)
CONTINUE
ENDIF
IF (IDRCTN.EQ.2) THEN
DO 20 I=1,K
Q(I)=V(I)
QTHETA(I)=THETA(I)
990 WRITE(10,990)K,I,Q(I),QTHETA(I)
20 FORMAT(1I2,2X,1I2,2X,1F10.4,1F10.1)
CONTINUE
ENDIF
C
RETURN
END

```

..., continued

```

SUBROUTINE SOLVE
IMPLICIT DOUBLE PRECISION (A-H,O-Z)
EXTERNAL BFUN,FCN
DIMENSION V(50),THETA(50),X(10),F(50),Q(50),BKAPPA(50),BTHTAO(50),
+BVO(50),BN(50),BWORK(90),BF(50),QTHETA(50),
+WK(130),FF(50)
CHARACTER*72 TITLE1
COMMON/AA/IN,IO,M,L,N,ITER
COMMON/DD/BKAPPA,BTHTAO,BVO,BN
COMMON/EE/V,THETA,J
COMMON/GG/BF
COMMON/HH/IDRCTN
COMMON/KK/ES,P,AMOIST
COMMON/LL/RHO,AMU
COMMON/MM/Q,QTHETA
COMMON/NN/K
COMMON/OO/JJ

```

```

C
IF(IDRCTN.EQ.1)THEN
WRITE(IO,91)TITLE
K=ITER
ENDIF
IF(IDRCTN.EQ.2)THEN
WRITE(IO,90)TITLE
K=5
ENDIF
C
DO 10 I=1,ITER
J=0
JJ=0
CALL ARRAY
C
IF(IDRCTN.EQ.1)THEN
MPOINT=M-K+1
CALL IFLSQ(FCN,Q,QTHETA,MPOINT,X,N,WK,IER)
ENDIF
IF(IDRCTN.EQ.2)THEN
MPOINT=K
CALL IFLSQ(FCN,Q,QTHETA,MPOINT,X,N,WK,IER)
ENDIF
C
BKAPPA(1)=1.0/X(3)
BTHTAO(1)=X(1)
BVO(1)=X(2)*BKAPPA(1)/2.0
EN=1.0
C
+ ALPHA = 32.174*(ABS((EN+1.0)/EN/BKAPPA(1))**EN)*P*(1.0-
(AMOIST*ES))/(AMU*RHO*ES)
RM = ALPHA*ABS(BVO(1))*RHO*ES/(1.0-(AMOIST*ES))
C
C
IF(IDRCTN.EQ.1)THEN
SUM=0.0
DO 30 II=1,M
FSUM=0.0
DO 31 III=1,N
FSUM = FSUM+(X(III)*Q(1)**(III-1))
F(II) = QTHETA(1)-FSUM
SUM=SUM+(F(II)**2)
30 CONTINUE
BF(1)=SUM/FLOAT(M-N)
ENDIF
IF(IDRCTN.EQ.2)THEN
SUM=0.0
DO 40 II=1,M
FFSUM=0.0
DO 41 III=1,N
FFSUM = FFSUM+(X(III)*Q(1)**(III-1))
FF(II) = QTHETA(1)-FFSUM
SUM=SUM+(FF(II)**2)
41

```

```

40          CONTINUE
          BF(1)=SUM/FLOAT(M-N)
          ENDIF
C
C          WRITE(10,121)BTHTAO(1),BKAPPA(1),BVO(1),BF(1),ALPHA, RM
C
C          IF(IDRCTN.EQ.1)THEN
C            K=K-1
C          ENDIF
C          IF(IDRCTN.EQ.2)THEN
C            K=K+1
C          ENDIF
C
C 10      CONTINUE
C
C          FORMAT STATEMENTS
90      FORMAT(/,2X,'ATHTAO',6X,'AKAPPA',9X,
+ 'AVO',8X,'VARIANCE',4X,'ALPHA',8X,'RM')
91      FORMAT(/,2X,'BTHTAO',6X,'BKAPPA',9X,
+ 'BVO',8X,'VARIANCE',4X,'ALPHA',8X,'RM')
121     FORMAT(1F8.1,2X,1E12.5,2X,1E12.5,2X,1E10.3,1X,1E10.3,
+1X,1E10.3)
C
C          RETURN
C          END
C
C
C          REAL FUNCTION FCN(KCOUNT,Q)
C          IMPLICIT DOUBLE PRECISION (A-H,O-Z)
C          REAL Q
C          INTEGER KCOUNT
C          COMMON/OO/JJ
C
C          JJ=JJ+1
C          IF(KCOUNT.EQ.1)THEN
C            FCN = 1.0
C          ENDIF
C          IF(KCOUNT.EQ.2)THEN
C            FCN = Q
C          ENDIF
C          IF(KCOUNT.EQ.3)THEN
C            FCN = Q**2
C          ENDIF
C
C          RETURN
C          END

```

The following is a typical data file which may be used with either COUNT FORTRAN or MERGE FORTRAN.

```

      m
      17
50 psi, 0 ppm, March 7, 1991
V, Volume(mL) THETA, (seconds)
122.      11.
322.      207.
422.      308.
522.      439.
622.      588.
722.      774.5
822.      981.5
922.     1202.5
1022.     1658.
1122.     1749.5
1222.     2081.
1322.     2398.
1422.     2758.
1522.     3150.5
1622.     3582.5
1722.     4011.
1822.     4472.
s(fract)  P(psi)      molal   rho(g/cu.cm)      mu(cP)
0.10      50.0 1.7555931 0.9971 0.8978518
.....

```

The following is an example of an output of COUNT FORTRAN.

```

      m
      17
50 psi, 0 ppm, March 7, 1991
vv(ML)  V(CUFT/SQFT)  V(METRES)  THETA(SECONDS)  FLOW(FT/S)
122.0    0.0956      0.029      11.0
322.0    0.2522      0.077      207.0    0.0007569
422.0    0.3306      0.101      308.0    0.0002543
522.0    0.4089      0.125      439.0    0.0001784
622.0    0.4872      0.149      588.0    0.0001332
722.0    0.5656      0.172      774.5    0.0001011
822.0    0.6439      0.196      961.5    0.0000815
922.0    0.7222      0.220     1202.5    0.0000651
1022.0   0.8006      0.244     1466.0    0.0000534
1122.0   0.8789      0.268     1749.5    0.0000448
1222.0   0.9572      0.292     2061.0    0.0000380
1322.0   1.0356      0.316     2398.0    0.0000327
1422.0   1.1139      0.340     2758.0    0.0000284
1522.0   1.1923      0.363     3150.5    0.0000249
1622.0   1.2706      0.387     3562.5    0.0000220
1722.0   1.3489      0.411     4011.0    0.0000195
1822.0   1.4273      0.435     4472.0    0.0000175

s(fract)  P(psi)  moist  rho(g/cu.cm)  mu(cP)
0.100     50.0    1.7556  0.9971        0.8979

S(FRACT)  P(LBF/SQ.FT.)  MOIST  RHO(LBM/CU.FT.)  MU(LBM/FT.S.)
0.100     7200.0  1.7556  62.2487        0.000603

P(KPA)    RHO(KG/CU.M.)
345.      997.1

BTHTAO    BKAPPA    BVO    VARIANCE    ALPHA    RM
-107.7    0.49182E-03  0.75680E-01  0.268E-02  0.207E+12  0.118E+12
 49.9     0.46991E-03  0.14707E-01  0.539E+01  0.216E+12  0.240E+11
 68.8     0.46730E-03  0.76107E-02  0.585E+01  0.218E+12  0.125E+11
 59.6     0.46663E-03  0.11133E-01  0.608E+01  0.217E+12  0.182E+11
 64.6     0.46786E-03  0.91254E-02  0.573E+01  0.217E+12  0.150E+11
 38.7     0.47214E-03  0.19915E-01  0.915E+01  0.215E+12  0.324E+11
 4.0      0.47841E-03  0.35286E-01  0.179E+02  0.213E+12  0.566E+11
 52.7     0.46910E-03  0.13075E-01  0.416E+01  0.217E+12  0.214E+11
 56.8     0.46829E-03  0.11191E-01  0.329E+01  0.217E+12  0.184E+11
 65.2     0.46650E-03  0.71479E-02  0.158E+01  0.218E+12  0.118E+11
 63.4     0.46690E-03  0.80271E-02  0.194E+01  0.218E+12  0.132E+11
 62.2     0.46719E-03  0.86499E-02  0.224E+01  0.218E+12  0.142E+11
 10.9     0.48245E-03  0.39314E-01  0.484E+02  0.211E+12  0.626E+11

ATHTAO    AKAPPA    AVO    VARIANCE    ALPHA    RM
-73.1     0.86533E-03  0.34083E+00  0.387E+01  0.118E+12  0.302E+12
-57.9     0.68046E-03  0.21346E+00  0.210E+03  0.149E+12  0.241E+12
-55.4     0.66198E-03  0.19986E+00  0.201E+01  0.154E+12  0.232E+12
-42.8     0.59649E-03  0.14837E+00  0.470E+01  0.171E+12  0.191E+12
-30.4     0.55254E-03  0.11135E+00  0.712E+02  0.184E+12  0.155E+12
-21.6     0.52939E-03  0.90439E-01  0.241E+01  0.192E+12  0.131E+12
-14.2     0.51417E-03  0.75723E-01  0.502E+03  0.198E+12  0.113E+12
 -8.2     0.50399E-03  0.65212E-01  0.153E+03  0.202E+12  0.994E+11
 -4.0     0.49799E-03  0.58816E-01  0.386E+02  0.204E+12  0.904E+11
  0.8     0.49209E-03  0.51739E-01  0.430E+02  0.207E+12  0.807E+11
  4.0     0.48864E-03  0.47486E-01  0.230E+02  0.208E+12  0.746E+11
  6.7     0.48428E-03  0.41817E-01  0.196E+02  0.210E+12  0.663E+11
 10.9     0.48245E-03  0.39314E-01  0.484E+02  0.211E+12  0.626E+11

```

The following is a copy of the programme MERGE FORTRAN.

```

C.....
C   THIS PROGRAMME IS FOR SOLVING FOR THE FOUR UNKNOWN PARAMETERS
C   USING FINITE DIFFERENCE LEVENBERG-MARQUARDT ALGORITHM TO
C   EVALUATE THE FOUR PARAMETERS KAPPA, VO, N, AND THETAO.
C   IT REQUIRES A INITIAL ESTIMATE OF THE FOUR PARAMETERS FROM
C   THE SUBROUTINE IFLSQ(...). THEN
C   IT USES IMSL SUBROUTINE ZXSSQ(...) TO ESTIMATE X(1,2,3,4).
C
C   USE F EXEC TO RUN THE PROGRAM.
C
C   M = NO. OF DATA POINTS
C   N,L = NO. OF PARAMETERS
C   X(1,2,...,4) = UNKNOWN PARAMETERS
C   F(I) = EXPT. VALUE MINUS YOUR MODEL
C   BKAPPA=X(1), BTHETAO=X(2), BVO=X(3), BN=X(4)
C   UNITS:   THETAO IN SECONDS
C           KAPPA IN SQUARE FEET PER SECOND
C           VO IN FEET
C           N IS DIMENSIONLESS
C           ALPHA IN FEET PER POUND
C           RM IN RECIPROCAL FEET.
C.....
C   PROGRAM MERGE
C   IMPLICIT DOUBLE PRECISION (A-H,O-Z)
C   EXTERNAL BFUN,FCN
C   DIMENSION V(50),THETA(50),Q(50),QTHETA(50),BKAPPA(50),
C   +BTHTAO(50),BVO(50),BN(50),F(50),X(4),BF(50),PARG(4),
C   +BXJAC(50,4),BXJTJ(10),BWORK(90)
C   COMMON/AA/IN,IO,M,L,N,ITER
C   COMMON/BB/F,X,IXJAC,NSIG,EPS,DELTA,MAXFN,IOPT
C   COMMON/CC/AKAPPA,ATHTAO,AN
C   COMMON/DD/BKAPPA,BTHTAO,BVO,BN
C   COMMON/EE/V,THETA,J
C   COMMON/GG/BF
C   COMMON/HH>IDRCTN
C   COMMON/KK/ES,P,AMOIST
C   COMMON/LL/RHO,AMU
C   COMMON/MM/Q,QTHETA
C   COMMON/NN/K
C   COMMON/OO/JJ
C
C   IN=15
C   IO=16
C   L=3
C   N=4
C   IXJAC=15
C   NSIG=3
C   EPS=0.
C   DELTA=0.
C   MAXFN=700
C   IOPT=1
C
C   CALL READ
C   DO 100 IDRCTN=1,2
100   CALL ENTEGO
C
C   STOP
C   END
C
C
C

```

```

SUBROUTINE READ
IMPLICIT DOUBLE PRECISION (A-H,O-Z)
DIMENSION VV(50),V(50),VMETRC(50),THETA(50),X(4),F(50)
CHARACTER*72 TITLE,TITLE1,TITLE2,TITLE3
COMMON/AA/IN,IO,M,L,N,ITER
COMMON/BB/F,X,IXJAC,NSIG,EPS,DELTA,MAXFN,IOPT
COMMON/EE/V,THETA,J
COMMON/KK/ES,P,AMOIST
COMMON/LL/RHO,AMU
COMMON/NN/K
C
READ(IN,50)TITLE
WRITE(10,50)TITLE
READ(IN,80)M
WRITE(10,80)M
ITER=M-4
C
READ(IN,50)TITLE
WRITE(10,50)TITLE
C
READ(IN,50) TITLE1
WRITE(10,80) TITLE2
C
DO 10 I=1,M
READ(IN,65) VV(I),THETA(I)
V(I) = VV(I)*0.00003531467/0.0450819
VMETRC(I) = V(I)
WRITE(10,70) VV(I),V(I),VMETRC(I),THETA(I)
10 CONTINUE
C
READ(IN,50)TITLE3
WRITE(10,85)TITLE3
C
READ(IN,400)ES,P,AMOIST,RHO,AMU
WRITE(10,400)ES,P,AMOIST,RHO,AMU
C
P = P*144.0
RHO = RHO/0.016018
AMU = AMU*6.7197*(10.0**(-4.0))
WRITE(10,500)TITLE
WRITE(10,450)ES,P,AMOIST,RHO,AMU
C
CONVERT TO METRIC
PMETRC = P/144.0*100.0/14.5038
RMETRC = RHO*0.016018*1000.0
WRITE(10,505)TITLE
WRITE(10,455)PMETRC,RMETRC
C
FORMAT STATEMENTS
50 FORMAT(A72)
60 FORMAT(4X,'VV(ML)',2X,'V(CUFT/SQFT)',9X,'V**2',
+2X,'THETA(SECONDS)')
65 FORMAT(2F10.1)
70 FORMAT(1F10.1,4X,1F10.4,3X,1F10.3,6X,1F10.1)
80 FORMAT(I10)
85 FORMAT(/,A72)
400 FORMAT(1F10.3,1F10.1,1F10.4,2F15.4,/)
450 FORMAT(1F10.3,1F10.1,6X,1F10.4,4X,1F10.4,5X,1F10.6)
455 FORMAT(1F10.0,6X,1F10.1)
500 FORMAT(2X,'S(FRACT)',5X,'P(LBF/SQ.FT.)',3X,'MOIST',3X,'RHO(LBM/FT.
+) ',2X,'MU(LBM/FT.S.)')
505 FORMAT(/,4X,'P(KPA)',3X,'RHO(KG/CU.M.)')
C
RETURN
END
C
C
C

```

..., continued

```

SUBROUTINE ARRAY
IMPLICIT DOUBLE PRECISION (A-H,O-Z)
DIMENSION V(50),THETA(50),Q(50),QTHETA(50)
COMMON/AA/IN,IO,M,L,N,ITER
COMMON/EE/V,THETA,J
COMMON/HH/IDRCTN
COMMON/MM/Q,QTHETA
COMMON/NN/K
C
IF (IDRCTN.EQ.1) THEN
DO 10 I=K,M
Q(I-K+1)=V(I)
QTHETA(I-K+1)=THETA(I)
C
WRITE(IO,990)K,I,Q(I-K+1),QTHETA(I-K+1)
10 CONTINUE
ENDIF
IF (IDRCTN.EQ.2) THEN
DO 20 I=1,K
Q(I)=V(I)
QTHETA(I)=THETA(I)
C
WRITE(IO,990)K,I,Q(I),QTHETA(I)
990 FORMAT(1I2,2X,1I2,2X,1F10.4,1F10.1)
20 CONTINUE
ENDIF
C
RETURN
END
C
C
C
SUBROUTINE ENTEGO
IMPLICIT DOUBLE PRECISION (A-H,O-Z)
EXTERNAL BFN,FCN
DIMENSION V(50),THETA(50),X(4),F(50),Q(50),BKAPPA(50),BTHTAO(50),
+BVO(50),BN(50),PARM(4),BXJAC(50,4),BXJJ(10),BWORK(90),BF(50),
+WK(18),QTHETA(50),FF(50),FLOW(50)
CHARACTER*72 TITLE
COMMON/AA/IN,IO,M,L,N,ITER
COMMON/BB/F,X,IXJAC,NSIG,EPS,DELTA,MAXFN,IOPT
COMMON/DD/BKAPPA,BTHTAO,BVO,BN
COMMON/EE/V,THETA,J
COMMON/GG/BF
COMMON/HH/IDRCTN
COMMON/KK/ES,P,AMOIST
COMMON/LL/RHO,AMU
COMMON/MM/Q,QTHETA
COMMON/NN/K
COMMON/OO/JJ
C
IF (IDRCTN.EQ.1) THEN
WRITE(IO,91)TITLE
K=ITER
ENDIF
IF (IDRCTN.EQ.2) THEN
WRITE(IO,90)TITLE
K=5
ENDIF
C
DO 10 I=1,ITER
C
IF (I.LE.1) THEN
J=0
JJ=0
CALL ARRAY
C
IF (IDRCTN.EQ.1) THEN
MPOINT=M-K+1
CALL IFLSQ(FCN,Q,QTHETA,MPOINT,X,L,WK,IER)
ENDIF
IF (IDRCTN.EQ.2) THEN
MPOINT=K
CALL IFLSQ(FCN,Q,QTHETA,MPOINT,X,L,WK,IER)
ENDIF
C

```

..., continued



```

WRITE(IO,120) BN(I),BTHTAO(I),BKAPPA(I),BVO(I),BF(I),ALPHA,RM
C
  IF(IDRCTN.EQ.1)THEN
    K=K-1
  ENDIF
  IF(IDRCTN.EQ.2)THEN
    K=K+1
  ENDIF
C  ENDIF
10 CONTINUE
C
C  F O R M A T   S T A T E M E N T S
90 FORMAT(/.2X,'AN',2X,'ATHTAO',6X,'AKAPPA',9X,
+'AVO',8X,'VARIANCE',4X,'ALPHA',8X,'RM')
91 FORMAT(/.2X,'BN',2X,'BTHTAO',6X,'BKAPPA',9X,
+'BVO',8X,'VARIANCE',4X,'ALPHA',8X,'RM')
120 FORMAT(1F4.2,1X,1F6.1,2X,1E12.5,2X,1E10.3,1X,1E10.3,
+1X,1E10.3)
121 FORMAT(1F4.2,1X,1F6.1,2X,1E12.5,2X,1E12.5,2X,1E10.3,1X,1E10.3,
+1X,1E10.3)
C
RETURN
END
C
C
C
REAL FUNCTION FCN(KCOUNT,Q)
IMPLICIT DOUBLE PRECISION (A-H,O-Z)
REAL Q
INTEGER KCOUNT
COMMON/OO/JJ
C
JJ=JJ+1
IF(KCOUNT.EQ.1)THEN
  FCN = 1.0
ENDIF
IF(KCOUNT.EQ.2)THEN
  FCN = Q
ENDIF
IF(KCOUNT.EQ.3)THEN
  FCN = Q**2
ENDIF
C
RETURN
END
C
C
C
SUBROUTINE BFUN(X,M,N,F)
IMPLICIT DOUBLE PRECISION (A-H,O-Z)
DIMENSION V(50),THETA(50),X(4),F(50),Q(50),QTHETA(50)
COMMON/EE/V,THETA,J
COMMON/HH/IDRCTN
COMMON/MM/Q,QTHETA
COMMON/NN/K
C
BKAPPA=X(1), BTHTAO=X(2), BVO=X(3), BN=X(4)
IF(IDRCTN.EQ.1)THEN
  DO 10 I=M,K,-1
    J=J+1
    TEMP = (1.0/ABS(X(4)))+1.0
    F(I) = QTHETA(I)-((((Q(I)+ABS(X(3)))**TEMP)-(ABS(X(3))
10 +**TEMP))/ABS(X(1)))-X(2)
    CONTINUE
  ENDIF
  IF(IDRCTN.EQ.2)THEN
    DO 20 I=1,K
      J=J+1
      TEMP = (1.0/ABS(X(4)))+1.0
      F(I) = QTHETA(I)-((((Q(I)+ABS(X(3)))**TEMP)-(ABS(X(3))
20 +**TEMP))/ABS(X(1)))-X(2)
    CONTINUE
  ENDIF
C
RETURN
END

```

The programme F EXEC is a file that was used to execute COUNT FORTRAN or MERGE FORTRAN.

```
FORTVS &1 (OPT(2)
GLOBAL TXTLIB VLNKMLIB VFORTLIB IMSLDLIB
LOAD &1 (CLEAR
GLOBAL LOADLIB VFLODLIB
FI 15 DISK &1 DATA
FI 16 DISK &1 OUTPUT A (RECFM F LRECL 132 BLOCK 132
CP Q T
START
CP Q T
*COPY &1 OUTPUT A &1 LISTING A (APPEND
ERASE &1 LISTING A
ERASE LOAD MAP A
ERASE &1 TEXT A
```

# Appendix B

## 10.1 Types of Average Molecular Weight

The term *monodisperse* refers to a polymer sample composed of molecules all having the same molecular weight. *Polydisperse* describes a polymer sample containing molecules having a range of molecular weights. It is reasonable to speak of an average molecular weight of a polydisperse sample.

### Types of Average Molecular Weight:

**Number-Average Molecular Weight  $\bar{M}_n$**  is given by

$$\bar{M}_n = \frac{\sum_i N_i M_i}{\sum_i N_i} \quad (\text{B.1})$$

where  $N_i$  is the number of molecules of the species  $i$  and  $M_i$  is the molecular weight.

The boiling point, freezing point, vapour pressure, osmotic pressure and end group analysis give number-average molecular weights (Tobolsky, 1971).

**Weight-Average Molecular Weight  $\bar{M}_w$**  is defined as

$$\bar{M}_w = \frac{\sum_i g_i M_i}{\sum_i g_i} \quad (\text{B.2})$$

where  $g_i$  is the weight and  $M_i$  is the molecular weight of each fraction.

Light scattering, diffusion, and ultracentrifugation give weight-average molecular weights (Tobolsky, 1971).

**z-Average Molecular Weight  $\overline{M}_z$  and z+1-Average Molecular Weight  $\overline{M}_{z+1}$  are**

$$\overline{M}_z = \frac{\sum_i N_i M_i^3}{\sum_i N_i N_i^2} \quad (\text{B.3})$$

$$\overline{M}_{z+1} = \frac{\sum_i N_i M_i^4}{\sum_i N_i N_i^3} \quad (\text{B.4})$$

This average molecular weight is not used often. It is determined by ultracentrifugation techniques (Smith, 1968).

**Viscosity-Average Molecular Weight  $\overline{M}_v$**  can be obtained from the determination of the intrinsic viscosity of a given polymer in an appropriate solvent. There exists a relation between the intrinsic viscosity and the molecular weight, and is named the Mark-Houwink equation.

$$[\eta] = K M^a \quad (\text{B.5})$$

where  $K$  and  $a$  are empirical constants that depend on the solvent and the temperature.

The viscosity average molecular weight is given by

$$\overline{M}_v = \frac{\sum_i N_i M_i^{a+1}}{\sum_i N_i M_i^a} \quad (\text{B.6})$$

**Peak-Average Molecular Weight  $\overline{M}_p$**  refers to the molecular weight at the peak of a molecular weight distribution curve (Keller and Odell, 1985).

#### Comparison of the Average Molecular Weights:

For a *monodisperse* polymer

$$\overline{M}_n = \overline{M}_v = \overline{M}_w = \overline{M}_z = \overline{M}_{z+1} \quad (\text{B.7})$$

For a *polydisperse* polymer

$$\overline{M}_n < \overline{M}_v < \overline{M}_w < \overline{M}_z < \overline{M}_{z+1} \quad (\text{B.8})$$

(Smith, 1968; Williams, 1971).

# Appendix C

## 11.1 Determination of the Viscosity-Average Molecular Weight of the Non-ionic and the Anionic Polyacrylamides

### Theory:

To describe the viscosity of solutions, the relative viscosity  $\eta_r$  is defined as the ratio of the solution viscosity  $\eta$  to the solvent viscosity  $\eta_s$ :

$$\eta_r = \frac{\eta}{\eta_s} \quad (\text{C.1})$$

This may be expanded in a Taylor series in the concentration  $c$  (Brandrup and Immergut, 1989):

$$\eta_r = 1 + [\eta]c + k' [\eta]^2 c^2 + \dots \quad (\text{C.2})$$

in which  $[\eta]$  and  $k'$  are independent of concentration. The coefficient  $[\eta]$  is called the intrinsic viscosity of the solution, and  $k'$  is called the Huggins coefficient. Neglecting the terms in the order of  $c^3$ , it follows that

$$\frac{\eta_r - 1}{c} = [\eta] + k' [\eta]^2 c \quad (\text{C.3})$$

Extrapolating a plot of  $\frac{\eta_r - 1}{c}$  versus  $c$  to zero concentration yields the value of the intrinsic viscosity (the intercept on the ordinate axis).

The Mark-Houwink equation (Bird et al., 1977a; Tobolsky, 1971; Billmeyer, 1984) relates the intrinsic viscosity at zero shear rate to the molecular weight:

$$[\eta]_0 = k' (\text{molecular weight})^a \quad (\text{C.4})$$

The constants  $k'$  and  $a$  are determined empirically for a given solvent and temperature. At very small shear rates the intrinsic viscosity  $[\eta]$  approaches  $[\eta]_0$ . In this case, the Mark-Houwink equation may be written as

$$[\eta] = k' (\text{molecular weight})^a \quad (\text{C.5})$$

The Mark-Houwink equation provides a convenient method for determining the molecular weight of a polydisperse sample of a linear polymer. The method involves comparing the intrinsic viscosities of samples of the polymer of carefully defined molecular weights. It can then be written that

$$[\eta] = k' \overline{M}_v^a \quad (\text{C.6})$$

Klein and Conrad (1978) have established that for aqueous, non-ionic polyacrylamide solutions at 25°C in the concentration range of 0 to 20% and in the average molecular weight range of  $5 \times 10^5$  to  $5 \times 10^6$ , the Mark-Houwink equation is

$$[\eta] = 4.9 \times 10^{-3} \overline{M}_v^{0.8} \quad (\text{C.7})$$

Cohen (1981) states the Mark-Houwink equation for anionic polyacrylamide which is 20% hydrolyzed (i.e., the percent of carboxyl and amide groups that are carboxyl groups is 20%) and of a molecular weight range of  $1 \times 10^6$  to  $3 \times 10^6$  to be

$$[\eta] = 3.13 \times 10^{-3} \overline{M}_v^{0.77} \quad (\text{C.8})$$

### Experimental Details:

A quantity of the stock polymer solution was weighed, and then diluted to the desired concentration. The range of concentrations chosen for this determination was that used in the filtration experiments. The viscosity of this solution was measured according to the ASTM specifications<sup>1</sup>. The viscosity of the solvent (distilled water) was 0.8936 cP (Perry, 1950). A plot of  $\frac{\eta_r - 1}{c}$  versus  $c$  was constructed.

<sup>1</sup>Standard Specification for Kinematic Glass Viscometers ASTM Designation: D 2515-66; and Standard Method for Test for Viscosity of Transparent and Opaque Liquids ASTM Designation: D445-65.

Table C.1 and Table C.2 list the results of the viscosity measurements.

**Table C.1: Concentrations and Corresponding Viscosity Numbers of Solutions of Non-ionic Polyacrylamide.**

$c$ (g/dL)	$\eta$ Pa · s	$\eta_r$	$\frac{\eta_r-1}{c}$ * (dL/g)	Date of Measurement	Date Solution Prepared
0.00098	1.082	1.211	215	Aug. 28, 1990	Aug. 16, 1990
0.00177	1.142	1.278	157	Sept. 10, 1990	Aug. 16, 1990
0.00249	1.144	1.281	113	Sept. 6, 1990	Aug. 16, 1990
0.00498	1.298	1.452	90.7	Sept. 4, 1990	Aug. 16, 1990
0.00748	1.432	1.602	80.5	Sept. 7, 1990	Aug. 16, 1990
0.00997	1.540	1.723	72.5	Sept. 7, 1990	Aug. 16, 1990
0.0308	2.379	2.662	53.9	Oct. 4, 1990	Oct. 2, 1990
0.0552	2.836	3.173	39.4	Oct. 4, 1990	Oct. 2, 1990

\* Each value of  $\frac{\eta_r-1}{c}$  listed is an average of two measurements.

**Table C.2: Concentrations and Corresponding Viscosity Numbers of Solutions of Anionic Polyacrylamide.**

$c$ (g/dL)	$\eta$ Pa · s	$\eta_r$	$\frac{\eta_r - 1}{c}$ * (dL/g)	Date of Measurement	Date Solution Prepared
0.00050	1.070	1.198	397	Aug. 30, 1990	Aug. 17, 1990
0.00093	1.140	1.276	298	Aug. 27, 1990	Aug. 17, 1990
0.00260	1.314	1.470	181	Aug. 26, 1990	Aug. 17, 1990
0.00500	1.584	1.772	155	Aug. 24, 1990	Aug. 17, 1990
0.00998	2.159	2.416	142	Aug. 22, 1990	Aug. 17, 1990
0.0299	3.711	4.152	105	Oct. 4, 1990	Oct. 4, 1990
0.0498	4.276	4.784	75.9	Oct. 5, 1990	Oct. 4, 1990

\* Each value of  $\frac{\eta_r - 1}{c}$  listed is an average of two measurements.

### Findings:

The plots of the viscosity number  $\frac{\eta_r - 1}{c}$  versus the concentration  $c$  for the two types of polyacrylamides used are depicted in Figures C.1 and C.2.

A straight line plot was expected, but, clearly, the plots are curves. This presents the problem as to how to extrapolate the curves accurately. Billmeyer (1984) suggested that for accuracy in extrapolating to  $c = 0$ , the solution concentration should be restricted to the range that gives relative viscosities between 1.1 and 1.5. Taking this into consideration, Figures C.1 and C.2 were extrapolated using only data with relative viscosities in this range. Table C.3 lists the results.

**Table C.3: Intrinsic Viscosities and Viscosity-Average Molecular Weights:**

Polymer Type	$[\eta]$	$\bar{M}_v$
Non-Ionic	287	$0.9 \times 10^6$
Anionic	448	$5.0 \times 10^6$

The curves in Figures C.1 and C.2 are unusual, but a similar result has been cited by Merrill, et al. (1962) with dilute solutions of high molecular weight polyisobutylene

(known to be viscoelastic) in a coaxial cylinder viscometer (shear rates exceeding  $10^4 \text{ s}^{-1}$ ). James and McLaren (1975) also reported a difficulty to determine the intrinsic viscosity of dilute high molecular weight polyethylene oxide, and dismiss their measurements as 'too dilute'. Furthermore, the dates on which each experiment was performed have been included in Tables E.1 and E.2 to indicate that the curves are not the result of solution 'aging'. One can speculate that a complicated flow phenomenon, viscoelastic in nature, is occurring. Further investigation is pertinent to extend the Mark-Houwink relation to accommodate viscoelastic effects.

### Sample Calculation of the Viscosity Number and Concentration:

A 5 ppm aqueous solution of anionic polyacrylamide (Pusher 500) was prepared. The temperature of all measurements was  $25^\circ\text{C}$ .

Amount of distilled water measured: 700.100 g

Amount of stock polymer solution measured: 36.909 g

Actual ppm:

$$\frac{(36.909) 99.8091 \times 10^{-6} \text{ grams}}{36.909 + 700.100 \text{ grams}} = 4.998 \times 10^{-6}$$

Kinematic Viscosity:

Trial Number	1	2	Average
Time (s)	4 min 20.2 s	4 min 20.6 s	4 min 20.4 s

$$\begin{aligned} \nu &= (260.4 \text{ s})(0.004123 \frac{\text{cm}^2}{\text{s}^2}) \\ &= 1.074 \frac{\text{cm}^2}{\text{s}} \end{aligned}$$

Density

Density of the polymer solution was found to be  $0.9970 \text{ g/cm}^3$ .

Dynamic Viscosity:

$$\eta = (1.074)(0.9970) = 1.070 \frac{\text{cm}^2}{\text{s}} \cdot \frac{\text{g}}{\text{cm}^3} \text{ or cP}$$

## Viscosity Number versus Concentration Non-ionic Polyacrylamide

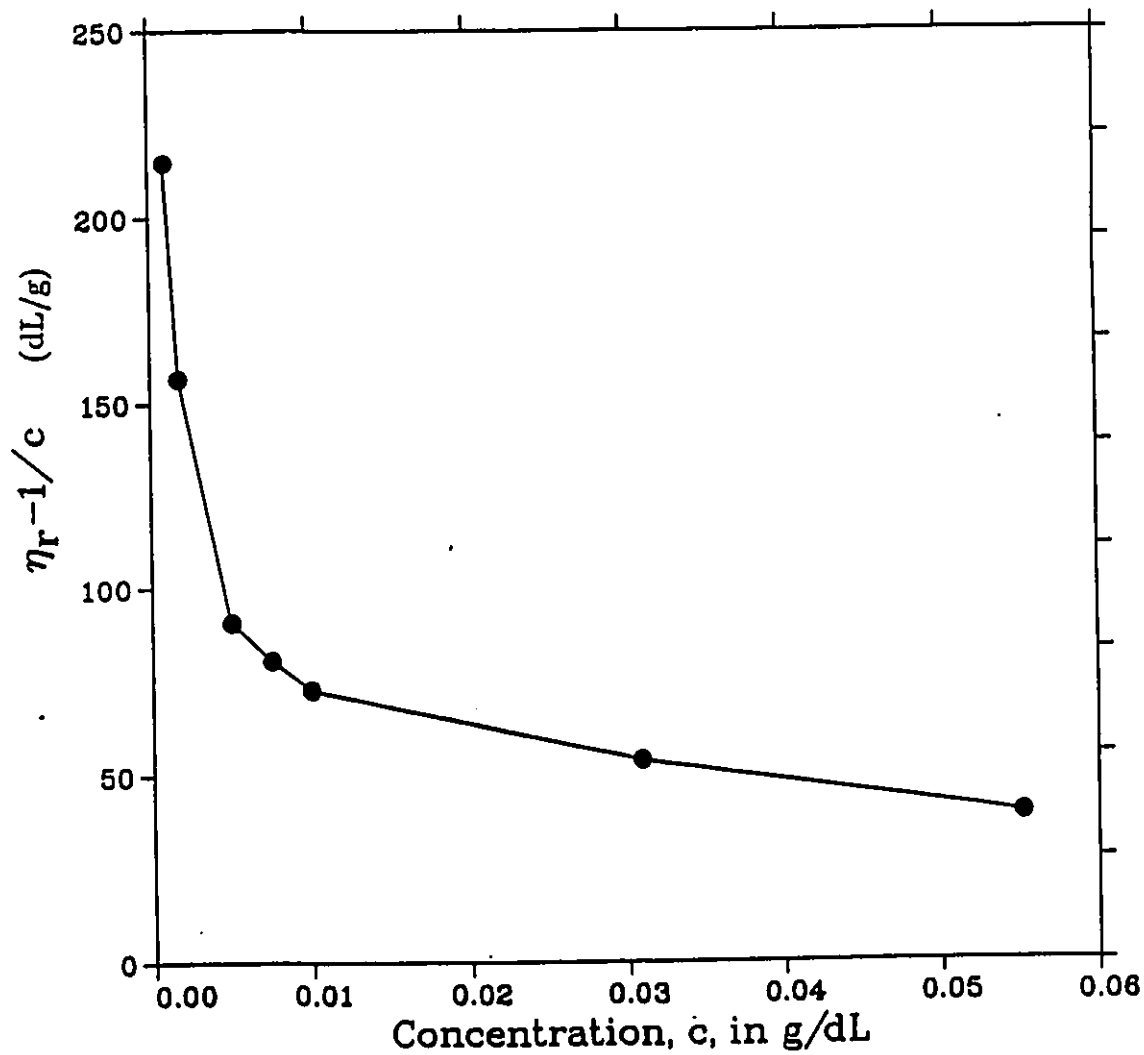


Figure C.1: Viscosity Number versus Concentration at 25°C for Aqueous Solutions of High Molecular Weight Non-Ionic Polyacrylamide.

# Viscosity Number versus Concentration

## Anionic Polyacrylamide

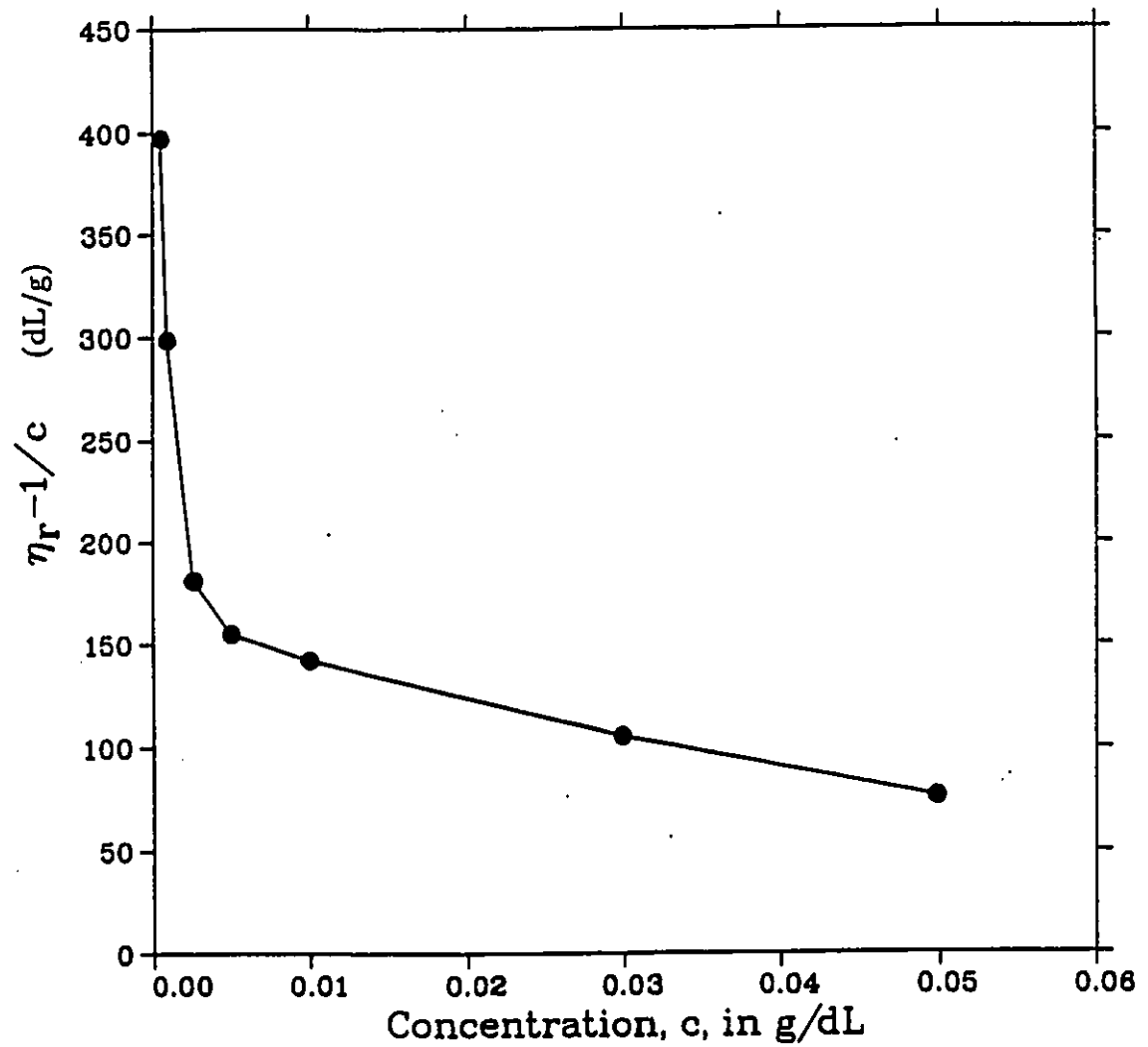


Figure C.2: Viscosity Number versus Concentration at 25°C for Aqueous Solutions of High Molecular Weight Anionic Polyacrylamide.

**Relative Viscosity:**

The viscosity of distilled water is 0.8936 cP (Perry, 1950)

$$\eta_r = \frac{\eta}{\eta_s} = \frac{1.070}{0.8936} = 1.198$$

**Concentration, g/dL:**

$$c = 4.998 \times 10^{-6} \frac{\text{g polymer}}{\text{g solution}} \times 0.9970 \frac{\text{g solution}}{\text{mL}} \times 100 \frac{\text{mL}}{1 \text{ dL}}$$

**Viscosity Number:**

$$\frac{\eta_r - 1}{c} = \frac{1.198 - 1}{0.0004998} = 397 \frac{\text{dL}}{\text{g}}$$

# Appendix D

## 12.1 Definitions of Configuration, Conformation, Composition, and Constitution

### Composition

Composition refers to the number and kinds of atoms present. It is expressed by the molecular formula.

### Configuration

Configuration refers to the different shapes a molecule can attain from the free rotation of atoms about single carbon-carbon bonds; or, the non-permanent arrangement of atoms in a molecule.

### Conformation

Conformation is the permanent arrangements of atoms in a molecule in 3-dimensional space. The following two molecules differ in configuration.

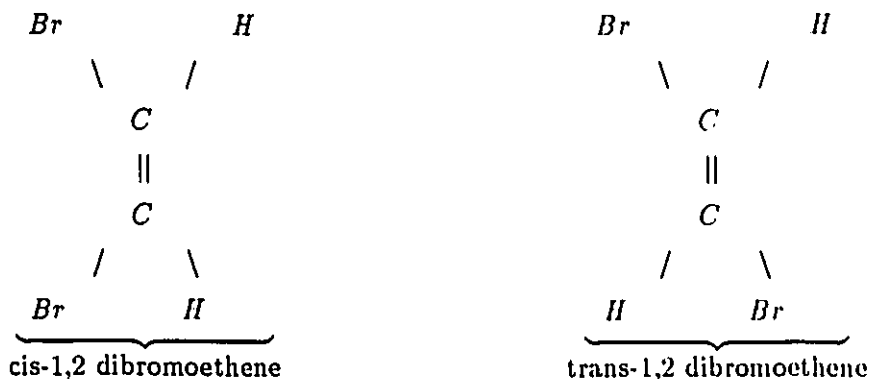
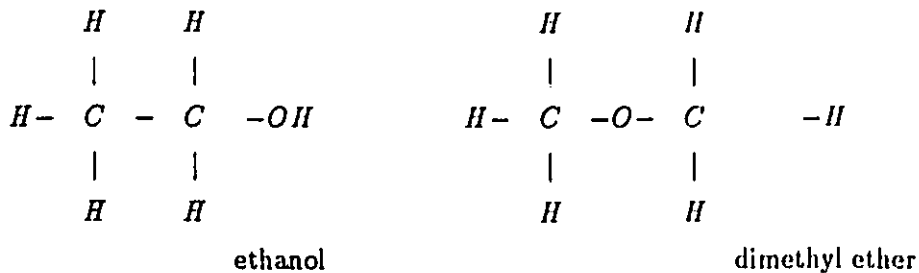


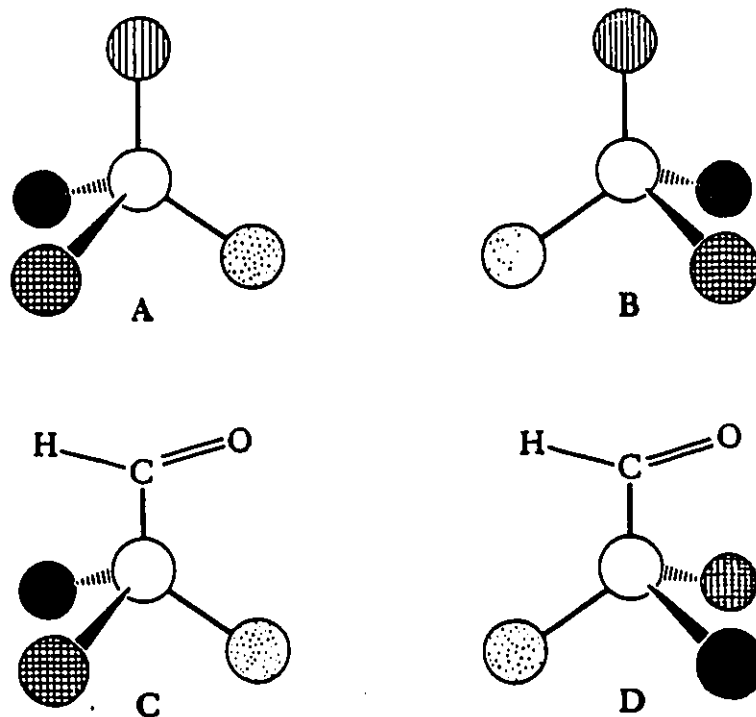
Figure D.1 gives an example to further illustrate the difference between the terms configuration and conformation.

### Constitution

Constitution is the order of linkage between the atoms and the kinds of bonds present. The following example compares ethanol and dimethyl ether.



Ethanol and dimethyl ether have the same composition, but differ in constitution.



A and B differ in configuration and are mirror images (enantiomers). They have the same composition and constitution.

C and D differ in conformation, but not in configuration. They have the same composition and constitution.

Figure D.1: Illustration of the difference between the terms configuration and conformation. Reproduced from Ternay (1976).

# Appendix E

## 13.1 Calibration Data for the Diaphragm Pressure Gauge

### Pressure Gauges

There were two pressure gauges utilized, a standard pressure gauge (USG, U.S.A., dial type with a range of 0 psi to 600 psi, subdivisions of 2 psi) and a diaphragm pressure gauge (ACCO Helicoid Gage, U.S.A., dial type with a range of 0 psi to 200 psi, subdivisions of 2 psi). For the location of the gauges, please refer to Figure 5.1. Both gauges provided readings of *gauge pressure*, not *absolute pressure*.

Before any experiments were performed, the diaphragm pressure gauge was calibrated against the standard gauge. The calibration involved filling the entire system with water, tightly capping the outlet of the filtering unit with a swage lock closure, and closing all other valves. Using the nitrogen gas, the autoclave was then pressurized to various levels, and the readings were recorded.

**Calibration Curve Data:**

<b>Standard Gauge Reading (psi)</b>	<b>Diaphragm Gauge Reading (psi)</b>
0	1.0
10	9.5
20	18.5
30	28.5
40	39.0
50	49.0
70	69.0
90	88.0
100	98.5
120	119.5

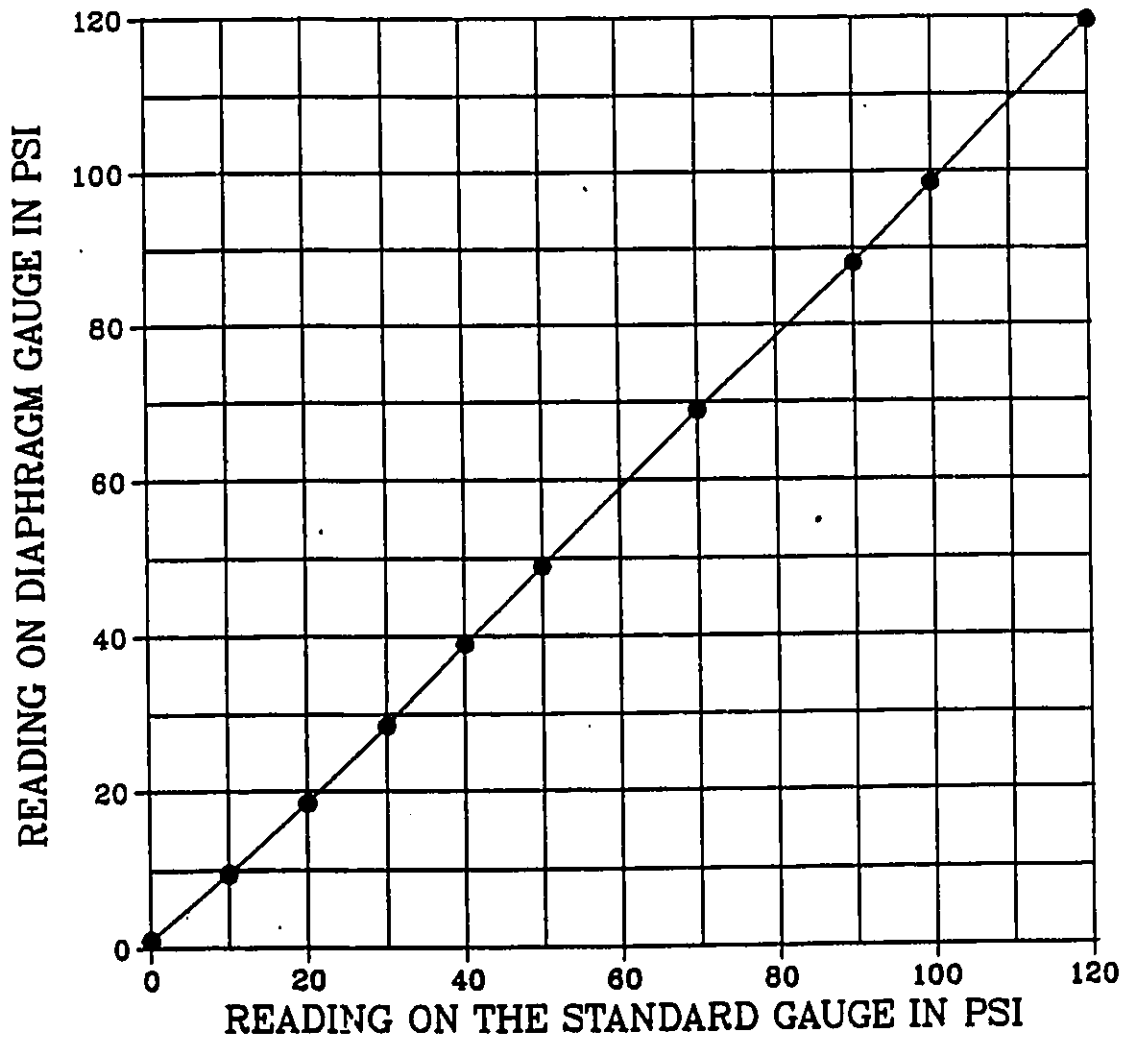


Figure E.1: Calibration Curve for the Diaphragm Pressure Gauge.

# Appendix F

## 14.1 Sample Calculation

A sample calculation to determine the amounts of stock polymer solution, calcium carbonate, and distilled water required for the experimental run of 10% $\frac{w}{w}$  CaCO<sub>3</sub> and 50 ppm of anionic polyacrylamide is presented.

Let  $x$  = mass of distilled water required

$z$  = mass of stock polymer solution required.

The mass of calcium carbonate is 775.0 grams.

The mass fraction of the polymer in the stock solution is 0.00479786.

The mass fraction of calcium carbonate required in the slurry is

$$0.1 = \frac{775.0}{x + z + 775.0} \quad (\text{F.1})$$

The mass fraction of polymer required in the slurry

$$50.0 \times 10^{-6} = \frac{0.00479786z}{x + z + 775.0} \quad (\text{F.2})$$

Rearranging these two equations,

$$x + z + 775.0 = \frac{775.0}{0.1} \quad (\text{F.3})$$

$$x + z + 775.0 = \frac{0.00479786z}{50.0 \times 10^{-6}} \quad (\text{F.4})$$

Solving Equation F.3 and Equation F.4,  $z$  may be evaluated.

$$z = \left( \frac{775.0}{0.1} \right) \left( \frac{50.0 \times 10^{-6}}{0.00479786} \right) = 80.76619 \quad (\text{F.5})$$

Solving Equation F.3 for  $x$ , one obtains

$$x = \frac{775.0}{.1} - 775.0 - 80.76619 = 6894.2 \quad (\text{F.6})$$

Therefore, the quantities of chemicals required in the slurry are as follows:

Stock polymer solution = 80.766 grams

Calcium carbonate = 775.0 grams

Distilled water = 6894.2 grams

# Appendix G

## 15.1 Estimation of the Volume in the Piping and the Cone above the Filter Cloth

The apparatus above the filter cloth, consisting of a plexiglass cone and a stainless steel pipe (as in Figure G.1), was filled with distilled water. The water was poured into a beaker and weighed.

Mass of Clean Beaker and Distilled Water	= 266.645 grams
Mass of Clean Beaker	= 144.713 grams
<hr/>	
Mass of Distilled Water	= 121.932 grams

After drying this section of the apparatus, the measurement was repeated and found to be 122.375 grams. The arithmetic average of the two measurements is 122.154 grams.

The density of the distilled water at 25°C was found to be 0.99704 g/mL using the digital density meter. Therefore, the volume occupied within the section of the filtration apparatus above the filter cloth was estimated to be

$$\text{volume} = 121.742/0.99704 \approx 122 \text{ mL}$$

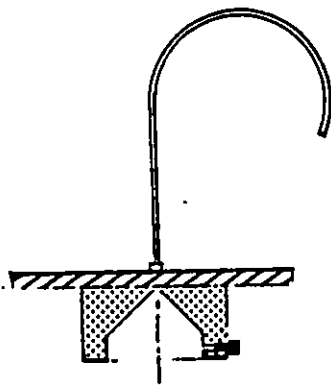


Figure G.1: Section of the Filtration Apparatus above the Filter Cloth.

# Appendix H

## 16.1 Filtration Data

The computer calculations were initially done in the *Imperial System* of units, and the following list of conversion factors were found useful to portray the results in *Système International* units.

### Conversion Factors:

<u>To Convert from</u>	<u>To</u>	<u>Multiply By</u>
$R_{ma}$ in $\frac{1}{ft}$	$R_{ma}$ in $\frac{1}{m}$	3.2808399
$\gamma_{av}$ in $\frac{ft}{lbm}$	$\gamma_{av}$ in $\frac{m}{kg}$	$\frac{2.204623}{3.2808399}$
$K_N$ in $\frac{ft}{s^2}$	$K_N$ in $\frac{m}{s^2}$	0.3048
$v_{me}$ in $ft$	$v_{me}$ in $m$	0.3048
pressure drop in $psi$	pressure drop in $kPa$	6.89473

345 kPa (50 psi)

0 ppm

---

Slurry solids fraction = 0.100  
Density of filtrate =  $997.1 \text{ kg} \cdot \text{m}^{-3}$   
Viscosity of filtrate =  $0.8979 \times 10^{-3} \text{ Pa} \cdot \text{s}$   
Moisture ratio = 1.76  
Porosity = 0.67

**Results of the Linear Least-Squares Estimation:**

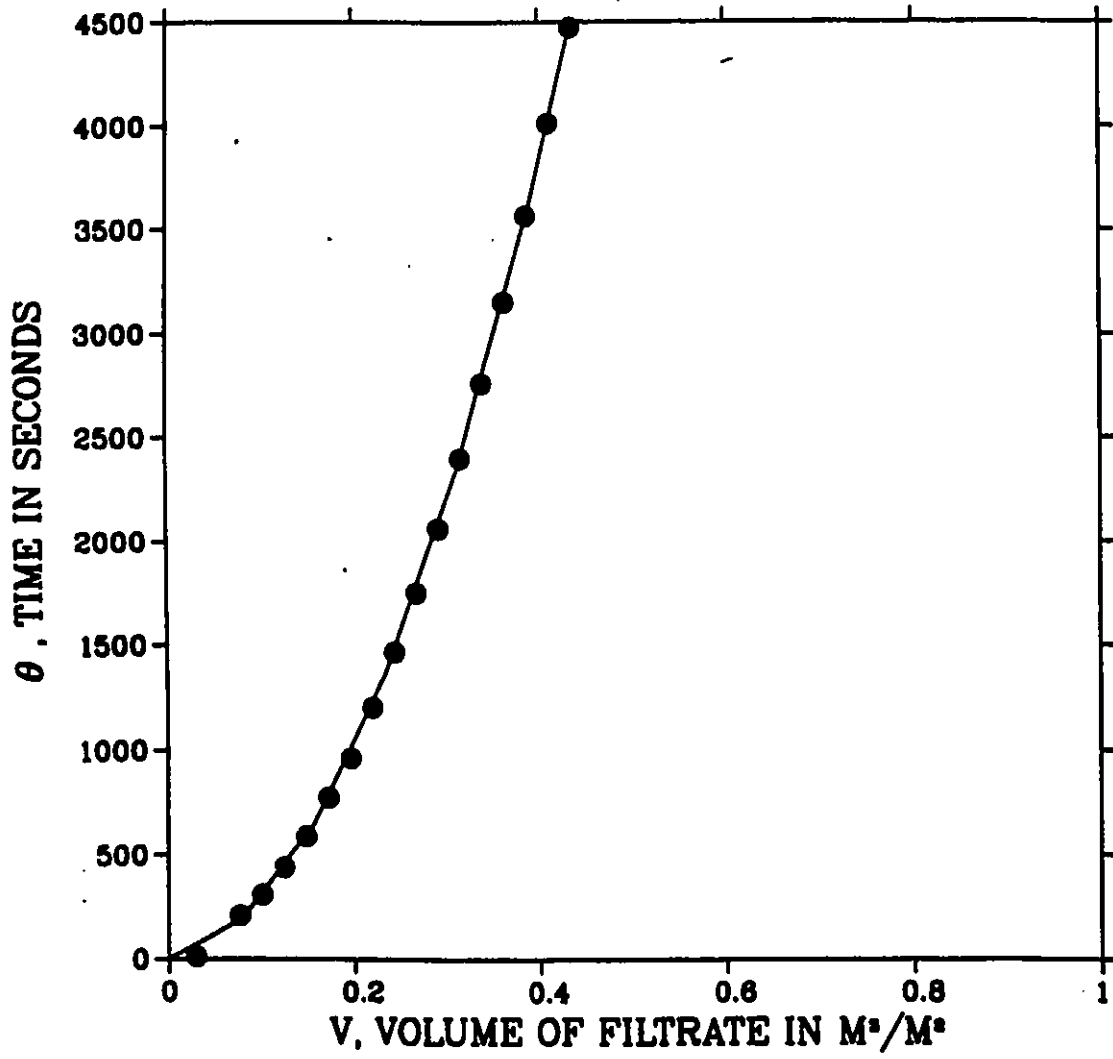
**Fitted Curve**

$\theta_0$  = 0.8 s  
 $v_{me}$  = 0.016 m  
 $K_N$  =  $0.00015 \text{ m} \cdot \text{s}^{-2}$   
 $R_{ma}$  =  $2.7 \times 10^{11} \text{ m}^{-1}$   
 $\gamma_{av}$  =  $1.4 \times 10^{11} \text{ m} \cdot \text{kg}^{-1}$   
variance = 0.007

**Experimental Data:**

volume of filtrate <i>mL</i>	volume of filtrate, <i>v</i> $\text{m}^3/\text{m}^2$	time, $\theta$ <i>s</i>
122.0	0.096	11.0
322.0	0.252	207.0
422.0	0.331	308.0
522.0	0.409	439.0
622.0	0.487	588.0
722.0	0.566	774.5
822.0	0.644	961.5
922.0	0.722	1202.5
1022.0	0.801	1466.0
1122.0	0.879	1749.5
1222.0	0.957	2061.0
1322.0	1.036	2398.0
1422.0	1.114	2758.0
1522.0	1.192	3150.5
1622.0	1.271	3562.5
1722.0	1.349	4011.0
1822.0	1.427	4472.0

345 kPa, 10 % CaCO<sub>3</sub>  
0 ppm



345 kPa (50 psi)  
Anionic Polyacrylamide  
25 ppm

---

Slurry solids fraction = 0.100  
Density of filtrate =  $997.1 \text{ kg} \cdot \text{m}^{-3}$   
Viscosity of filtrate =  $1.0072 \times 10^{-3} \text{ Pa} \cdot \text{s}$   
Moisture ratio = 1.73  
Porosity = 0.66

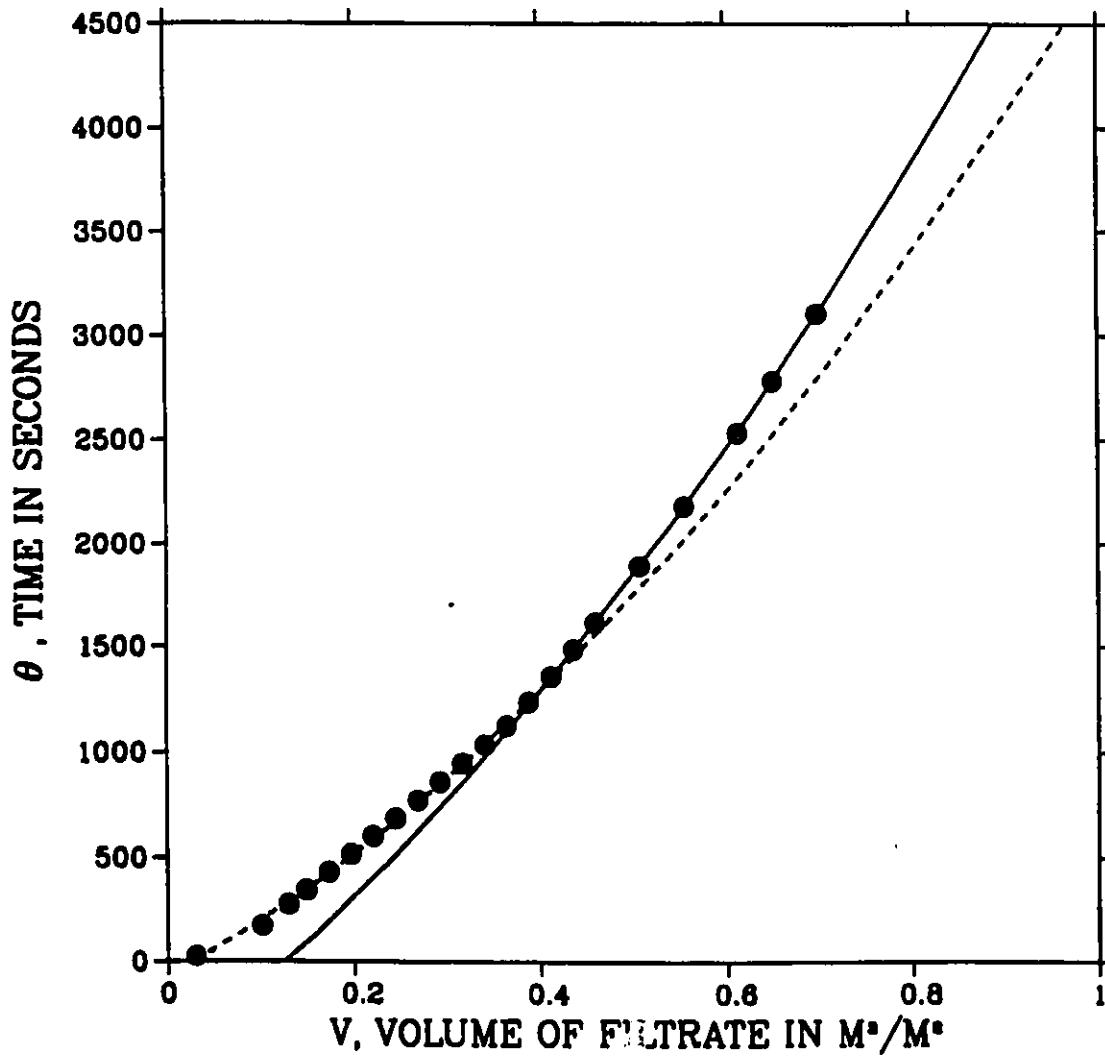
Results of the Linear Least-Squares Estimation:  
Fitted Curve A                      Fitted Curve B

$\theta_0$	=	-70.8 s	$\theta_0$	=	-474.5 s
$v_{me}$	=	0.53 m	$v_{me}$	=	0.73 m
$K_N$	=	$0.0014 \text{ m} \cdot \text{s}^{-2}$	$K_N$	=	$0.0014 \text{ m} \cdot \text{s}^{-2}$
$R_{ma}$	=	$8.5 \times 10^{11} \text{ m}^{-1}$	$R_{ma}$	=	$11.8 \times 10^{11} \text{ m}^{-1}$
$\gamma_{av}$	=	$0.13 \times 10^{11} \text{ m} \cdot \text{kg}^{-1}$	$\gamma_{av}$	=	$0.13 \times 10^{11} \text{ m} \cdot \text{kg}^{-1}$
variance	=	0.12	variance	=	0.015

Experimental Data:

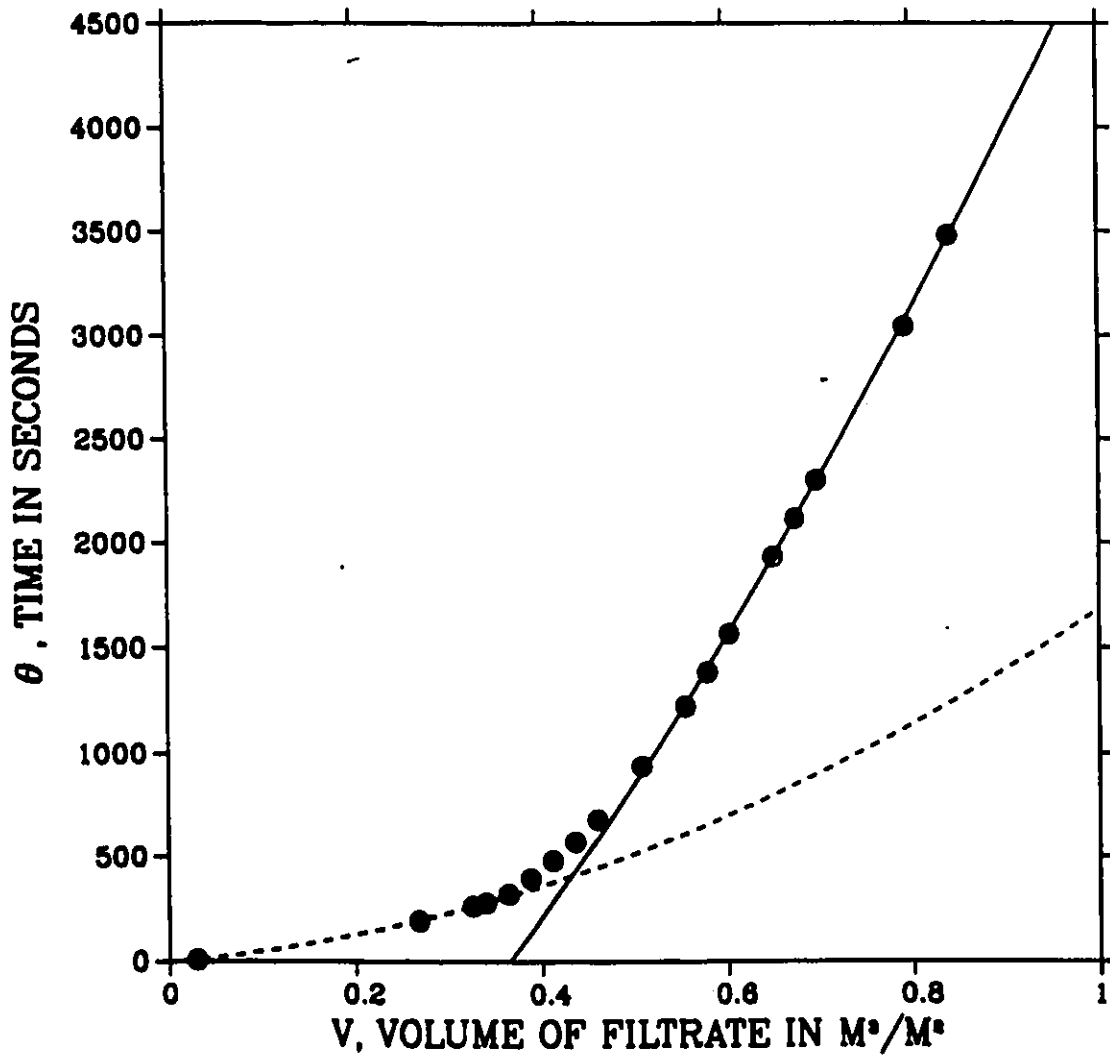
volume of filtrate <i>mL</i>	volume of filtrate, <i>v</i> $m^3/m^2$	time, $\theta$ <i>s</i>
122.0	0.096	24.0
422.0	0.331	172.0
542.0	0.425	275.0
622.0	0.487	344.0
722.0	0.566	430.0
822.0	0.644	515.0
922.0	0.722	600.0
1022.0	0.801	686.0
1122.0	0.879	772.0
1222.0	0.957	859.0
1322.0	1.036	946.0
1422.0	1.114	1034.0
1522.0	1.192	1126.5
1622.0	1.271	1236.0
1722.0	1.349	1356.5
1822.0	1.427	1486.0
1922.0	1.506	1614.0
2122.0	1.662	1890.0
2322.0	1.819	2180.0
2562.0	2.007	2531.5
2722.0	2.132	2780.0
2922.0	2.289	3102.0

345 kPa, 10 % CaCO<sub>3</sub>  
Anionic Polyacrylamide<sup>3</sup>  
25 ppm





345 kPa, 10 % CaCO<sub>3</sub>  
Anionic Polyacrylamide<sup>s</sup>  
50 ppm



345 kPa (50 psi)  
Non-ionic Polyacrylamide  
25 ppm

---

Slurry solids fraction = 0.100  
Density of filtrate =  $997.1 \text{ kg} \cdot \text{m}^{-3}$   
Viscosity of filtrate =  $1.0142 \times 10^{-3} \text{ Pa} \cdot \text{s}$   
Moisture ratio = 1.63  
Porosity = 0.63

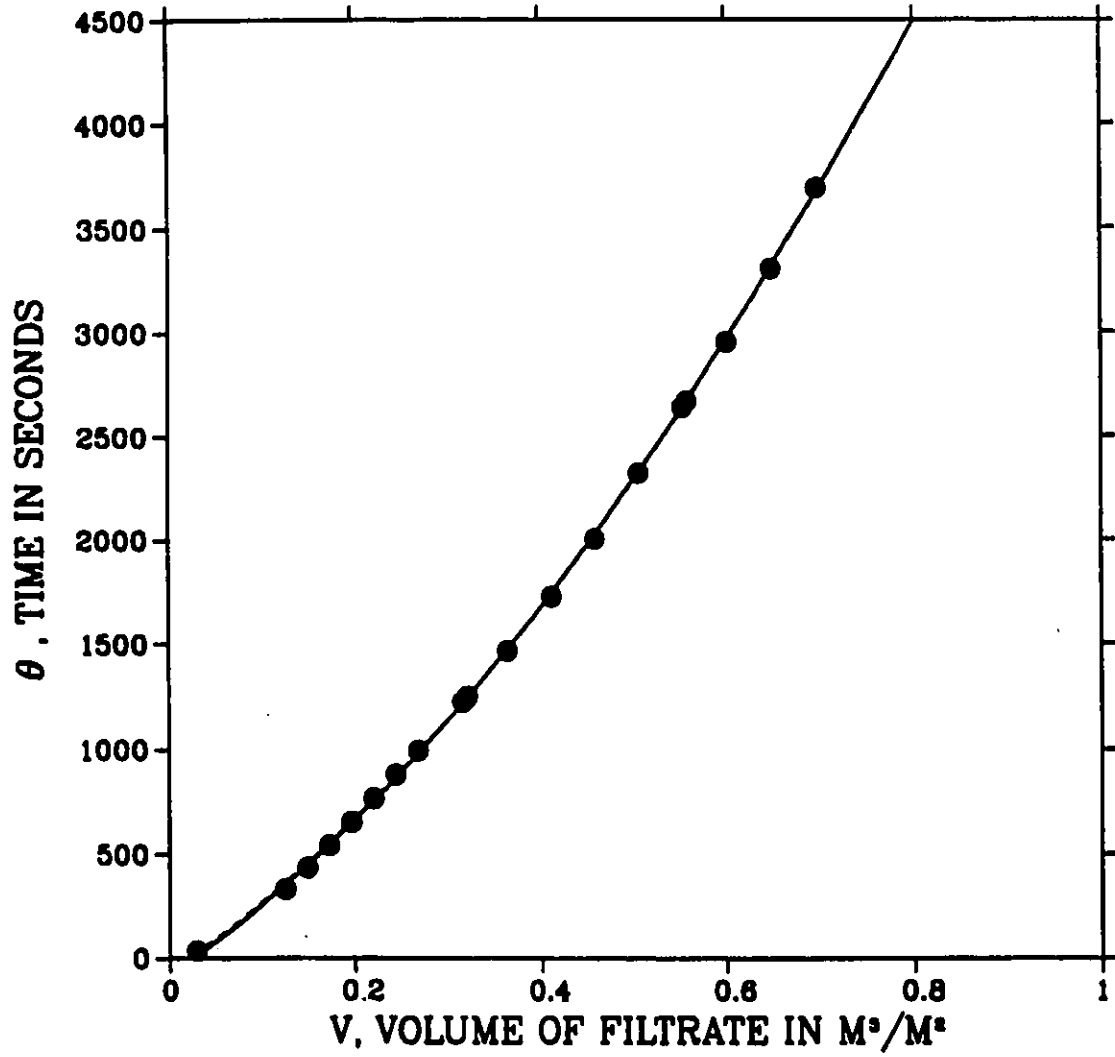
**Results of the Linear Least-Squares Estimation:**  
**Fitted Curve A**                      **Fitted Curve B**

$\theta_0$	=	-71.8 s	$\theta_0$	=	-85.9 s
$v_{me}$	=	0.016 m	$v_{me}$	=	0.46 m
$K_N$	=	$0.0011 \text{ m} \cdot \text{s}^{-2}$	$K_N$	=	$0.0010 \text{ m} \cdot \text{s}^{-2}$
$R_{ma}$	=	$10.6 \times 10^{11} \text{ m}^{-1}$	$R_{ma}$	=	$10.5 \times 10^{11} \text{ m}^{-1}$
$\gamma_{av}$	=	$0.2 \times 10^{11} \text{ m} \cdot \text{kg}^{-1}$	$\gamma_{av}$	=	$0.2 \times 10^{11} \text{ m} \cdot \text{kg}^{-1}$
variance	=	8.2	variance	=	20.1

Experimental Data:

volume of filtrate <i>mL</i>	volume of filtrate, <i>v</i> $m^3/m^2$	time, $\theta$ <i>s</i>
122	0.0290	35.5
522	0.125	331.5
622	0.149	434.0
722	0.172	542.0
822	0.196	653.0
922	0.220	765.5
1022	0.244	880.0
1122	0.268	994.0
1322	0.316	1225.0
1342	0.320	1249.0
1522	0.363	1466.5
1582	0.378	1402.0
1722	0.411	1725.0
1922	0.459	2003.5
2122	0.507	2320.0
2322	0.554	2640.0
2342	0.559	2670.5
2522	0.602	2950.5
2722	0.650	3300.5
2922	0.698	3688.0

345 kPa, 10 % CaCO<sub>3</sub>  
Non-ionic Polyacrylamide  
25 ppm



345 kPa (50 psi)  
 Non-ionic Polyacrylamide  
 50 ppm

---

Slurry solids fraction = 0.100  
 Density of filtrate =  $997.2 \text{ kg} \cdot \text{m}^{-3}$   
 Viscosity of filtrate =  $1.0174 \text{ Pa} \cdot \text{s}$   
 Moisture ratio = 2.12  
 Porosity = 0.63

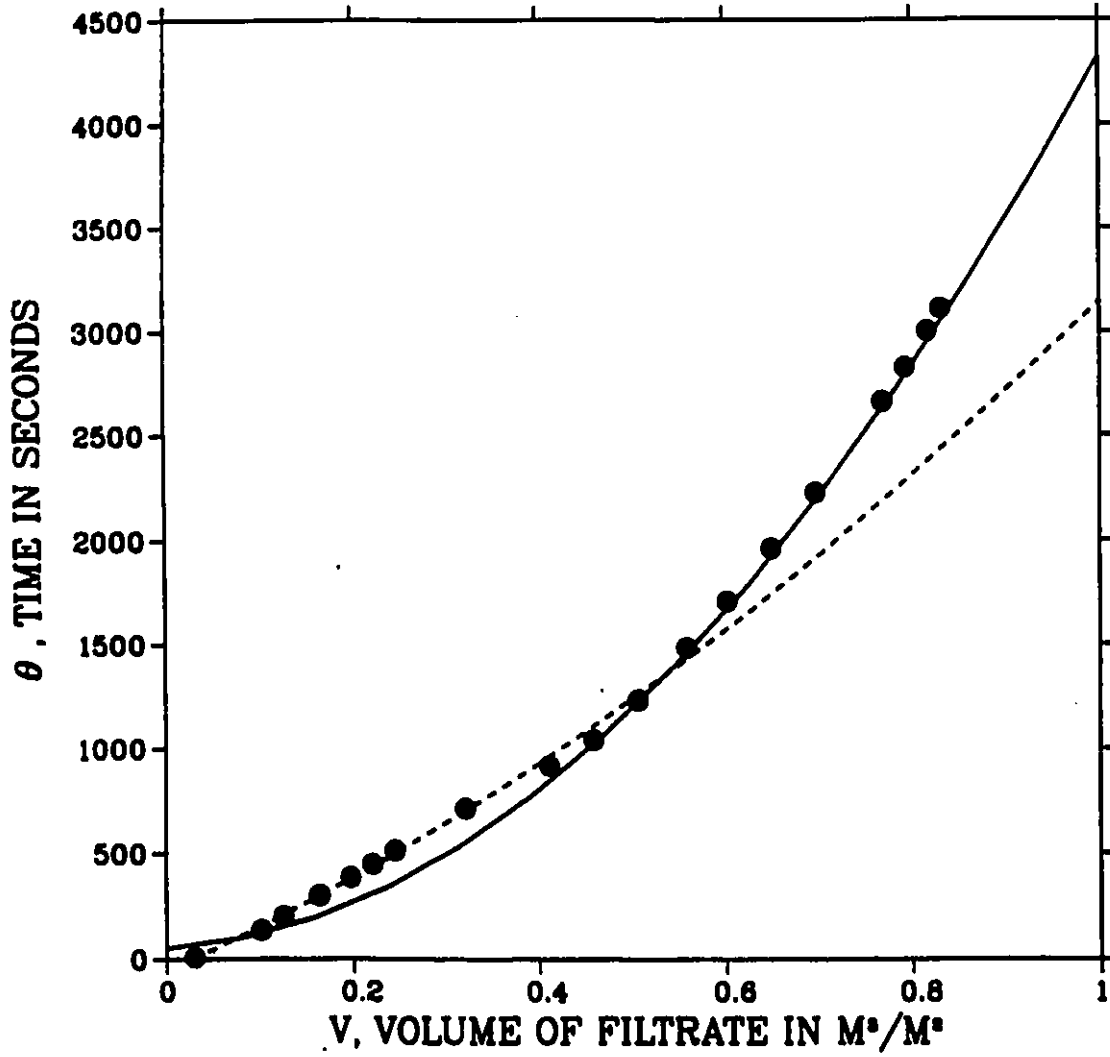
**Results of the Linear Least-Squares Estimation:**  
**Fitted Curve A** **Fitted Curve B**

$\theta_0$ = -54.8 s $v_{me}$ = 0.79 m $K_N$ = $0.0027 \text{ m} \cdot \text{s}^{-2}$ $R_{ma}$ = $6.6 \times 10^{11} \text{ m}^{-1}$ $\gamma_{av}$ = $0.07 \times 10^{11} \text{ m} \cdot \text{kg}^{-1}$ variance = 13.6	$\theta_0$ = 51.5 s $v_{me}$ = 0.037 m $K_N$ = $0.00082 \text{ m} \cdot \text{s}^{-2}$ $R_{ma}$ = $1.0 \times 10^{11} \text{ m}^{-1}$ $\gamma_{av}$ = $0.22 \times 10^{11} \text{ m} \cdot \text{kg}^{-1}$ variance = 7.7
--	--

**Experimental Data:**

volume of filtrate <i>mL</i>	volume of filtrate, <i>v</i> $\text{m}^3/\text{m}^2$	time, $\theta$ <i>s</i>
122	0.0290	7.0
1722	0.411	917.0
1922	0.459	1040.5
2122	0.507	1229.5
2342	0.559	1483.0
2522	0.602	1708.0
2722	0.650	1960.0
2922	0.698	2226.0
3222	0.769	2660.0
3322	0.793	2825.0
3422	0.817	3001.0
3482	0.831	3109.0

345 kPa, 10 % CaCO<sub>3</sub>  
Non-ionic Polyacrylamide  
50 ppm



517 kPa (75 psi)

0 ppm

---

Slurry solids fraction = 0.100  
Density of filtrate = 997.1 kg/m<sup>3</sup>  
Viscosity of filtrate = 0.899 × 10<sup>-3</sup> Pa · s  
Moisture ratio = 1.66  
Porosity = 0.64

**Results of the Linear Least-Squares Estimation:**

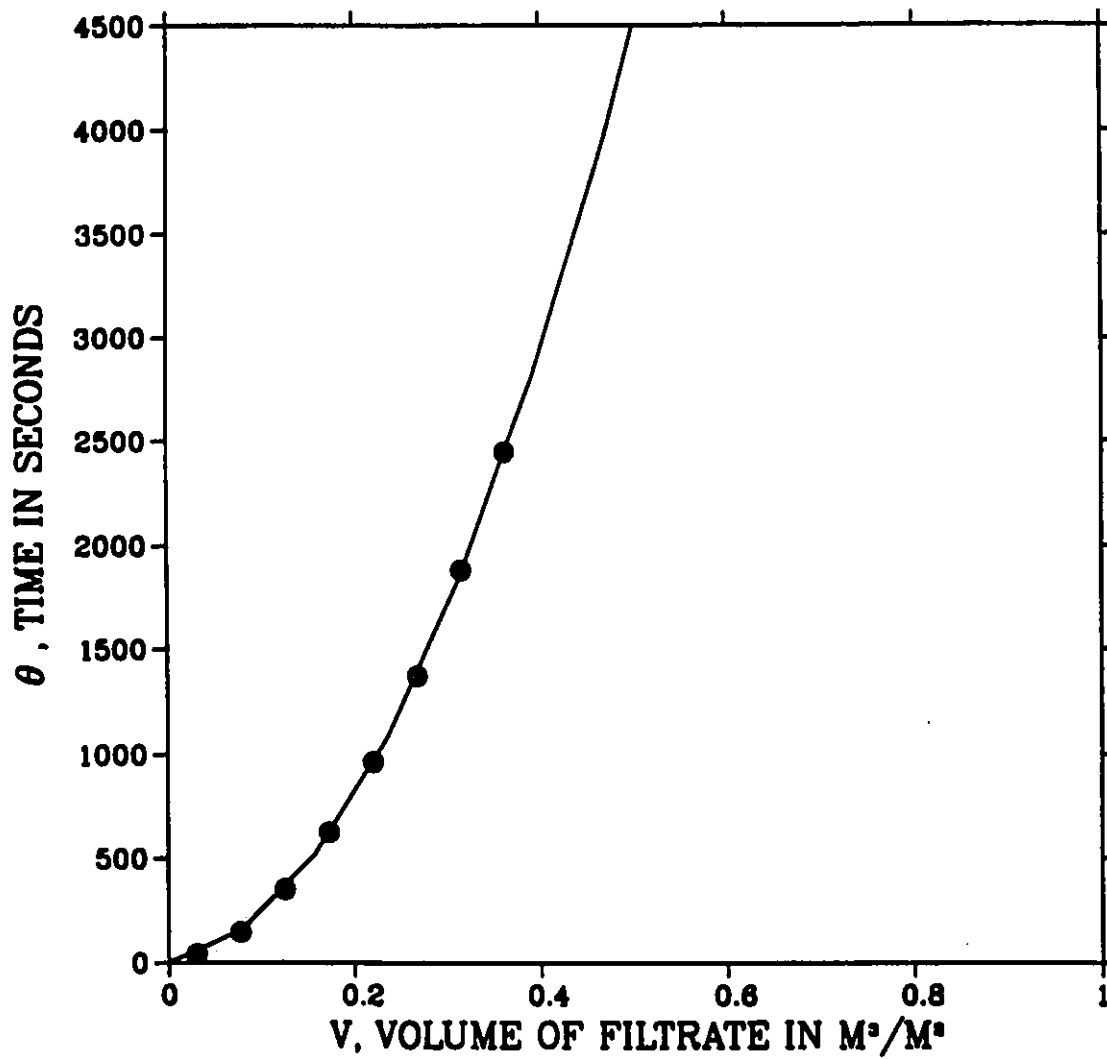
Fitted Curve A

Fitted Curve B

$\theta_0$  = 0.4 s  
 $v_{me}$  = 0.023 m  
 $K_N$  = 0.00018 m · s<sup>-2</sup>  
 $R_{ma}$  = 0.5 × 10<sup>11</sup> m<sup>-1</sup>  
 $\gamma_{av}$  = 1.9 × 10<sup>11</sup> m · kg<sup>-1</sup>  
variance = 27.9

volume of filtrate mL	volume of filtrate, $v$ m <sup>3</sup> /m <sup>2</sup>	time, $\theta$ s
122.0	0.096	40.0
322.0	0.252	146.0
522.0	0.409	351.5
722.0	0.566	626.0
922.0	0.722	963.0
1122.0	0.879	1372.0
1322.0	1.036	1879.0
1522.0	1.192	2445.0

517 kPa, 10 %  $\text{CaCO}_3$   
0 ppm



517 kPa (75 psi)  
 Anionic Polyacrylamide  
 25 ppm

---

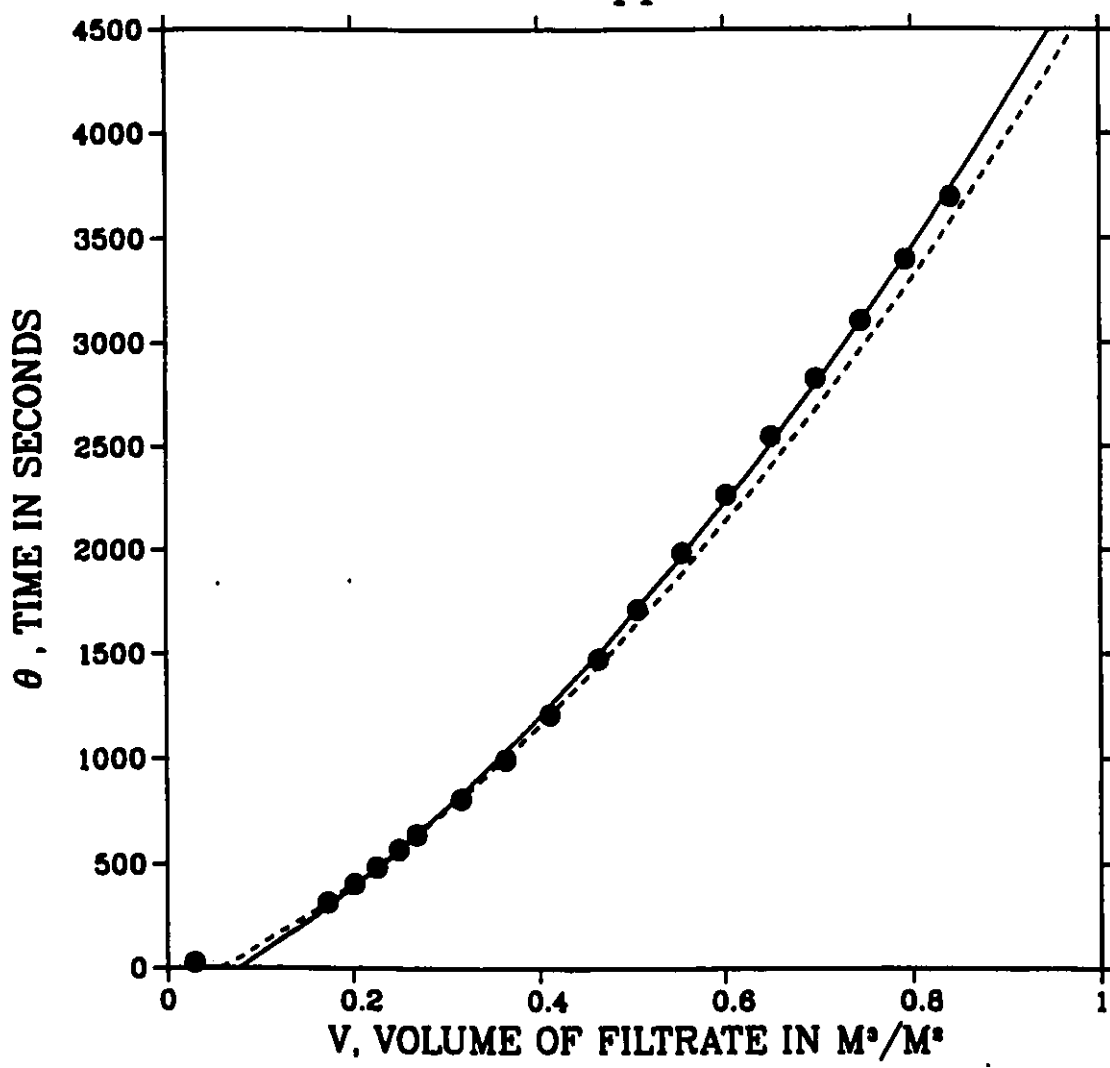
Slurry solids fraction = 0.100  
 Density of filtrate = 997.1 kg/m<sup>3</sup>  
 Viscosity of filtrate = 1.0130 × 10<sup>-3</sup> Pa · s  
 Moisture ratio = 1.67  
 Porosity = 0.65

**Results of the Linear Least-Squares Estimation:**  
Fitted Curve A                      Fitted Curve B

$\theta_0$ = -134.0 s $v_{mc}$ = 0.40 m $K_N$ = 0.0012 m · s <sup>-2</sup> $R_{ma}$ = 11.0 × 10 <sup>11</sup> m <sup>-1</sup> $\gamma_{av}$ = 0.2 × 10 <sup>11</sup> m · kg <sup>-1</sup> variance = 11.2	$\theta_0$ = -203.8 s $v_{mc}$ = 0.46 m $K_N$ = 0.0012 m · s <sup>-2</sup> $R_{ma}$ = 12.4 × 10 <sup>11</sup> m <sup>-1</sup> $\gamma_{av}$ = 0.2 × 10 <sup>11</sup> m · kg <sup>-1</sup> variance = 1970.0
--	--

volume of filtrate mL	volume of filtrate, $v$ m <sup>3</sup> /m <sup>2</sup>	time, $\theta$ s
122.0	0.096	25.0
722.0	0.566	316.0
842.0	0.660	405.0
942.0	0.738	486.0
1042.0	0.816	570.5
1122.0	0.879	640.5
1322.0	1.036	810.0
1522.0	1.192	995.0
1722.0	1.349	1208.0
1942.0	1.521	1475.5
2122.0	1.662	1710.0
2322.0	1.819	1983.0
2522.0	1.976	2262.0
2722.0	2.132	2544.0
2922.0	2.289	2822.0
3122.0	2.446	3101.5
3322.0	2.602	3395.0
3522.0	2.759	3692.0

517 kPa, 10 % CaCO<sub>3</sub>  
Anionic Polyacrylamide<sup>3</sup>  
25 ppm



517 kPa (75 psi)  
 Anionic Polyacrylamide  
 50 ppm

---

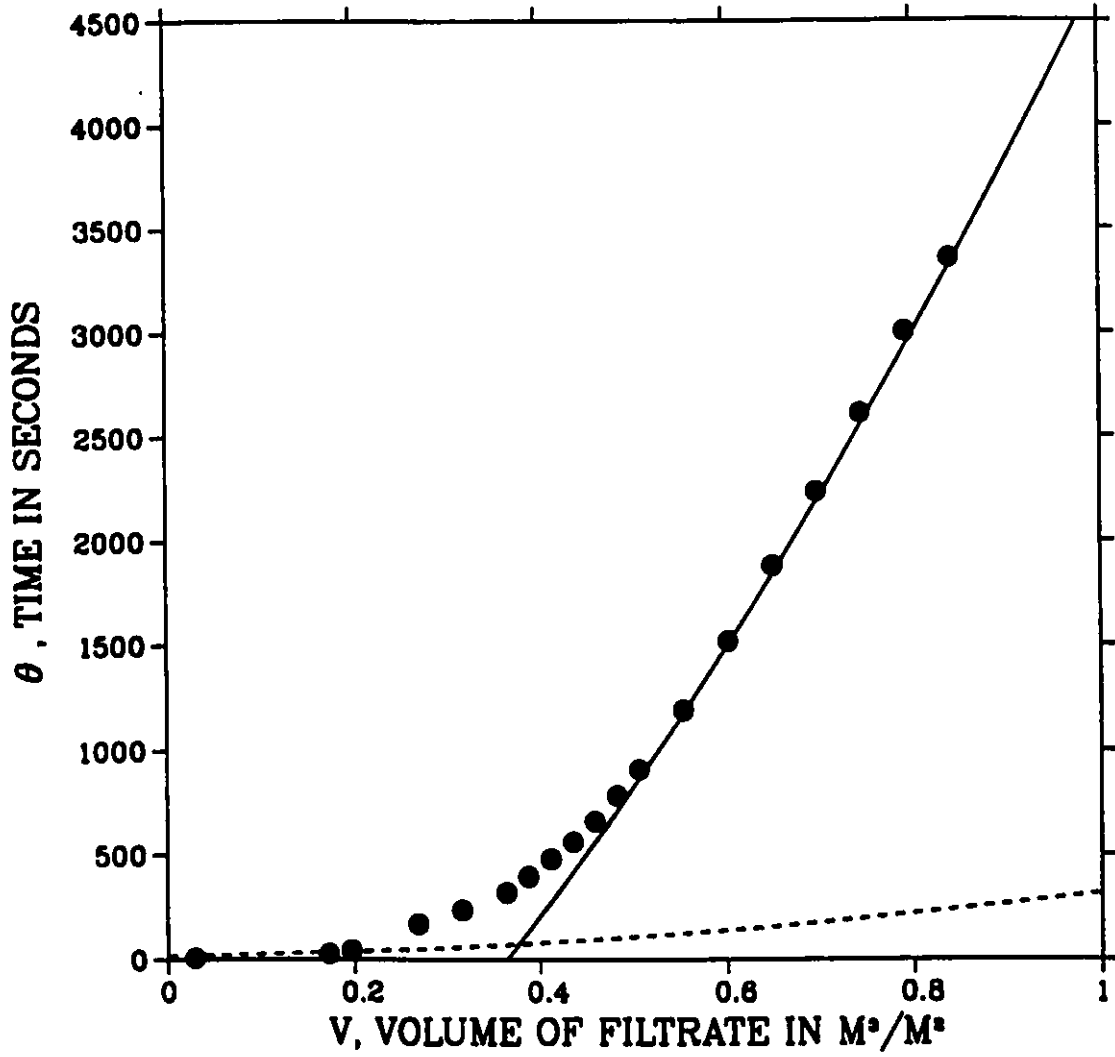
Slurry solids fraction = 0.10  
 Density of filtrate =  $997.2 \text{ kg} \cdot \text{m}^{-3}$   
 Viscosity of filtrate =  $1.0127 \times 10^{-3} \text{ Pa} \cdot \text{s}$   
 Moisture ratio = 1.92  
 Porosity = 0.71

**Results of the Linear Least-Squares Estimation:**  
Fitted Curve A                      Fitted Curve B

$\theta_0$ = 16.0 s $v_{me}$ = 0.12 m $K_N$ = $0.0013 \text{ m} \cdot \text{s}^{-2}$ $R_{ma}$ = $0.3 \times 10^{11} \text{ m}^{-i}$ $\gamma_{av}$ = $0.02 \times 10^{11} \text{ m} \cdot \text{kg}^{-1}$ variance = 44.7	$\theta_0$ = -1689.0 s $v_{me}$ = 0.64 m $K_N$ = $0.0012 \text{ m} \cdot \text{s}^{-2}$ $R_{ma}$ = $18.8 \times 10^{11} \text{ m}^{-1}$ $\gamma_{av}$ = $0.2 \times 10^{11} \text{ m} \cdot \text{kg}^{-1}$ variance = 2.5
---	---

volume of filtrate <i>mL</i>	volume of filtrate, <i>v</i> $\text{m}^3/\text{m}^2$	time, $\theta$ <i>s</i>
122	0.029	5.0
722	0.172	25.5
822	0.196	42.5
1122	0.268	168.0
1322	0.316	235.0
1522	0.363	320.0
1622	0.387	396.0
1722	0.411	479.0
1822	0.435	560.5
1922	0.459	660.5
2022	0.483	782.0
2122	0.507	907.0
2322	0.554	1190.0
2522	0.602	1517.0
2722	0.650	1879.0
2922	0.698	2234.0
3122	0.745	2612.0
3322	0.793	3001.0
3522	0.841	3354.5

517 kPa, 10 % CaCO<sub>3</sub>  
Anionic Polyacrylamide  
50 ppm



517 kPa (75 psi)  
 Anionic Polyacrylamide  
 100 ppm

---

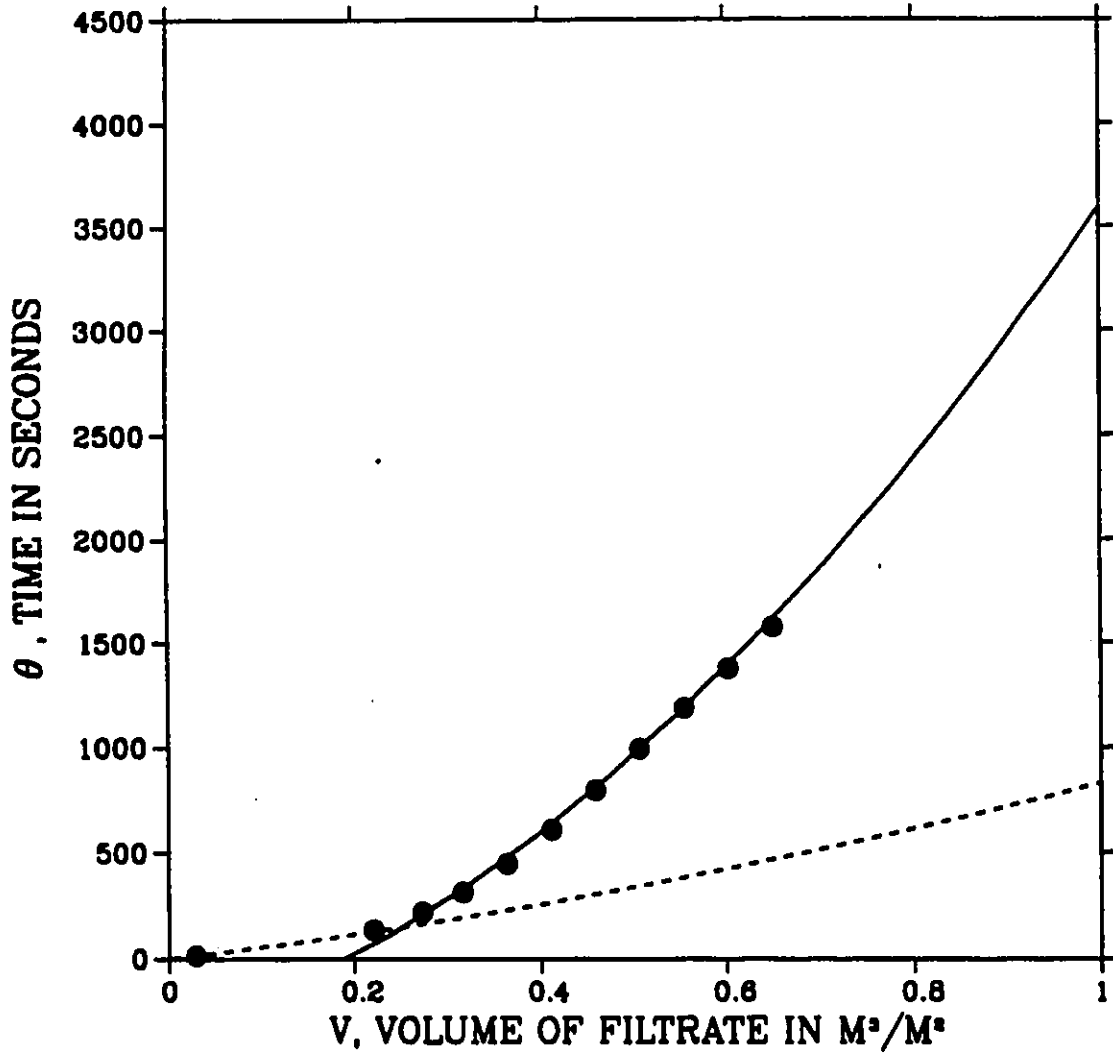
Slurry solids fraction = 0.10  
 Density of filtrate =  $997.1 \text{ kg} \cdot \text{m}^{-3}$   
 Viscosity of filtrate =  $1.0212 \times 10^{-3} \text{ Pa} \cdot \text{s}$   
 Moisture ratio = 2.28  
 Porosity = 0.78

**Results of the Linear Least-Squares Estimation:**  
Fitted Curve A Fitted Curve B

$\theta_0$ = -1.6 s $v_{me}$ = 0.85 m $K_N$ = $0.0107 \text{ m} \cdot \text{s}^{-2}$ $R_{ma}$ = $2.7 \times 10^{11} \text{ m}^{-1}$ $\gamma_{av}$ = $0.03 \times 10^{11} \text{ m} \cdot \text{kg}^{-1}$ variance = 0.00095	$\theta_0$ = -346.1 s $v_{me}$ = 0.25 m $K_N$ = $0.0012 \text{ m} \cdot \text{s}^{-2}$ $R_{ma}$ = $6.7 \times 10^{11} \text{ m}^{-1}$ $\gamma_{av}$ = $0.2 \times 10^{11} \text{ m} \cdot \text{kg}^{-1}$ variance = 2.1
--	---

volume of filtrate <i>mL</i>	volume of filtrate, <i>v</i> $\text{m}^3/\text{m}^2$	time, $\theta$ <i>s</i>
122.0	0.096	14.0
300.0	0.235	23.0
400.0	0.313	32.0
500.0	0.392	42.0
600.0	0.470	58.0
700.0	0.548	77.0
800.0	0.627	98.0
922.0	0.722	135.0
1100.0	0.862	173.0
1142.0	0.895	219.0
1322.0	1.036	314.0
1522.0	1.192	447.0
1722.0	1.349	610.0
1922.0	1.506	796.0
2122.0	1.662	993.0
2322.0	1.819	1187.0
2522.0	1.976	1376.0
2722.0	2.132	1577.0

517 kPa, 10 % CaCO<sub>3</sub>  
Anionic Polyacrylamide<sup>3</sup>  
100 ppm



517 kPa (75 psi)  
 Non-ionic Polyacrylamide  
 25 ppm

---

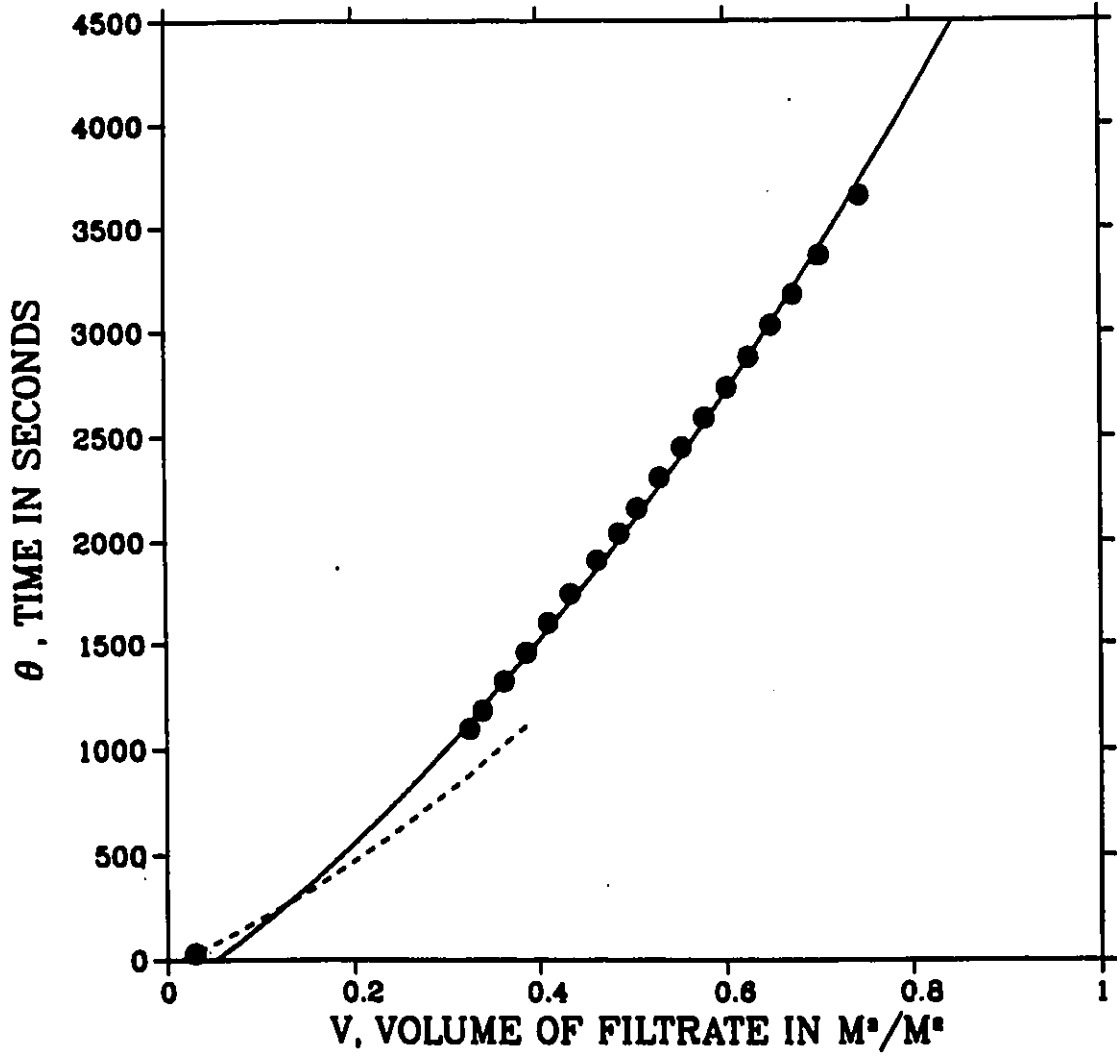
Slurry solids fraction = 0.100  
 Density of filtrate = 997.1 kg/m<sup>3</sup>  
 Viscosity of filtrate = 1.0175 × 10<sup>-3</sup> Pa · s  
 Moisture ratio = 1.55  
 Porosity = 0.60

**Results of the Linear Least-Squares Estimation:**  
Fitted Curve A Fitted Curve B

$\theta_0$ = -33.2 s $v_{me}$ = 0.43 m $K_N$ = 0.0014 m · s <sup>-2</sup> $R_{ma}$ = 10.3 × 10 <sup>11</sup> m <sup>-1</sup> $\gamma_{av}$ = 0.2 × 10 <sup>11</sup> m · kg <sup>-1</sup> variance = 21.9	$\theta_0$ = -165.1 s $v_{me}$ = 0.49 m $K_N$ = 0.0011 m · s <sup>-2</sup> $R_{ma}$ = 15.2 × 10 <sup>11</sup> m <sup>-1</sup> $\gamma_{av}$ = 0.3 × 10 <sup>11</sup> m · kg <sup>-1</sup> variance = 12.4
---	--

volume of filtrate mL	volume of filtrate, $v$ m <sup>3</sup> /m <sup>2</sup>	time, $\theta$ s
122	0.0290	31.0
1362	0.325	1095.0
1422	0.340	1180.0
1522	0.363	1319.0
1582	0.378	1402.0
1622	0.387	1457.0
1722	0.411	1602
1822	0.435	1742.5
1942	0.464	1905.5
2042	0.488	2037.0
2122	0.507	2157.0
2222	0.531	2303.0
2322	0.554	2447.0
2422	0.578	2588.0
2522	0.602	2730.5
2622	0.626	2876.0
2722	0.650	3029.0
2822	0.674	3176.5
2942	0.702	3365.5
3122	0.745	3656.0

517 kPa, 10 % CaCO<sub>3</sub>  
Non-ionic Polyacrylamide  
25 ppm



517 kPa (75 psi)  
 Non-ionic Polyacrylamide  
 50 ppm

---

Slurry solids fraction = 0.100  
 Density of filtrate =  $997.1 \text{ kg} \cdot \text{m}^{-3}$   
 Viscosity of filtrate =  $1.0019 \times 10^{-3} \text{ Pa} \cdot \text{s}$   
 Moisture ratio = 1.56  
 Porosity = 0.60

**Results of the Linear Least-Squares Estimation:**

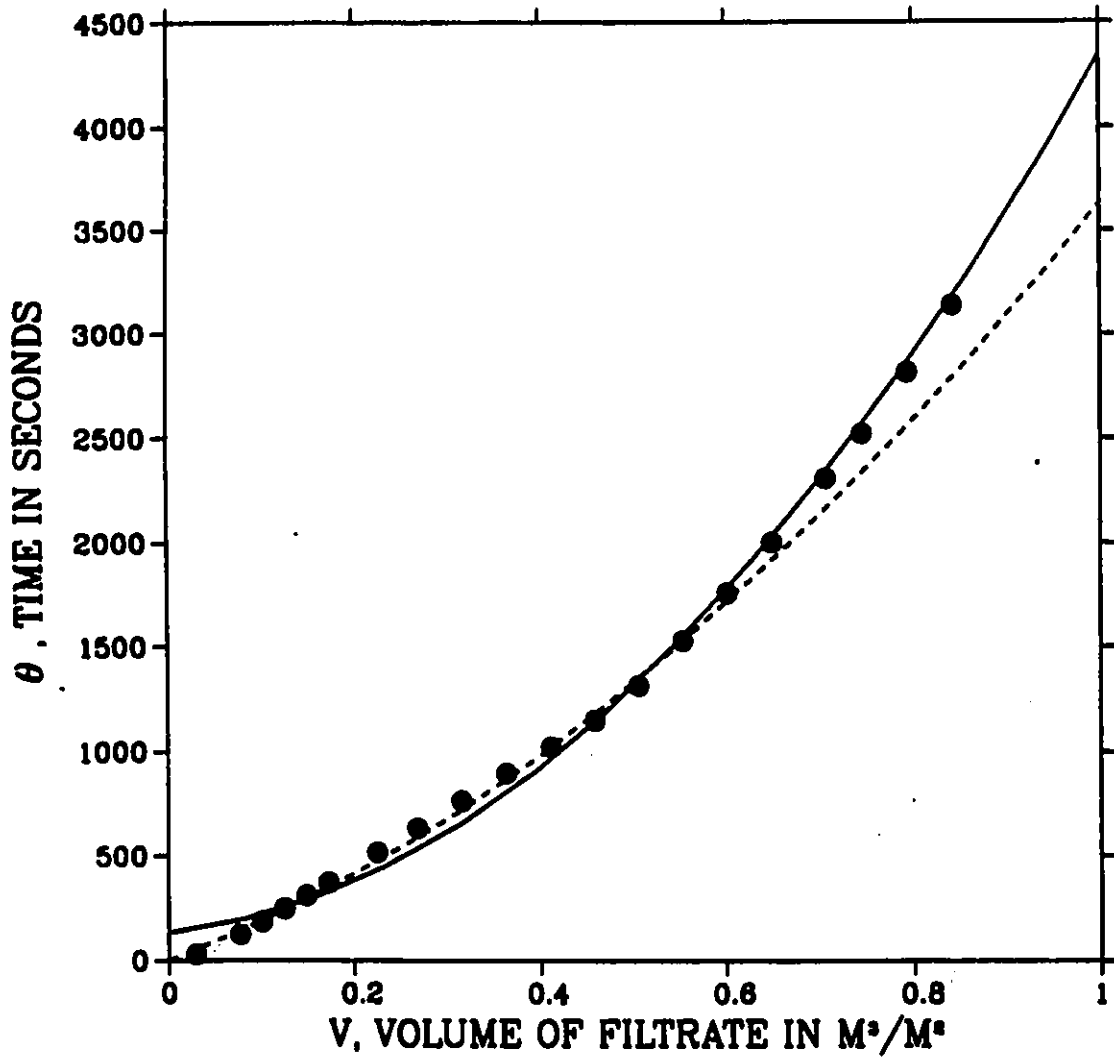
**Fitted Curve A**

**Fitted Curve B**

$\theta_0$	=	-0.1 s	$\theta_0$	=	131.3 s
$v_{me}$	=	0.43 m	$v_{me}$	=	0.067 m
$K_N$	=	$0.0017 \text{ m} \cdot \text{s}^{-2}$	$K_N$	=	$0.00088 \text{ m} \cdot \text{s}^{-2}$
$R_{ma}$	=	$8.8 \times 10^{11} \text{ m}^{-1}$	$R_{ma}$	=	$2.5 \times 10^{11} \text{ m}^{-1}$
$\gamma_{av}$	=	$0.2 \times 10^{11} \text{ m} \cdot \text{kg}^{-1}$	$\gamma_{av}$	=	$0.3 \times 10^{11} \text{ m} \cdot \text{kg}^{-1}$
variance	=	2690.0	variance	=	24.3

volume of filtrate <i>mL</i>	volume of filtrate, <i>v</i> $\text{m}^3/\text{m}^2$	time, $\theta$ <i>s</i>
122	0.029	28.0
322	0.077	124.0
422	0.101	184.0
522	0.125	246.0
622	0.149	308.5
722	0.172	370.5
942	0.225	514.5
1122	0.268	633.5
1322	0.316	764.0
1522	0.363	895.0
1722	0.411	1020.0
1922	0.459	1147.5
2122	0.507	1312.5
2322	0.554	1528.0
2522	0.602	1754.5
2722	0.650	1998.0
2962	0.707	2305.0
3122	0.745	2520.5
3322	0.793	2814.0
3522	0.841	3135.0

517 kPa, 10 % CaCO<sub>3</sub>  
Non-ionic Polyacrylamide  
50 ppm



689 kPa (100 psi)

0 ppm

---

Slurry solids fraction = 0.10  
Density of filtrate =  $997.1 \text{ kg} \cdot \text{m}^{-3}$   
Viscosity of filtrate =  $0.8959 \times 10^{-3} \text{ Pa} \cdot \text{s}$   
Moisture ratio = 1.18  
Porosity = 0.62

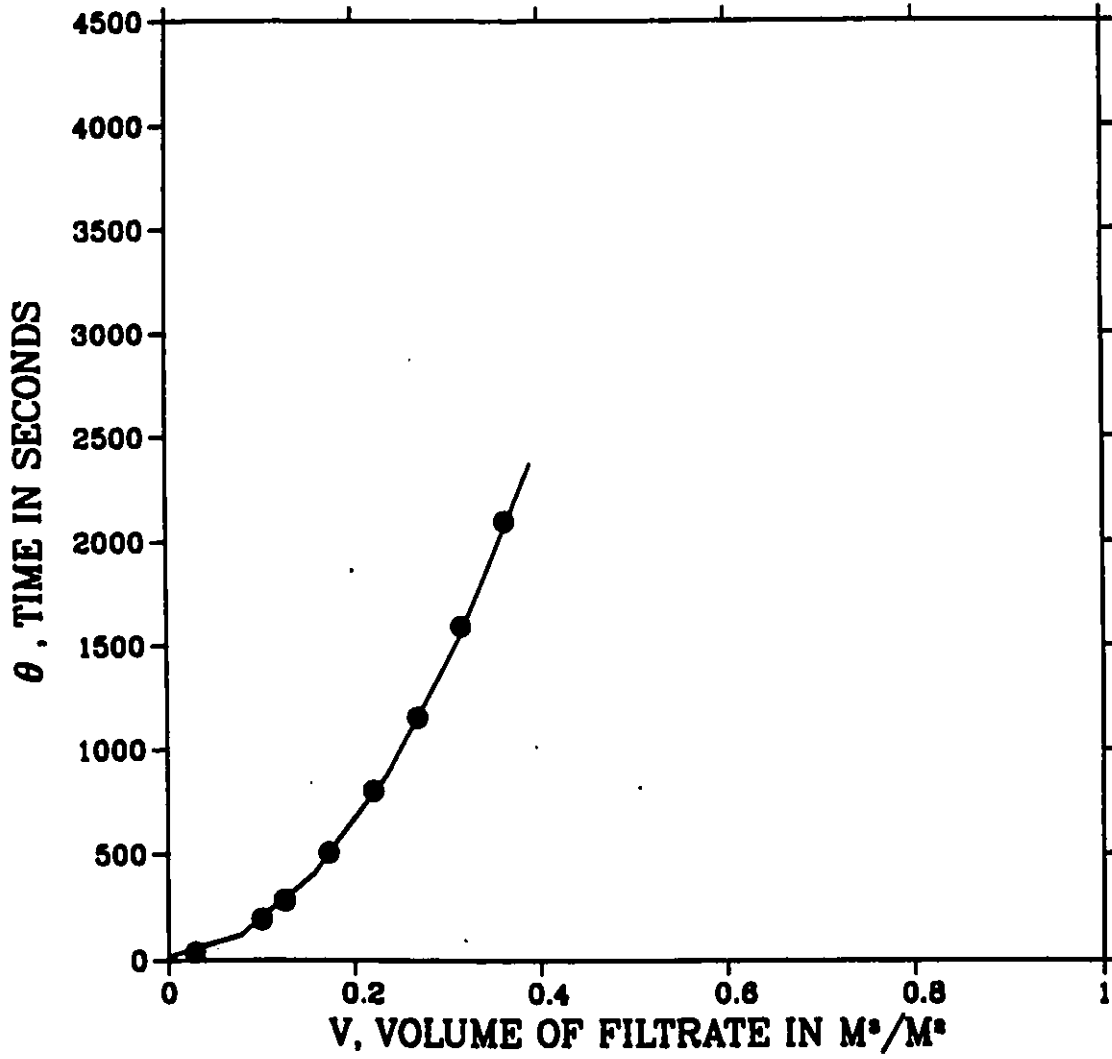
**Results of the Linear Least-Squares Estimation:**

**Fitted Curve**

$\theta_0$  = 15.7 s  
 $v_{me}$  = 0.0055 m  
 $K_N$  =  $0.00021 \text{ m} \cdot \text{s}^{-2}$   
 $R_{ma}$  =  $1.4 \times 10^{11} \text{ m}^{-1}$   
 $\gamma_{av}$  =  $2.2 \times 10^{11} \text{ m} \cdot \text{kg}^{-1}$   
variance = 0.00093

volume of filtrate mL	volume of filtrate, $v$ $\text{m}^3/\text{m}^2$	time, $\theta$ s
122.0	0.096	34.5
422.0	0.331	192.0
522.0	0.409	280.5
722.0	0.566	505.5
922.0	0.722	800.0
1122.0	0.879	1154.0
1322.0	1.036	1592.5
1522.0	1.192	2096.5

689 kPa, 10 %  $\text{CaCO}_3$   
0 ppm



689 kPa (100 psi)  
Anionic Polyacrylamide  
25 ppm

---

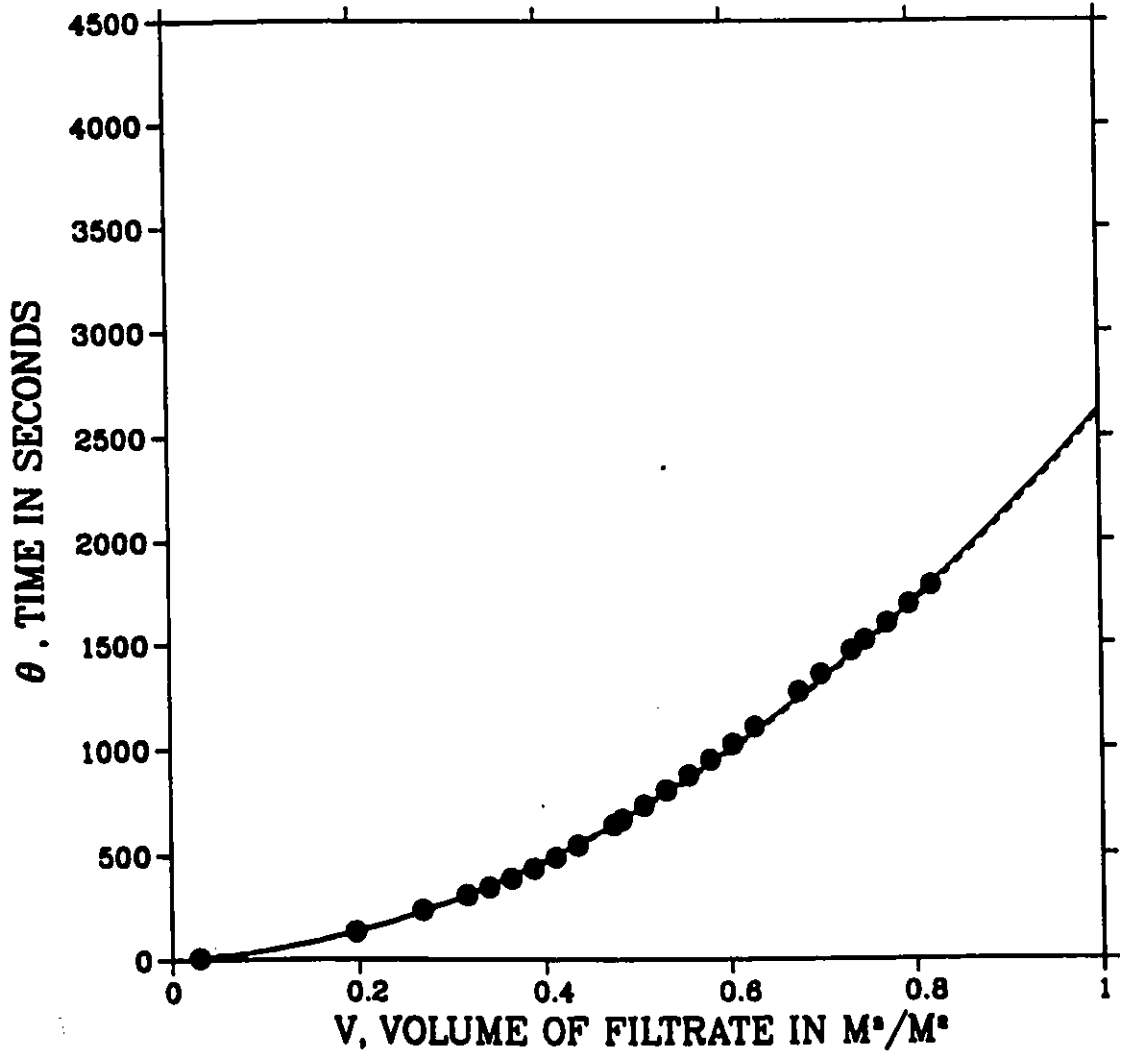
Slurry solids fraction = 0.10  
Density of filtrate =  $997.1 \text{ kg} \cdot \text{m}^{-3}$   
Viscosity of filtrate =  $1.0008 \times 10^{-3} \text{ Pa} \cdot \text{s}$   
Moisture ratio = 1.74  
Porosity = 0.67

**Results of the Linear Least-Squares Estimation:**  
**Fitted Curve A**                      **Fitted Curve B**

$\theta_0$	=	-4.5 s	$\theta_0$	=	-8.8 s
$v_{mc}$	=	0.046 m	$v_{mc}$	=	0.052 m
$K_N$	=	$0.0014 \text{ m} \cdot \text{s}^{-2}$	$K_N$	=	$0.0014 \text{ m} \cdot \text{s}^{-2}$
$R_{ma}$	=	$1.4 \times 10^{11} \text{ m}^{-1}$	$R_{ma}$	=	$1.7 \times 10^{11} \text{ m}^{-1}$
$\gamma_{av}$	=	$0.3 \times 10^{11} \text{ m} \cdot \text{kg}^{-1}$	$\gamma_{av}$	=	$0.3 \times 10^{11} \text{ m} \cdot \text{kg}^{-1}$
variance	=	56.0	variance	=	45.3

volume of filtrate <i>mL</i>	volume of filtrate, <i>v</i> $m^3/m^2$	time, $\theta$ <i>s</i>
122.0	0.096	7.0
822.0	0.644	133.0
1122.0	0.879	236.5
1322.0	1.036	308.0
1422.0	1.114	345.0
1522.0	1.192	386.0
1622.0	1.271	434.0
1722.0	1.349	487.0
1822.0	1.427	545.0
1982.0	1.553	642.5
2022.0	1.584	667.5
2122.0	1.662	733.0
2222.0	1.741	804.0
2322.0	1.819	874.5
2422.0	1.897	947.0
2522.0	1.976	1021.5
2622.0	2.054	1102.5
2822.0	2.211	1271.0
2922.0	2.289	1354.0
3062.0	2.399	1466.0
3122.0	2.446	1516.0
3222.0	2.524	1600.0
3322.0	2.602	1689.0
3422.0	2.681	1780.0

689 kPa, 10 % CaCO<sub>3</sub>  
Anionic Polyacrylamide<sup>3</sup>  
25 ppm



689 kPa (100 psi)  
 Anionic Polyacrylamide  
 50 ppm

---

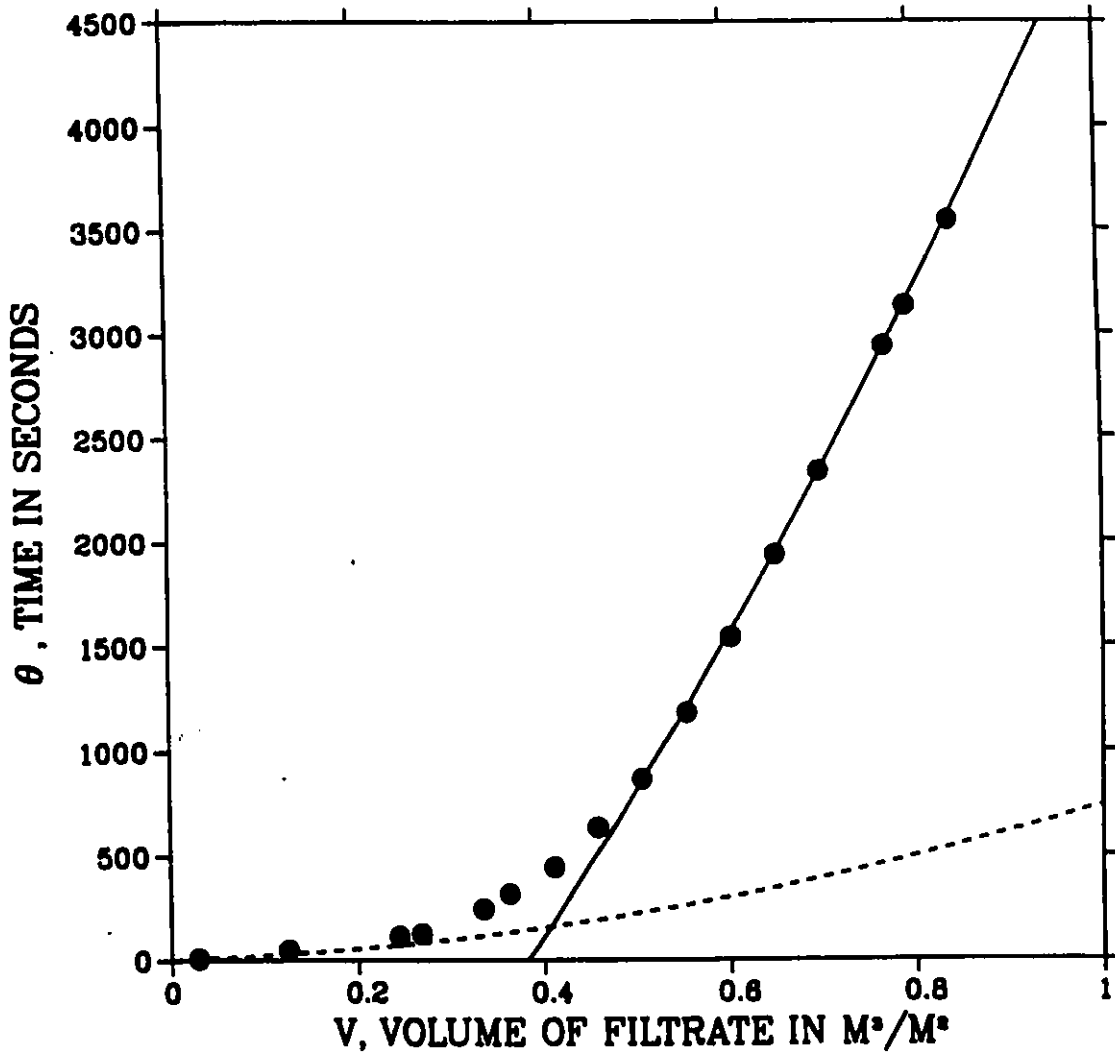
Slurry solids fraction = 0.10  
 Density of filtrate =  $997.1 \text{ kg} \cdot \text{m}^{-3}$   
 Viscosity of filtrate =  $1.0076 \times 10^{-3} \text{ Pa} \cdot \text{s}$   
 Moisture ratio = 1.73  
 Porosity = 0.67

**Results of the Linear Least-Squares Estimation:**  
Fitted Curve A Fitted Curve B

$\theta_0$	= -0.5 s	$\theta_0$	= -2138.2 s
$v_{me}$	= 0.13 m	$v_{me}$	= 0.88 m
$K_N$	= $0.0055 \text{ m} \cdot \text{s}^{-2}$	$K_N$	= $0.0012 \text{ m} \cdot \text{s}^{-2}$
$R_{ma}$	= $1.0 \times 10^{11} \text{ m}^{-1}$	$R_{ma}$	= $31.2 \times 10^{11} \text{ m}^{-1}$
$\gamma_{av}$	= $0.07 \times 10^{11} \text{ m} \cdot \text{kg}^{-1}$	$\gamma_{av}$	= $0.3 \times 10^{11} \text{ m} \cdot \text{kg}^{-1}$
variance	= 0.0016	variance	= 0.69

volume of filtrate <i>mL</i>	volume of filtrate, <i>v</i> $\text{m}^3/\text{m}^2$	time, $\theta$ <i>s</i>
122.0	0.096	6.5
522.0	0.409	46.0
1022.0	0.801	111.5
1122.0	0.879	125.0
1402.0	1.098	244.0
1522.0	1.192	317.5
1722.0	1.349	445.0
1922.0	1.506	634.0
2122.0	1.662	865.0
2322.0	1.819	1182.5
2522.0	1.976	1540.5
2722.0	2.132	1936.0
2922.0	2.289	2336.5
3222.0	2.524	2937.5
3322.0	2.602	3130.0
3522.0	2.759	3542.5

689 kPa, 10 % CaCO<sub>3</sub>  
Anionic Polyacrylamide<sup>3</sup>  
50 ppm



689 kPa (100 psi)  
 Anionic Polyacrylamide  
 50 ppm  
 0.5 Molar NaCl

---

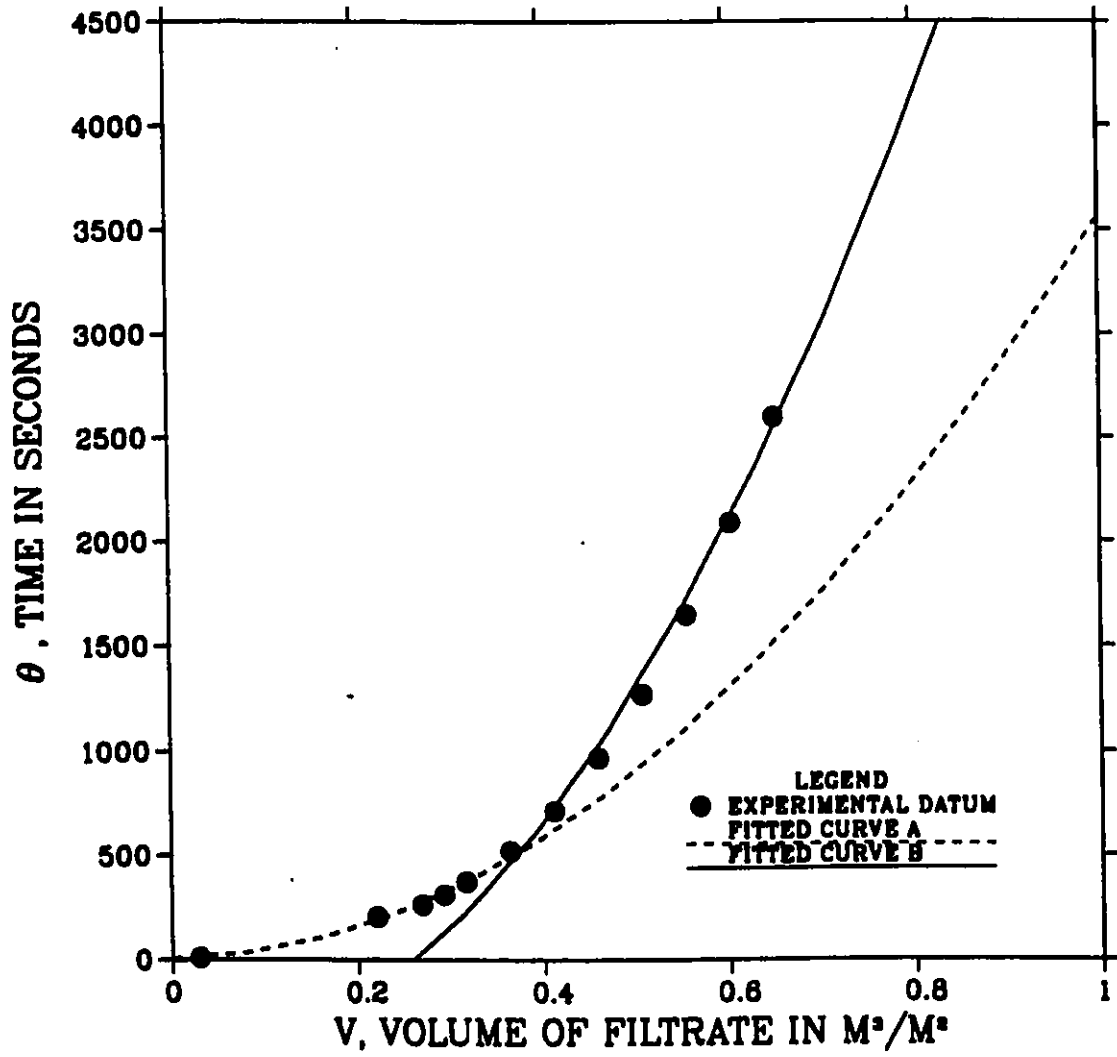
Slurry solids fraction = 0.10  
 Density of filtrate =  $1017.2 \text{ kg} \cdot \text{m}^{-3}$   
 Viscosity of filtrate =  $1.0682 \times 10^{-3} \text{ Pa} \cdot \text{s}$   
 Moisture ratio = 1.67  
 Porosity = 0.65

**Results of the Linear Least-Squares Estimation:**  
Fitted Curve A Fitted Curve B

$\theta_0$ = 4.7 s $v_{mc}$ = 0.0098 m $K_N$ = $0.00094 \text{ m} \cdot \text{s}^{-2}$ $R_{ma}$ = $0.4 \times 10^{11} \text{ m}^{-1}$ $\gamma_{av}$ = $0.47 \times 10^{11} \text{ m} \cdot \text{kg}^{-1}$ variance = 1.5	$\theta_0$ = -488.0 s $v_{mc}$ = 0.0000057 m $K_N$ = $0.00046 \text{ m} \cdot \text{s}^{-2}$ $R_{ma}$ = $0.004 \times 10^{11} \text{ m}^{-1}$ $\gamma_{av}$ = $0.6 \times 10^{11} \text{ m} \cdot \text{kg}^{-1}$ variance = 1060.0
--	--

volume of filtrate mL	volume of filtrate, $v$ $\text{m}^3/\text{m}^2$	time, $\theta$ s
122	0.029	7.0
922	0.220	202.5
1122	0.268	262.5
1222	0.292	310.5
1322	0.316	373.0
1522	0.363	520.0
1722	0.411	714.0
1922	0.459	967.0
2122	0.507	1267.0
2322	0.554	1645.0
2522	0.602	2085.0
2722	0.650	2595.0

689 kPa, 10 % CaCO<sub>3</sub>  
Anionic Polyacrylamide<sup>3</sup>  
50 ppm, 0.5 M NaCl



689 kPa (100 psi)  
Anionic Polyacrylamide  
100 ppm

---

Slurry solids fraction = 0.10  
Density of filtrate =  $997.1 \text{ kg} \cdot \text{m}^{-3}$   
Viscosity of filtrate =  $1.0389 \times 10^{-3} \text{ Pa} \cdot \text{s}$   
Moisture ratio = 2.14  
Porosity = 0.76

**Results of the Linear Least-Squares Estimation:**

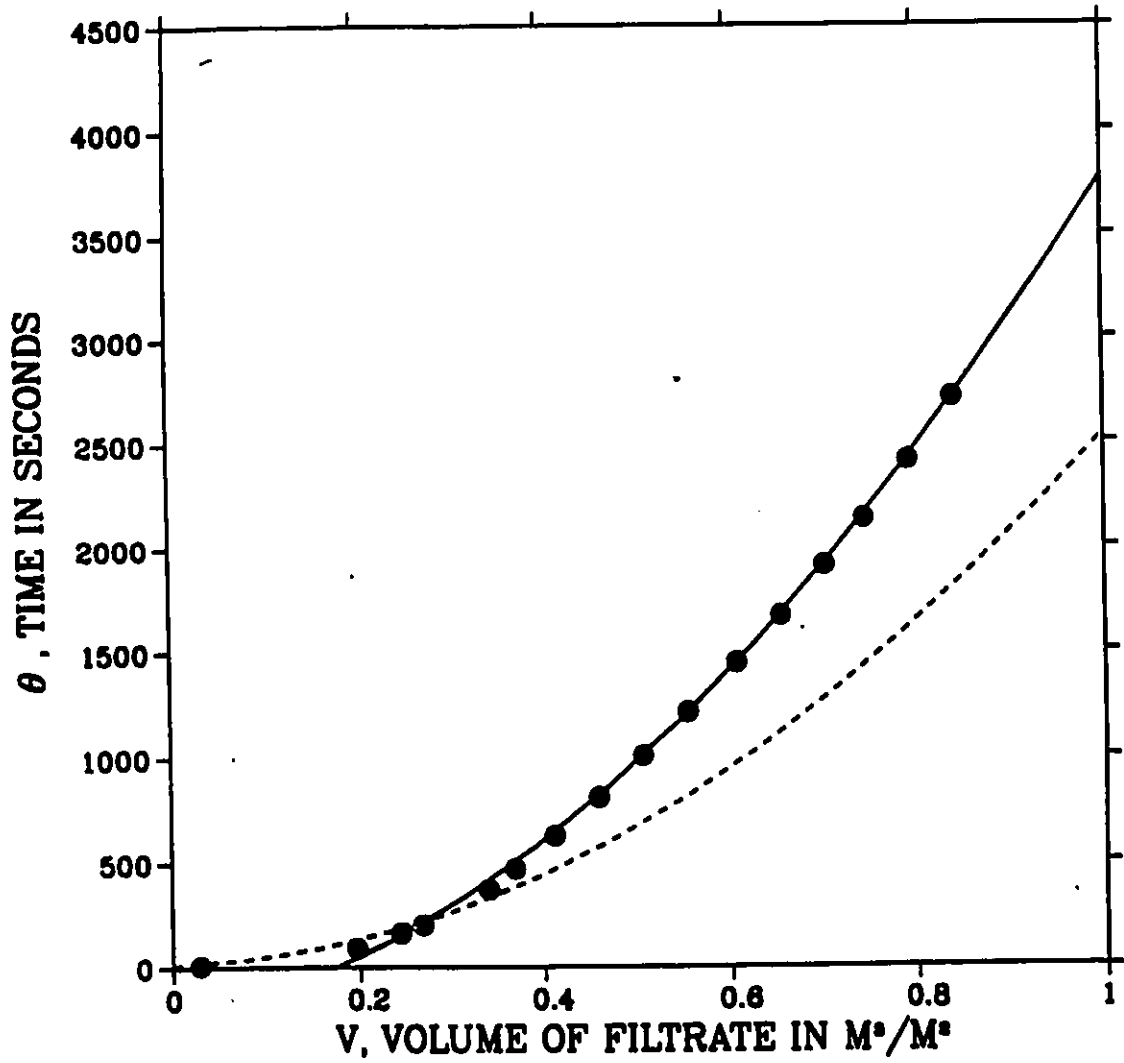
**Fitted Curve A**

**Fitted Curve B**

$\theta_0$	=	10.4 s	$\theta_0$	=	-264.8 s
$v_{me}$	=	0.027 m	$v_{me}$	=	0.16 m
$K_N$	=	$0.0014 \text{ m} \cdot \text{s}^{-2}$	$K_N$	=	$0.0011 \text{ m} \cdot \text{s}^{-2}$
$R_{ma}$	=	$0.9 \times 10^{11} \text{ m}^{-1}$	$R_{ma}$	=	$6.3 \times 10^{11} \text{ m}^{-1}$
$\gamma_{av}$	=	$0.3 \times 10^{11} \text{ m} \cdot \text{kg}^{-1}$	$\gamma_{av}$	=	$0.3 \times 10^{11} \text{ m} \cdot \text{kg}^{-1}$
variance	=	59.7	variance	=	0.012

volume of filtrate <i>mL</i>	volume of filtrate, <i>v</i> $m^3/m^2$	time, $\theta$ <i>s</i>
122.0	0.096	8.5
200.0	0.157	10.0
300.0	0.235	13.0
400.0	0.313	20.0
500.0	0.392	29.0
600.0	0.470	43.0
700.0	0.548	61.0
822.0	0.644	90.0
1022.0	0.801	160.0
1122.0	0.879	200.0
1200.0	0.940	242.0
1300.0	1.018	301.0
1422.0	1.114	370.0
1542.0	1.208	471.0
1722.0	1.349	628.0
1922.0	1.506	810.5
2122.0	1.662	1006.0
2322.0	1.819	1213.0
2542.0	1.991	1447.0
2742.0	2.148	1672.0
2942.0	2.305	1912.5
3122.0	2.446	2138.0
3322.0	2.602	2414.5
3522.0	2.759	2711.0

689 kPa, 10 % CaCO<sub>3</sub>  
Anionic Polyacrylamide  
100 ppm



689 kPa (100 psi)  
Non-ionic Polyacrylamide  
25 ppm

---

Slurry solids fraction = 0.10  
Density of filtrate =  $997.1 \text{ kg} \cdot \text{m}^{-3}$   
Viscosity of filtrate =  $1.0171 \times 10^{-3} \text{ Pa} \cdot \text{s}$   
Moisture ratio = 1.53  
Porosity = 0.59

**Results of the Linear Least-Squares Estimation:**

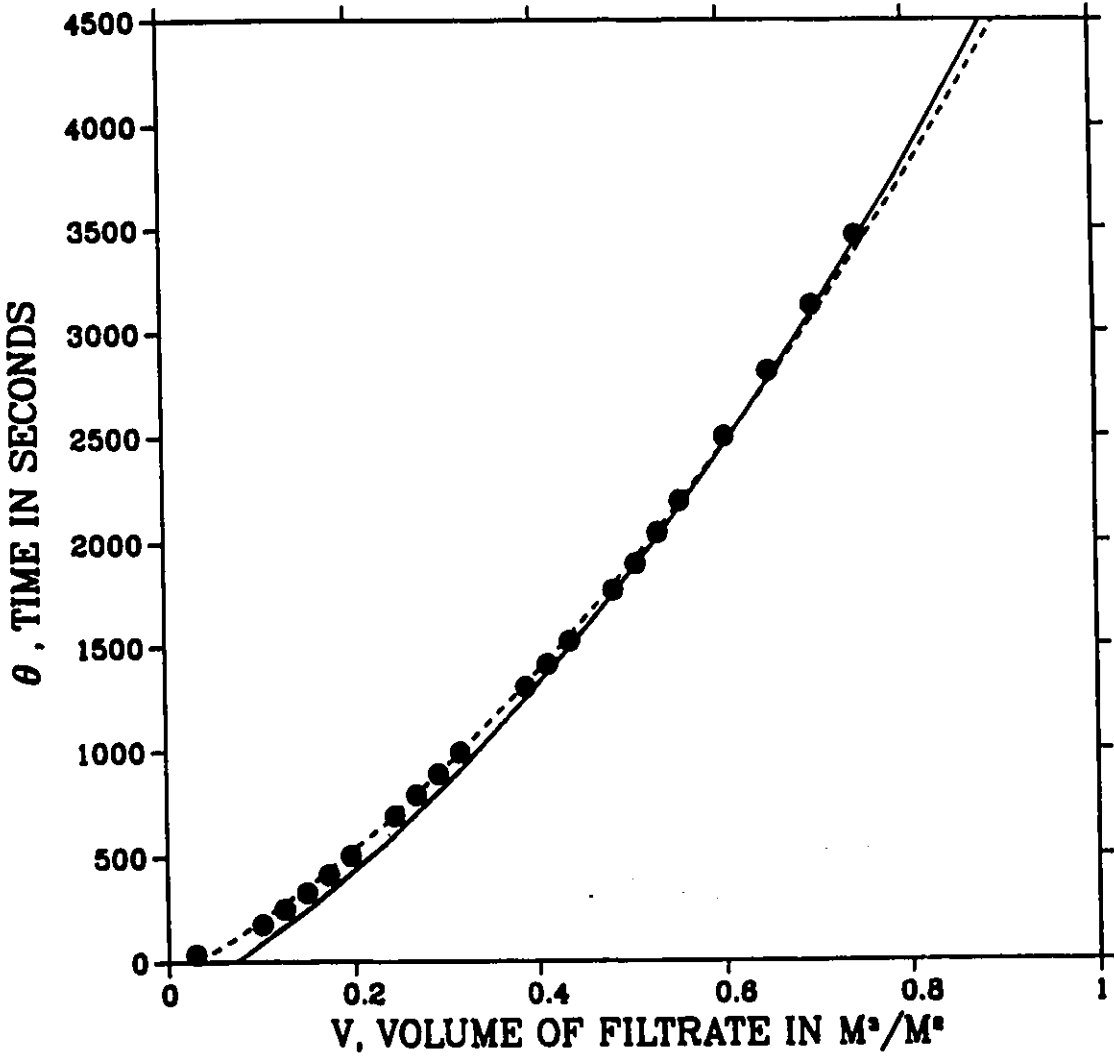
**Fitted Curve A**

**Fitted Curve B**

$\theta_0$	=	-83.6 s	$\theta_0$	=	-199.8 s
$v_{me}$	=	0.43 m	$v_{me}$	=	0.40 m
$K_N$	=	$0.0011 \text{ m} \cdot \text{s}^{-2}$	$K_N$	=	$0.0010 \text{ m} \cdot \text{s}^{-2}$
$R_{ma}$	=	$16.7 \times 10^{11} \text{ m}^{-1}$	$R_{ma}$	=	$17.3 \times 10^{11} \text{ m}^{-1}$
$\gamma_{av}$	=	$0.3 \times 10^{11} \text{ m} \cdot \text{kg}^{-1}$	$\gamma_{av}$	=	$0.4 \times 10^{11} \text{ m} \cdot \text{kg}^{-1}$
variance	=	11.3	variance	=	2.8

volume of filtrate <i>mL</i>	volume of filtrate, <i>v</i> $m^3/m^2$	time, $\theta$ <i>s</i>
122.0	0.096	34.0
422.0	0.331	175.0
522.0	0.409	247.0
622.0	0.487	327.0
722.0	0.566	411.0
822.0	0.644	501.5
1022.0	0.801	693.0
1122.0	0.879	791.0
1222.0	0.957	890.0
1322.0	1.036	991.0
1422.0	1.114	1094.0
1522.0	1.192	1257.0
1622.0	1.271	1302.0
1722.0	1.349	1411.0
1822.0	1.427	1524.5
2022.0	1.584	1771.0
2122.0	1.662	1897.0
2222.0	1.741	2046.0
2322.0	1.819	2196.0
2522.0	1.976	2500.0
2722.0	2.132	2813.0
2922.0	2.289	3128.5
3122.0	2.446	3467.0

689 kPa, 10 % CaCO<sub>3</sub>  
Non-ionic Polyacrylamide  
25 ppm



689 kPa (100 psi)  
Non-ionic Polyacrylamide  
50 ppm

---

Slurry solids fraction = 0.10  
Density of filtrate =  $997.1 \text{ kg} \cdot \text{m}^{-3}$   
Viscosity of filtrate =  $1.0068 \times 10^{-3} \text{ Pa} \cdot \text{s}$   
Moisture ratio = 1.54  
Porosity = 0.59

**Results of the Linear Least-Squares Estimation:**

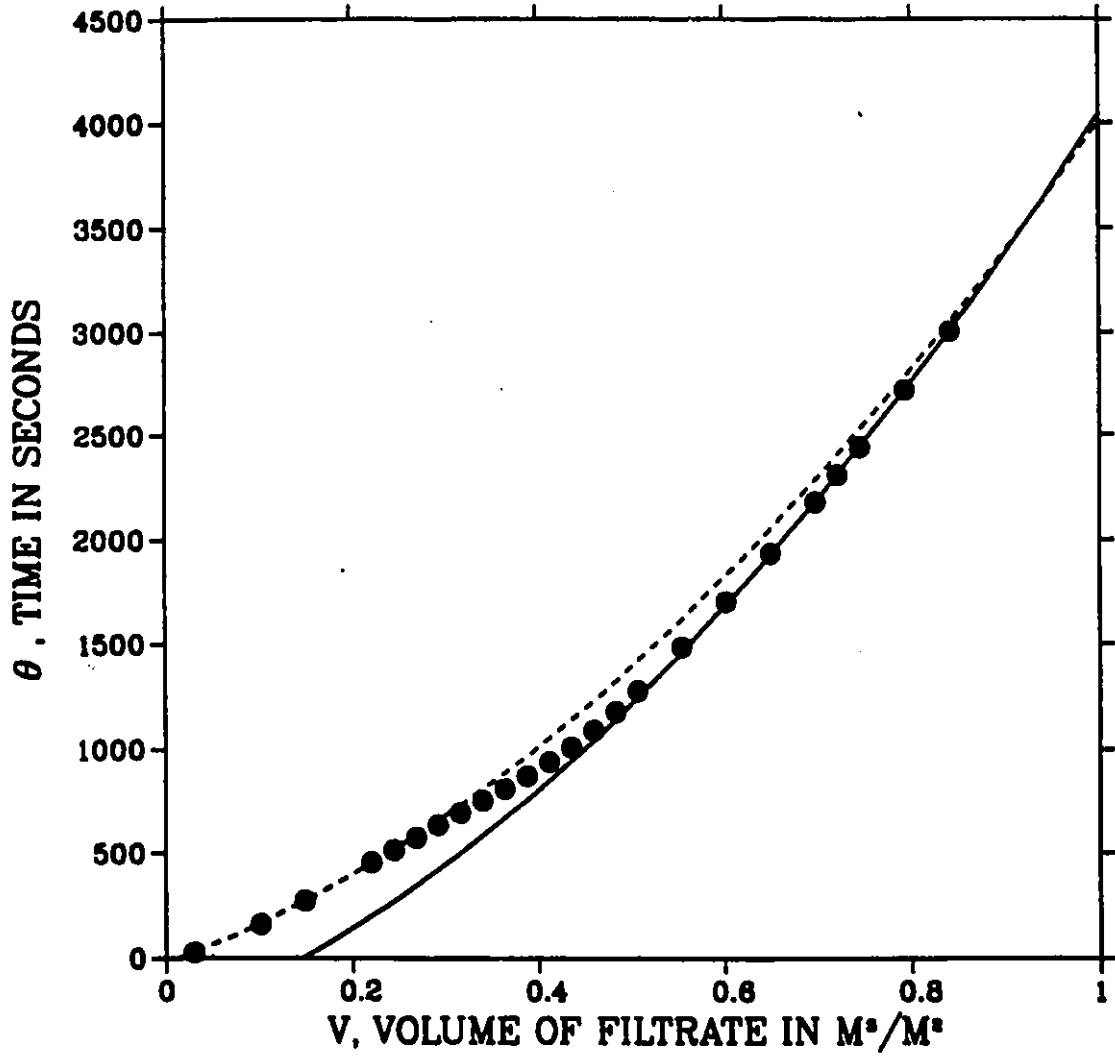
**Fitted Curve A**

**Fitted Curve B**

$\theta_0$	=	-23.6 s	$\theta_0$	=	-313.0 s
$v_{me}$	=	0.34 m	$v_{me}$	=	0.34 m
$K_N$	=	$0.0014 \text{ m} \cdot \text{s}^{-2}$	$K_N$	=	$0.0012 \text{ m} \cdot \text{s}^{-2}$
$R_{ma}$	=	$13.9 \times 10^{11} \text{ m}^{-1}$	$R_{ma}$	=	$15.0 \times 10^{11} \text{ m}^{-1}$
$\gamma_{av}$	=	$0.4 \times 10^{11} \text{ m} \cdot \text{kg}^{-1}$	$\gamma_{av}$	=	$0.4 \times 10^{11} \text{ m} \cdot \text{kg}^{-1}$
variance	=	1.7	variance	=	0.90

volume of filtrate <i>mL</i>	volume of filtrate, <i>v</i> $m^3/m^2$	time, $\theta$ <i>s</i>
122.0	0.096	27.0
422.0	0.331	161.0
622.0	0.487	272.5
922.0	0.722	454.5
1022.0	0.801	513.0
1122.0	0.879	574.0
1222.0	0.957	635.0
1322.0	1.036	694.0
1422.0	1.114	752.5
1522.0	1.192	810.5
1622.0	1.271	873.0
1722.0	1.349	939.0
1822.0	1.427	1009.0
1922.0	1.506	1090.0
2022.0	1.584	1179.0
2122.0	1.662	1277.0
2322.0	1.819	1485.5
2522.0	1.976	1701.0
2722.0	2.132	1932.5
2922.0	2.289	2176.5
3022.0	2.367	2305.0
3122.0	2.446	2437.5
3322.0	2.602	2715.0
3522.0	2.759	3000.0

689 kPa, 10 % CaCO<sub>3</sub>  
Non-ionic Polyacrylamide  
50 ppm



689 kPa (100 psi)  
Non-ionic Polyacrylamide  
100 ppm

---

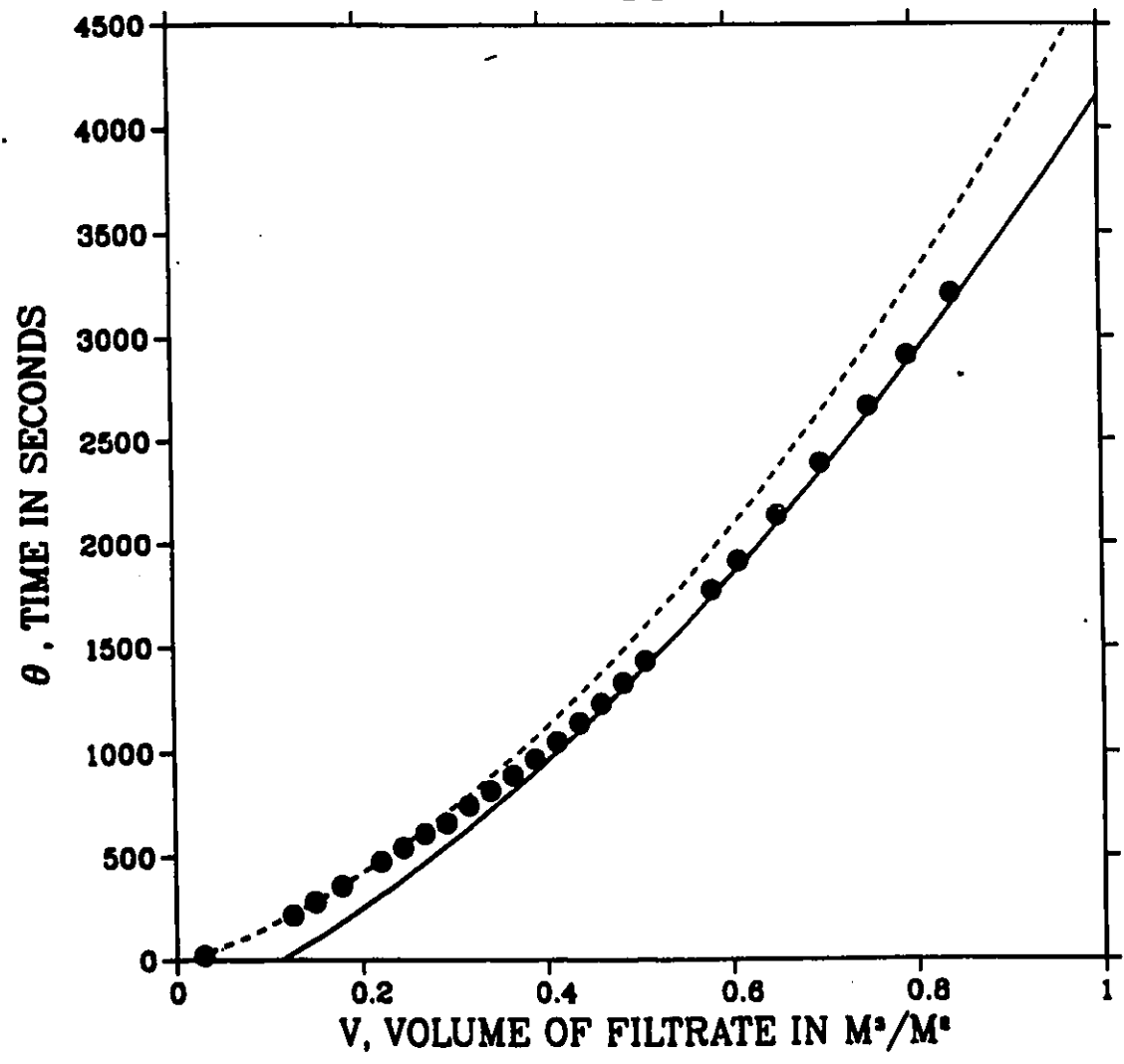
Slurry solids fraction = 0.10  
Density of filtrate =  $997.1 \text{ kg} \cdot \text{m}^{-3}$   
Viscosity of filtrate =  $1.0199 \times 10^{-3} \text{ Pa} \cdot \text{s}$   
Moisture ratio = 1.55  
Porosity = 0.60

**Results of the Linear Least-Squares Estimation:**  
**Fitted Curve A**                      **Fitted Curve B**

$\theta_0$	=	-29.3 s	$\theta_0$	=	-278.5 s
$v_{me}$	=	0.25 m	$v_{me}$	=	0.49 m
$K_N$	=	$0.0010 \text{ m} \cdot \text{s}^{-2}$	$K_N$	=	$0.0015 \text{ m} \cdot \text{s}^{-2}$
$R_{ma}$	=	$10.8 \times 10^{11} \text{ m}^{-1}$	$R_{ma}$	=	$15.2 \times 10^{11} \text{ m}^{-1}$
$\gamma_{av}$	=	$0.4 \times 10^{11} \text{ m} \cdot \text{kg}^{-1}$	$\gamma_{av}$	=	$0.3 \times 10^{11} \text{ m} \cdot \text{kg}^{-1}$
variance	=	0.22	variance	=	12.2

volume of filtrate <i>mL</i>	volume of filtrate, <i>v</i> $m^3/m^2$	time, $\theta$ <i>s</i>
122.0	0.096	20.5
522.0	0.409	216.5
622.0	0.487	280.0
742.0	0.581	357.0
922.0	0.722	476.0
1022.0	0.801	542.5
1122.0	0.879	611.0
1222.0	0.957	661.0
1322.0	1.036	745.0
1422.0	1.114	815.5
1522.0	1.192	890.0
1622.0	1.271	967.0
1722.0	1.349	1050.0
1822.0	1.427	1140.0
1922.0	1.506	1231.5
2022.0	1.584	1330.0
2122.0	1.662	1434.0
2422.0	1.897	1773.0
2542.0	1.991	1913.0
2722.0	2.132	2134.0
2922.0	2.289	2386.5
3142.0	2.461	2665.0
3322.0	2.602	2910.0
3522.0	2.759	3206.5

689 kPa, 10 % CaCO<sub>3</sub>  
Non-ionic Polyacrylamide  
100 ppm



# Appendix I

## 17.1 Verification of Assumptions

1. *In filtration the gravitational forces across the cake are considered to be negligible in comparison to the pressure forces.*

In the worst case, the gauge pressure drop across the cake is 50 psi, and the cake was 0.040 metres thick. The density of the fluid flowing through the filter cake is  $997.1 \text{ kg/m}^3$ . The gravitational acceleration in the Ottawa area is  $9.80606 \text{ m} \cdot \text{s}^{-2}$ .

$$\begin{aligned} \text{pressure force:} & \quad (50 \text{ psi}) \left( \frac{101.325 \text{ kPa}}{14.7 \text{ psi}} \right) & = & \quad 344.6 \text{ kPa} \\ \text{gravitational force:} & \quad (997.1 \frac{\text{kg}}{\text{m}^3})(9.80606 \frac{\text{m}}{\text{s}^2})(0.040 \text{ m}) & = & \quad 0.4 \text{ kPa} \end{aligned}$$

Since the gravitational force of 0.4 kPa is much less than the pressure force of 344.6 kPa, then the assumption to neglect the gravitational force is acceptable.

2. *The fluid flowing through the filter cake is a dilute aqueous solution of polyacrylamide. In other words, a quantity of polyacrylamide remains in the aqueous solution after flocculation has occurred.*

The experiments of Daza (1991) were tailored to complement the work described in this thesis. Aqueous polyacrylamide solutions (25 ppm, 50 ppm, 100 ppm; non-ionic and anionic) were prepared in graduated cylinders. Calcium carbonate, 10%  $\frac{w}{w}$ , was added, and the cylinders were inverted three times. The viscosities of the supernatant were taken. The graduated cylinders were then inverted many more times to observe

Table I.1: Viscosities in  $Pa \cdot s$  of the Non-ionic Polyacrylamide (Daza, 1991).

Polymer Concentration	Viscosity of the fresh solution $Pa \cdot s$	Viscosity after three inversions $Pa \cdot s$	Viscosity after several inversions $Pa \cdot s$
25 ppm	0.0011	0.00095	0.00091
50 ppm	0.0012	0.0010	0.00092
100 ppm	0.0014	0.0012	0.00094

Table K.2: Viscosities in  $Pa \cdot s$  of the Anionic Polyacrylamide (Daza, 1991).

Polymer Concentration	Viscosity of fresh solution $Pa \cdot s$	Viscosity after three inversions $Pa \cdot s$	Viscosity after several inversions $Pa \cdot s$
25 ppm	0.0012	0.0011	0.00091
50 ppm	0.0017	0.0013	0.00093
100 ppm	0.0028	0.0021	0.0011

the effect of much agitation of the solution viscosities. Table I.1 and Table I.1 displays the results of these experiments.

It is evident from the two previous tables that flocculation does not remove all of the polymer from the aqueous solution. There still remains polymer in the solution that will propagate the viscoelastic effects as it flows through the filter cake.

3. *The amount of nitrogen gas which dissolves into the slurry during a filtration run is negligible.*

Henry's Law at 25° for nitrogen gas is

$$P = H x \quad (I.1)$$

where  $P$  is the partial pressure in *atmospheres* of the gas above the liquid,  $H$  is Henry's constant, reported as  $8.65 \times 10^4$  in Perry (1950), and  $x$  is the mole fraction of the gas dissolved in the liquid. Therefore,

$$x = \frac{P}{H} \quad (I.2)$$

$$\begin{aligned}
&= \frac{100 \frac{\text{lb}_f}{\text{in}^2}}{8.65 \times 10^4} \left( \frac{1 \text{ atm}}{14.7 \frac{\text{lb}_f}{\text{in}^2}} \right) \\
&= 0.0000786 \text{ mole fraction of nitrogen.}
\end{aligned}$$

These mole fractions of nitrogen listed in the previous table represent quantities that would be present in the water at equilibrium. However, the duration of the experiments performed was relatively brief; thus, the amount of nitrogen dissolved in the slurry was insignificant. Therefore, the use of nitrogen gas to drive the slurry through the system was considered to have had no effect on the slurry characteristics, nor on the cake characteristics.

4. *In Non-Newtonian filtration, the slurry concentration has little effect on the filtration, even for concentrated slurries of compressible materials (Shirato, 1985).*

A weight fraction of 0.10 of calcium carbonate in the slurry was found satisfactory for the purpose of this study because filter cakes of appreciable thickness were obtained. Previous work involving polymers in constant pressure filtration employed slurry concentrations of  $\text{CaCO}_3$  of 2.5%  $\frac{w}{w}$  (Rao, 1970; Fu, 1977). It would seem that direct comparisons of work in this thesis to their work should not be done. However, it is shown on p.52, Figure 2.7 of Shirato (1985) that at a slurry solids fraction below 0.20, the variations in the quantities  $\frac{q}{q_1}$ ,  $\frac{r}{r_1}$ , and  $\frac{cz}{q_1}$  with  $\frac{w}{w_0}$  are negligible. Therefore, it is reasonable to make comparisons of experimental results of Rao (1970) and Fu (1977) to the results obtained in this thesis.